

**HOLISTIC WATERSHED MANAGEMENT FOR EXISTING AND FUTURE LAND
USE DEVELOPMENT ACTIVITIES: OPPORTUNITIES FOR ACTION FOR LOCAL
DECISION MAKERS: PHASE 1 – MODELING AND DEVELOPMENT OF FLOW
DURATION CURVES (FDC 1 PROJECT)**

**SUPPORT FOR SOUTHEAST NEW ENGLAND PROGRAM (SNEP)
COMMUNICATIONS STRATEGY AND TECHNICAL ASSISTANCE**

FINAL PROJECT REPORT

SEPTEMBER 30, 2021

Prepared for:

U.S. EPA Region 1



Prepared by:

Paradigm Environmental



Great Lakes Environmental Center



Blanket Purchase Agreement: BPA-68HE0118A0001-0003

Requisition Number: PR-R1-20-00322

Order: 68HE0121F0001

EXECUTIVE SUMMARY

This report presents a proof-of-concept demonstration of flow duration curve (FDC) development and watershed management analyses using the Region 1 Opti-Tool and associated models. The results represent the first phase of a two-phase project that is intended to investigate the impacts and potential benefits of next-generation new development and/or redevelopment (nD/rD) practices, referred to here as Conservation Development (CD) practices, on watershed hydrology and stream health. Conservation Development practices include among other things, de-emphasis on use and application of impervious cover (IC), an increasing role of landscape architecture to achieve enhanced evapotranspiration (ET), on-site groundwater recharge and better geospatial distribution of nD/rD site runoff, conservation of naturally vegetated areas, and incorporation of architectural features (e.g., green roofs) for increased sustainability, resilience, and preservation of the pre-development hydrological condition. This report advances these goals by quantifying the impacts of land cover and climate change on FDCs and investigates the ability of distributed Green Infrastructure (GI) Stormwater Control Measures (SCMs) to influence the frequency and distribution of long-term streamflows. The report provides the foundation for an analytical framework that includes tools (Opti-Tool) and metrics (i.e., ecosurplus and ecodeficit) to help quantify both the hydrologic impacts of the existing condition and the potential benefits of hydrograph restoration associated with GI stormwater management activities.

The project leveraged an existing calibrated continuous simulation watershed model for the Taunton River Basin. The existing Hydrological Simulation Program – FORTRAN (HSPF) model was converted into the Loading Simulation Program in C++ (LSPC) model, which is based on the same algorithms as the original HSPF model but has expanded functionality to provide seamless linkage to EPA’s System for Urban Stormwater Treatment and Analysis Integration (SUSTAIN) model and to SUSTAIN’s excel spreadsheet-based derivative, the Stormwater Management Optimization Tool (Opti-Tool). LSPC was used to develop FDCs for streamflows representative of pre-development, existing, and highly developed watershed conditions as well as climate change scenarios while the Opti-Tool was used to demonstrate the impacts of optimized stormwater retrofit management strategies for improving FDC conditions.

The study supports a growing body of evidence that highlights the complex and sometimes surprising relationships that can exist between watershed development and streamflow. For the study sub-watersheds, located in the Northeast United States, the impact which development has on streamflow can vary depending on the intensity of development. Relatively low levels of development can increase flows across the entire FDC, while development conditions with large amounts of directly connected IC can increase high flows but reduce baseflows. The results highlight four major mechanisms for FDC alteration: (1) the initial removal of vegetation from a watershed reduces the ability for the watershed to store and attenuate water as well as to return it to the atmosphere (2) an increase in impervious surfaces reduces opportunities for infiltration and further reduces ET (3) conveying impervious surface runoff directly to receiving waters increases flows, especially high flows (4) conveying impervious surface runoff to infiltration based SCMs reduces high flows but can increase low flows via additional groundwater recharge. Evapotranspiration plays an important role in ‘natural’ flow regimes and as watershed development increases, the associated reduction in ET throughout the landscape can result in higher flows across the FDC. The loss of vegetative cover (forests), as well as an increase in impervious surfaces, shifts the water balance towards higher flows. As impervious surfaces increase, baseflows may again start to fall due to more water being conveyed immediately to receiving waters with fewer opportunities for infiltration. Additionally, hydromodification such as diversions and point sources can also impact flows, although in this case, the study watersheds had minimal water withdrawals or discharges. The implementation of SCMs that disconnect existing impervious surfaces can reduce high flows and increase baseflows. The results presented in this report improve our understanding of the extent to which management strategies for implementing infiltration-based SCMs can restore predevelopment streamflow and improve watershed functions. While SCM implementation can mitigate some of the impacts of watershed development, it may be difficult to attain pre-development

watershed functions without landscape-level strategies that promote additional evapotranspiration and attenuation of water throughout the watershed.

Summary of an optimized GI SCM solution (knee of the curve) results for study sub-watersheds (analysis period 2000-2020)

Study Sub-Watershed	Pilot Tributary	Lower Hodges Brook	Upper Hodges Brook
Drainage Area to the Outlet (acre)	1,457	2,505	1,336
Total Impervious Area (%)	4%	20%	32%
Average Design Storage Volume for the Selected Solution (i.e., Runoff Depth Captured from IC)	0.40 inch	0.33 inch	0.41 inch
FDC Difference between Existing Conditions and SCM Implementation for the Selected Solution	Result	Result	Result
High Flows [<10%] (gallons/year)	-38,859,725	-433,792,645	-545,640,325
Moist Condition [10% - 40%] (gallons/year)	5,974,685	45,228,610	74,162,160
Mid-range Flows [40% - 60%] (gallons/year)	2,743,340	52,862,950	67,586,685
Dry Condition [60% - 90%] (gallons/year)	3,747,455	52,206,315	52,988,510
Low Flows [>90%] (gallons/year)	2,911,970	26,144,950	21,413,090
WQ Benefits and Costs of an Optimized Solution	Result	Result	Result
TSS Load Removed (tons/year)	12	85	63
	(23% reduction from baseline)	(50% reduction from baseline)	(51% reduction from baseline)
TN Load Removed (pounds/year)	239	1,894	1,560
	(12% reduction from baseline)	(32% reduction from baseline)	(36% reduction from baseline)
TP Load Removed (pounds/year)	35	262	211
	(10% reduction from baseline)	(32% reduction from baseline)	(37% reduction from baseline)
Zn Load Removed (pounds/year)	29	245	196
	(21% reduction from baseline)	(50% reduction from baseline)	(53% reduction from baseline)
Cost per Ton TSS Removed (\$)	\$40,724	\$40,181	\$52,487
Cost per Pound TN Removed (\$)	\$2,018	\$1,806	\$2,124
Cost per Pound TP Removed (\$)	\$13,889	\$13,051	\$15,682
Cost per Pound Zn Removed (\$)	\$16,576	\$13,971	\$16,893

The results of the streamflow modeling analysis support many well-established concepts about how impervious surfaces influence streamflow, especially stormflows. Additionally, the results suggest that the impact development has on baseflows can vary depending on the intensity of development. Compared to pre-development/forested conditions, development, including development that includes disconnected impervious surfaces, increased baseflows. However, baseflows fell below pre-development conditions when the amount of connected impervious surfaces was substantially increased. The results support the findings of previous research efforts into the impact of development on streamflow, although results may be impacted by the geography and climate of the study area.

Table of Contents

Executive Summary	i
1. Introduction	1
1.1 Background	1
1.2 Project Objectives	1
2. Wading River Watershed – Available Data and Existing Conditions	3
2.1 Data/Information Assessment	3
2.1.1 Landscape Data	3
2.1.2 Dams and Reservoirs	3
2.1.3 Water Use	3
2.1.4 Meteorology Data	4
2.1.5 Streamflow Data	9
2.1.6 Existing Models	10
2.1.7 Study Sub-watersheds Identification and Prioritization	16
2.2 Climate Data: Historic Trends and Future Conditions	16
2.2.1 Historic Trends	18
2.2.2 Future Conditions	18
3. Model Application	20
3.1 Watershed Modeling Approach	20
3.2 SCM Modeling Approach with FDC Attenuation Objective	22
3.3 LSPC Model Configuration, Calibration, and Validation	22
3.3.1 Model Configuration	22
3.3.2 Hydrology Calibration and Validation	34
3.3.3 HRU Based Water Quality Calibration	35
3.4 Opti-Tool Background and Updates	37
4. Hydrologic Streamflow Modeling Analyses	38
4.1 LSPC Streamflow Modeling Results	38
4.1.1 Baseline Unit-Area Analysis	38
4.1.2 Relationships Between Impervious Cover and Watershed Function	38
4.1.3 Pollutant Export	54
4.1.4 Latent Heat and Carbon Sequestration	54
4.1.5 Climate Change Scenarios	58
4.2 Opti-Tool Optimization of SCMs to Achieve Flow Duration Curve Objectives	70
4.2.1 GIS Screening to Identify SCM Opportunities	70
4.2.2 Estimating SCM Footprints and Drainage Treatment Areas	70
4.2.3 Opti-Tool Setup	74
4.3 Optimization Results	82
4.4 Conclusions	98

5. Future Work - Phase II..... 100

6. References 101

List of Figures

Figure 2-1. Wading River watershed location within Taunton basin.....	5
Figure 2-2. Meteorology and streamflow gage locations.....	6
Figure 2-3. Flow duration curve 1925-2020. Wading River.	11
Figure 2-4. Flow duration curves by decade. Wading River.	11
Figure 2-5. Enlarged section of Figure 2-4 showing the low flow portion of flow duration curves by decade. Wading River.	12
Figure 2-6. Enlarged section of Figure 2-4 showing the high flow portion of flow duration curves by decade. Wading River.	12
Figure 2-7. Ecosurplus and ecodeficit for the Wading River for 2001-2019 vs. 1972-1990. Black dots represent inflection points where the two curves change between surplus and a deficit.	13
Figure 2-8. HSPF subbasins for the Wading River.	15
Figure 2-9. Selected sub-watersheds in the Wading River watershed.....	17
Figure 2-10. Representative Concentration Pathways for climate change analysis (International Institute for Applied Systems Analysis, 2009).	19
Figure 3-1. Conceptual representation of the LSPC model development cycle.....	21
Figure 3-2. Hydrology model schematic for LSPC (based on Stanford Watershed Model).	21
Figure 3-3. LSPC and Opti-Tool linkage schematic for integrated watershed-SCM hydrology modeling.	22
Figure 3-4. LSPC model configuration and calibration components.	23
Figure 3-5. Mapped HRUs process (spatial overlay of land use – land cover, soil, and slope layers).	26
Figure 3-6. Mapped HRUs for the Taunton basin.	28
Figure 3-7. Mapped HRUs for Lower Hodges Brook (top left), Upper Hodges Brook (top right), Pilot Tributary (bottom left), and Wading River (bottom right).	29
Figure 3-8. Translation sequence from MIA to DCIA.....	30
Figure 3-9. Relationships between Mapped and Directly Connected Impervious Area (Sutherland 2000).	30
Figure 3-10. Peppered HRUs representing the effective impervious areas for Upper Hodges Brook (MIA on left and EIA on right).	32
Figure 4-1. Water Balance for LSPC Hydrological Response Units, Summarized by Land Use. Baseline Simulation 2000-2020.	39
Figure 4-2. Water Balance for LSPC Hydrological Response Units, Summarized by Soil Group. Baseline Simulation 2000-2020.	40
Figure 4-3. Water Balance for LSPC sub-watersheds.	41
Figure 4-4. Standard FDC (top) and Normalized FDCs (bottom) for the three study watersheds.	42
Figure 4-5. Ecosurplus and Ecodeficit for Upper Hodges compared to Lower Hodges.....	43
Figure 4-6. Average monthly discharge and runoff depth for the three study watersheds.....	45
Figure 4-7. Flow Duration Curves for Upper Hodges Brook watershed for baseline, predevelopment, EIA=TIA, and EIA=0 conditions. Baseline FDC is black with a yellow highlight.,.....	46
Figure 4-8. High flow (top) and low flow (bottom) sections of the FDC-presented in Figure 4-7 Baseline FDC is black with a yellow highlight.	47
Figure 4-9. Water balances and Ecosurplus and Ecodeficit for Upper Hodges Brook watershed for baseline and EIA=TIA conditions. EIA=TIA reflects an increase in directly connected impervious surfaces. Black dots indicate places where FDCs cross.	48
Figure 4-10. Water balances and Ecosurplus for Upper Hodges Brook watershed for baseline and forested/pre-development conditions. Ecosurplus calculated relative to forested/pre-development conditions.	49
Figure 4-11. Water balances and Ecosurplus/Ecodeficit for Upper Hodges Brook watershed for baseline and EIA = 0 (all existing impervious surfaces disconnected). Ecosurplus/Ecodeficit calculated relative to baseline/existing condition. Black dots indicate places where FDCs cross each other.....	50
Figure 4-12. Average (top) and minimum (bottom) monthly flows for land use scenarios. Minimum flows are presented on a logarithmic scale.....	51
Figure 4-13. Three-day minimum (top) and maximum (bottom) flow for land use scenarios.	52
Figure 4-14. Pollutant export comparisons across land use scenarios.	54

Figure 4-15. Average Annual Latent Heat Flux for Hodges Brook (top left), Upper Hodges Brook (top right), Pilot Tributary (bottom left), and Wading River (bottom right).	56
Figure 4-16. Ensemble results for ecosurplus and ecodeficits.	59
Figure 4-17. Ecodeficit FDCs at the Wading River USGS Gage (01109000) under baseline and climate change scenarios for RCP 8.5 (top) and RCP 4.5 (bottom).	60
Figure 4-18. Ecosuplus FDCs at the Wading River USGS Gage (01109000) under baseline and climate change scenarios for RCP 8.5 (top) and RCP 4.5 (bottom).	61
Figure 4-19. Results for the wet, median, and dry models for ecodeficits based on an RCP 4.5 scenario. Results are for the Wading River USGS Gage (01109000) under comparing baseline (2000-2020) to future climate scenarios (2079-2099).	62
Figure 4-20. Results for the wet, median, and dry models for ecodeficits based on an RCP 8.5 scenario. Results are for Wading River USGS Gage (01109000) comparing baseline (2000-2020) to future climate scenarios (2079-2099).	63
Figure 4-21. Results for the wet, median, and dry models for ecosurpluses based on an RCP 4.5 scenario. Results are for Wading River USGS Gage (01109000) comparing baseline (2000-2020) to future climate scenarios (2079-2099).	64
Figure 4-22. Results for the wet, median, and dry models for ecosurpluses based on an RCP 8.5 scenario. Results are for the Wading River USGS Gage (01109000) comparing baseline (2000-2020) to future climate scenarios (2079-2099).	65
Figure 4-23. Percent change in annual average precipitation and temperature from baseline conditions for the selected models presented in Table 4-6.	67
Figure 4-24. SCM opportunities for Wading River (top left), Upper Hodges Brook (top right), Pilot Tributary (bottom left), and Lower Hodges Brook (bottom right).	72
Figure 4-25. Opti-Tool baseline verification for Pilot Tributary (top), Lower Hodges (middle), and Upper Hodges (bottom) sub-watersheds. Sub-watersheds ordered from top to bottom as least developed (Pilot Tributary) to most Developed (Upper Hodges).	77
Figure 4-26. Opti-Tool FDC cost-effectiveness curves for Pilot Tributary (top), Lower Hodges (middle), and Upper Hodges (bottom) sub-watersheds. The maximum solutions are highlighted. Sub-watersheds ordered from top to bottom as least developed (Pilot Tributary) to most Developed (Upper Hodges).	83
Figure 4-27. Opti-Tool FDC cost-effectiveness curves for Pilot Tributary (top), Lower Hodges (middle), and Upper Hodges (bottom) sub-watersheds. Highly cost-effective solutions, located around the knee of the curves, are highlighted. Sub-watersheds ordered from top to bottom as least developed (Pilot Tributary) to most Developed (Upper Hodges).	84
Figure 4-28. Opti-Tool FDCs for Pilot Tributary (top), Lower Hodges (middle), and Upper Hodges (bottom) sub-watersheds. Results are based on the solutions highlighted in Figure 4-27. Sub-watersheds ordered from top to bottom as least developed (Pilot Tributary) to most Developed (Upper Hodges).	85
Figure 4-29. Annotated flow duration curve. Adapted from U.S. EPA, 2007.	86
Figure 4-30. Comparison of FDCs resulting from optimized SCM implementation under baseline conditions and those same SCMs under climate change conditions for Upper Hodges sub-watershed. Graphs highlight separate sections of the same FDCs. The top graph shows the high flows and the bottom graph highlight the low flows.	92
Figure 4-31. Evaluation of the response of optimized SCM implementation to climate change scenarios (RCP 4.5 Ecodeficit Models for Upper Hodges sub-watershed.	93
Figure 4-32. Evaluation of the response of optimized SCM implementation to climate change scenarios (RCP 4.5 Ecosurplus Models for Upper Hodges sub-watershed.	94
Figure 4-33. Evaluation of the response of optimized SCM implementation to climate change scenarios (RCP 8.5 Ecodeficit Models for Upper Hodges sub-watershed.	95
Figure 4-34. Evaluation of the response of optimized SCM implementation to climate change scenarios (RCP 8.5 Ecosurplus Models for Upper Hodges sub-watershed.	96
Figure 4-35. Evaluation of the impact of optimized BMP implementation to bankfull discharge for the Upper Hodges watershed.	97

Figure 4-36. From (Hawley and Vietz, 2016). Bed-sediment mobilization along a sensitivity gradient. Q_c = critical discharge for incipient motion, Q_2 = 2-y peak discharge, $Q_{c2} = Q_c$ standardized by Q_2 , Q_{c2} = mean threshold values for each particle size. 98

List of Tables

Table 2-1. Summary of NCDC gauge location metadata.....	7
Table 2-2. Precipitation analysis for T.F. Green Airport. Red to blue shading indicates years below and above median values, respectively with darker shading representing larger magnitudes	7
Table 2-3. Precipitation summary for T.F. Green Airport	9
Table 2-4. IHA parameter comparison for observed historical and current conditions.....	14
Table 3-1. Final HRU categories.....	27
Table 3-2. Mapped Impervious Area (MIA) and Effective Impervious Area (EIA) distribution in Wading River watershed.....	31
Table 3-3. HSPF and LSPC Model area comparison for Wading River watershed	31
Table 3-4. Summary of climate data input requirements by LSPC module	34
Table 3-5. Calibration and Validation Simulation Periods for the LSPC Wading River Model.....	34
Table 3-6. Summary of annual average pollutant loading rate calibrated to HRU type for the study area.	36
Table 4-1. Land Use Scenarios simulated using Upper Hodges Brook sub-watershed	45
Table 4-2. Comparison of average 3-day minimum and maximum flows for baseline and land use scenarios	53
Table 4-3. Summary of average monthly flows and percent differences for land use scenarios.....	53
Table 4-4. Carbon benefits and associated activities, indicators, and calculation methods (Brill et.al., 2021)	57
Table 4-5. InVEST carbon model results for three pilot sub-watersheds	58
Table 4-6. Selected models from ensemble results for future climate projections (2079-2099)	59
Table 4-7. Summary of ecosurpluses and ecodeficits (millions of gallons per year) for RCP 4.5 and 8.5 scenarios	66
Table 4-8. Percent change in 3-day minimum and maximum flows for RCP 4.5 and 8.5 scenarios compared to baseline simulation	67
Table 4-9. Dry days and days with precipitation for the selected future climate scenarios compared to the historical, observed conditions.....	68
Table 4-10. Percent change for average annual and monthly precipitation for future climate scenarios compared to the historical, observed conditions.....	68
Table 4-11. Percent change for average maximum consecutive dry days for the future climate scenarios compared to the historical, observed conditions.....	69
Table 4-12. Percent change in average maximum daily temperature for the selected future climate scenarios compared to the historical, observed conditions.....	69
Table 4-13. Percent change in average minimum daily temperature for the selected future climate scenarios compared to the historical, observed conditions.....	69
Table 4-14. Percent change in average daily temperature for the selected future climate scenarios compared to the historical, observed conditions	70
Table 4-15. Site suitability criteria for stormwater management categories	71
Table 4-16. SCM Design Specifications.....	73
Table 4-17. Precipitation analysis for the baseline model period	76
Table 4-18. Impervious area treated by SCMs (impervious cover disconnection) in the three study sub-watersheds.....	78
Table 4-19. Potential SCM opportunity areas (maximum modeled footprints) in the three study sub-watersheds.....	80
Table 4-20. Average daily flow by flow regime (gallons per day) for Pilot Tributary sub-watershed. Results are based on the FDCs shown in Figure 4-28.....	86
Table 4-21. Average daily flow by flow regime (gallons per day) for Lower Hodges sub-watershed. Results are based on the FDCs shown in Figure 4-28.....	87
Table 4-22. Average daily flow by flow regime (gallons per day) for Upper Hodges sub-watershed. Results are based on the FDCs shown in Figure 4-28.....	87
Table 4-23. Pollutant load reductions (%) from the surface runoff for the best solutions (highlighted in Figure 4-27) for the study sub-watersheds.	87

Table 4-24. Optimized SCM opportunities for the maximum solution (highlighted in Figure 4-26) for the Upper Hodges sub-watershed. 88

Table 4-25. Optimized SCM opportunities for the best solutions (highlighted in Figure 4-27) for the Upper Hodges sub-watershed..... 89

1. INTRODUCTION

1.1 Background

Freshwater ecosystems are affected by all characteristics of a long-term flow regime (Walsh et al., 2015). Changes in land cover resulting in the removal of vegetation (forests) and increased impervious cover tend to be a primary driver behind declining hydrologic and water quality conditions. Stormwater management is often focused on matching pre-development peak flows for a small set of design storms, meeting a limited set of intended control conditions for flow, water quality, and groundwater recharge. Less attention is paid to the cumulative geomorphic and ecological degradation resulting from changes in the frequency, magnitude, and duration of disturbances over the entire flow regime. For example, while existing detention standards attenuate the peak flow of a large storm, they provide little to no attenuation for lesser flow rates. Increased runoff volumes from the impervious cover that is detained and released can result in a prolonged period of elevated streamflow that can impact the ecosystem of the receiving waters (Reichold et al., 2010).

Changes to the frequency and magnitude of discharges, as well as associated impacts to water quality, stream geomorphology, and habitat conditions can be measured by changes in watershed hydrology. Flow duration curves (FDCs) are cumulative frequency curves that provide a valuable indication of hydrological conditions by showing the percent of the time when specific discharges were equaled or exceeded during a given period (Searcy, 1959). The applications of FDCs have included their use in quantifying the effect of channel and floodplain processes on channel characteristics (Naito and Parker, 2019) and their ability to inform predictions of stream erosion (Fan and Li, 2004). Reichold et al., (2010) developed an optimization framework to identify land use patterns that minimize impacts to FDCs. A team that included Paradigm Environmental applied the EPA System for Urban Stormwater Treatment and Analysis Integration (SUSTAIN) FDC optimization approach to watershed-scale stormwater planning efforts in the Puget Sound region (Northwest Hydraulic Consultants, 2017). The Wading River watershed and its sub-watersheds, which are in the larger Taunton River basin in southeastern Massachusetts provided an excellent opportunity as a study site for which to further develop the application of FDCs. The area has long-term streamflow and meteorological monitoring records, a mix of land development patterns, and is within the modeling domain of an existing and calibrated HSPF model (Barbaro & Sorenson, 2013).

1.2 Project Objectives

The purpose of this project is to develop and present a hydrological modeling framework that can be used to quantify the changes to watershed functions associated with landscape conversion to impervious cover and the mitigating benefits of distributed Stormwater Control Measures (SCMs). Phase 1 of the project provides the foundation for which Phase 2 of the project can be established; Phase 2 includes consideration of not only conventional SCMs but Conservation Development (CD) practices as well. Watershed management that is informed by CD practices allows for sustainable development while protecting an area's natural resources and functions. Phase 1 of this project, which includes this final report and associated [technical memos](#) provides tools and metrics to assess a full range of hydrological impacts due to watershed development and increased impervious cover (IC) conversion.

One of the objectives of the overall project, including Phase 2, is to develop relationships between FDCs and watershed development that can be applied to other watersheds with similar physical characteristics and to present these relationships in clear and simple terms. The results are intended to inform the development of both restoration plans and protective management strategies that address the impact of future growth and increase climate resiliency. This will help make the connection between the science of urban stream ecology and management strategies that are accessible to watershed managers, engineers, and developers. The modeling approach in Phase 2 is expected to investigate and quantify the benefits of conserving existing

resources, such as forested areas and wetlands, as well as implementing next-generation nD/rD practices that could be incentivized or required through local regulations. The work is also expected to highlight the challenges, costs, and limitations of traditional stormwater management approaches that do not account for the multiple ecological and hydrologic functions that are often substantially altered in developed watersheds. The FDCs and optimization results can highlight cost-effective solutions that will help support decision-making as well as public outreach and education efforts. Overall, the project, including Phase 2, will provide a body of technical documentation that can support communities, especially in the Southeast New England Program (SNEP) region who may consider the adoption of protective ordinances that build resiliency and promote the restoration/protection of local and regional water resources.

To achieve project objectives, a weight-of-evidence approach used several different sources of data, including historical observations, previous studies, and modeling. Available data, including historical observations, were first used to evaluate the existing conditions of the Wading River (Section 2). This included generating historical and current FDCs using observed flow records. An EPA Loading Simulation Program – C++ (LSPC) model was then configured and calibrated for the Wading River watershed (Section 3), a tributary to the Taunton River. The most recent twenty-year period, 2000-2020 was used for baseline conditions. Following calibration, the LSPC model was then used to investigate how land use and climate change conditions impact FDCs (Section 4). The analysis included unit-area modeling at the Hydrologic Response Unit (HRU) level to elucidate differences in the water balance for various land uses and soil types. The FDCs of three sub-watersheds with varying amounts of impervious cover were assessed. Further investigation on the impact of imperviousness was conducted by varying the land use of one of the three study sub-watersheds over a range of development, from pre-development/forested conditions to fully connected impervious surfaces. Future climate conditions were simulated in the Wading River watershed and the impact to flow metrics and water balances were quantified. The impact of land use change on carbon sequestration and heat flux was also assessed.

While LSPC was used to establish baseline conditions and quantify the impacts of land use and climate change, the EPA Region 1's Stormwater Management Optimization Tool (Opti-Tool) was used to explicitly investigate the ability of stormwater management strategies to mitigate these impacts. A key contribution of this project was expanding functionality to the Opti-Tool, which included adding a groundwater/aquifer component and an FDC evaluation factor for cost-benefit optimization of strategic locations and sizes of SCMs. The expanded functionality enhances the simulation of SCMs and allows optimization simulations to identify optimal and most cost-effective management strategies to address impacts associated with FDCs and associated critical flow regimes. The Opti-Tool FDC evaluation factor can be used in future work (Phase 2 of the project) to investigate the impacts of CD practices on watershed hydrology, stream health, and overall pollutant load export.

2. WADING RIVER WATERSHED – AVAILABLE DATA AND EXISTING CONDITIONS

This section presents a summary review of the available data and existing conditions of the Taunton River Basin and the Wading River watershed (Figure 2-1). A more detailed discussion can be found in the [Task 5 Memo](#). Additionally, Appendix A of this final report contains several associated maps and tables relevant to the discussion below. The available hydrological, meteorological, and geospatial data for modeling the Wading River watershed and the larger Taunton basin are summarized and analyzed (Section 2.1). This includes identifying trends in streamflow, precipitation, and land use/land cover. Candidate study sub-watersheds, located within the Wading River watershed and representing a range of imperviousness, are identified for the development of FDCs. Past, current, and future climate data, including a description of the downscaling method used to derive the hourly boundary condition time series needed for continuous hydrological modeling, are presented in Section 2.2.

2.1 Data/Information Assessment

2.1.1 Landscape Data

Several land use/land cover layers were downloaded and assessed. Land use data sources included the Multi-Resolution Land Characteristics (MRLC) Consortium, National Atmospheric and Oceanic Administration (NOAA), the United States Department of Agriculture National Agricultural Statistics Service (USDA NASS), and the Massachusetts Bureau of Geographic Information (MassGIS). Elevation data were acquired from the United States Geological Survey 3D Elevation Program (USGS 3DEP), surficial materials data were acquired from the USGS Scientific Investigations Map 3402 – Surficial Materials of Massachusetts (USGS SIM 3402) and MassGIS. Soil data were acquired from the Natural Resources Conservation Service (USDA NRCS). Historical land use was available for the Taunton basin for 1971, 1985, 1999, and 2005. The most recent land use data available was for 2016. However, this data did not conform to the land use classification scheme used in the historical datasets. This data also included land cover classifications that identify impervious surfaces. Additional impervious surface data were available for the years 2001, 2006, and 2011.

2.1.2 Dams and Reservoirs

There are several small dams within the Wading River watershed. Dam locations were acquired from the Dams_Pt shapefile available from MassGIS. Many of these were built in the 17th and 18th centuries to support industry in the area (Norton Conservation Commission, 2010) and appear to be generally small structures (dam locations can be found in Appendix A). These dams were not explicitly represented in the LSPC model, the reaches in the Wading River were simulated using an open-channel flow equation (Section 3.3.1.5). The largest impoundment in the Wading River watershed is the Lake Mirimichi dam. A 1730 map shows a pond existing in the current location of Lake Mirimichi. Between 1925 and 1927, the larger dam was built to supply drinking water (Friends of Lake Mirimichi, 2020). During this time, a USGS gage (Wading River 01109000) was also installed downstream.

2.1.3 Water Use

Water use information, including public water supply (PWS) and non-PWS data, were obtained from the eASR and eARF databases, respectively, provided by Massachusetts DCR. The facilities located within the Wading River watershed are presented in Appendix A. The only major surface water withdrawal is from Blakes Pond, for which consumptive use data were available between 2009 and 2019. Agriculture land use comprises a relatively small percentage of the watershed (See Appendix A) and no data were available concerning agricultural water use or hydrological modifications such as tile drainage and ditch systems.

However, these may play an important role in the FDCs of more agriculturally dominated watersheds and should be considered in these areas.

2.1.4 Meteorology Data

One meteorology gauge was located within the Taunton basin, another meteorology gauge was located at T.F. Green International Airport in Providence Rhode Island, approximately 15 miles southwest of the watershed (Figure 2-2). Both daily and hourly precipitation data were available as part of historical climate data from the NCDC Global Historic Climate Network (GHNC) and Local Climate Data (LCD) gauge located at the Taunton Municipal Airport (WBAN 54777). A coincident set of records was available from the Providence, RI Airport (WBAN 14765) and was used for comparison purposes and for filling gaps in the observed time series at the Taunton Municipal Airport location. While these two locations are only 25 miles apart, they do have different orientations to the coast which may result in some differences in observed climate patterns slightly different. The Providence Airport gauge sits on the western edge of the Providence River approximately three miles from the mouth where it meets Narragansett Bay while the Taunton Municipal Airport gauge sits approximately 20 miles inland northwest of Narragansett Bay and approximately 20 miles west of Cape Cod. Table 2-1 summarizes station metadata for these gauges.

The records for the Taunton Municipal Airport and a second Taunton gauge (WBAN 98367) were ultimately combined during data processing as their periods of record were complimentary with only a short duration of overlap during 2005 (Table 2-1). Between the combined records for Taunton and the Providence Airport, a common 73-year period beginning January 1, 1948, was available. Limited data gaps (missing records) were found during the data review for the most recent 40-year period (1981-2020) at both the Providence and combined Taunton gauges, with intervals flagged as suspect accounting for less than 1% of the long-term time series. More significant data gaps during the pre-1981 period of record were filled at the respective gauge using the normal-ratio method with data from the other gauge. Table 2-2 presents annual precipitation totals for the entire period of record for the T.F. Green Airport, comparing each year against long-term precipitation trends. Table 2-3 presents a summary of rainfall trends from the most recent 21-year period (2000-2020) compared to the long-term 73-year period (1948-2020) comparing the total annual average precipitation and distribution of storm events by depth.

2.1.4.1 Temperature

Daily and hourly air temperature data were available as part of the same data sets (GHNC and LCD) used for obtaining the precipitation data. The hourly air temperature data were assessed for data gaps by reviewing the quality flags provided with the raw data and reviewing summary statistics. Data quality was assessed using NCDC-supplied flagging like the precipitation data presented in the previous section. Values were filled forward to patch short-term data gaps. One outlier maximum temperature value of 148 degrees Fahrenheit was found in the Providence Airport gauge (72506814765) daily records on January 26, 1962, but was not present in the hourly records. This outlier was replaced by the maximum temperature of 43 degrees Fahrenheit found in the corresponding hourly data set. Daily maximum and minimum temperatures were derived from hourly temperature data by searching the 24 hours between midnight and midnight of each day for the highest and lowest temperatures. Missing values were filled with the maximum/minimum daily temperature found in the corresponding hourly data sets, and any remaining missing values without coincident hourly data were filled by linear interpolation of the time series. Large gaps were filled using the more complete daily records which were disaggregated using a typical 24-hour diurnal based on the hourly observations.

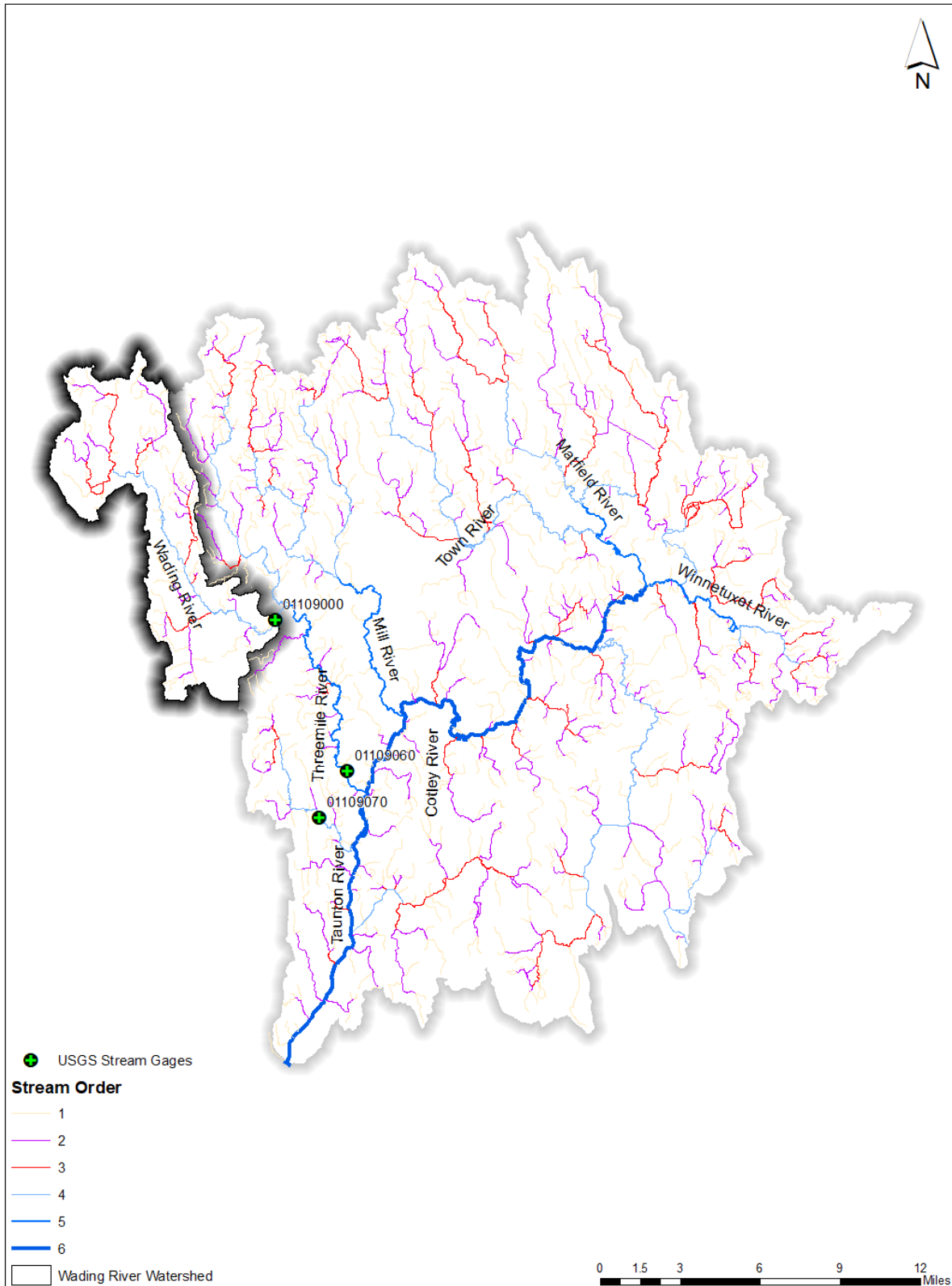


Figure 2-1. Wading River watershed location within Taunton basin.

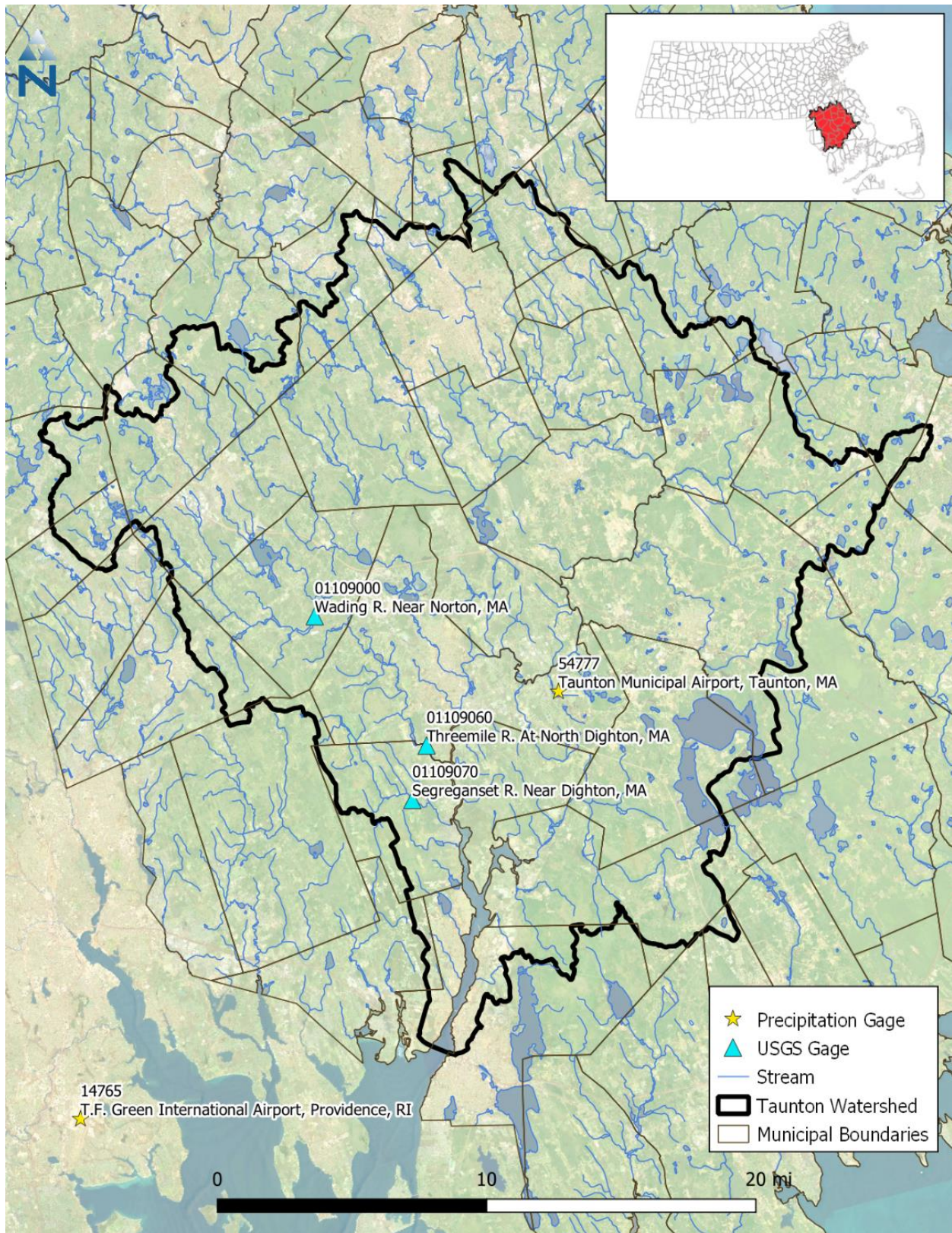


Figure 2-2. Meteorology and streamflow gage locations.

Table 2-1. Summary of NCDC gauge location metadata

Station Name	Station ID	Data Period	Latitude	Longitude	Elevation (ft.)
Providence, RI	14765	1942-2021	41.7225	-71.4325	16.8
Taunton Municipal Airport, MA	54777	2005-2021	41.87556	-71.0211	13.1
Taunton, MA	98367	1942-2005	41.90028	-71.0658	Not Available

Table 2-2. Precipitation analysis for T.F. Green Airport. Red to blue shading indicates years below and above median values, respectively with darker shading representing larger magnitudes

T.F. Green Airport - Providence, RI								
Year	Rainfall (in)	Percentile	Difference (in.)		Number of Rain Days per Year:			
		10th %	Last 20 Years	All Years	≥ 0.1in	≥ 0.5in	≥ 1.0in	≥ 1.5in
		Average						
		90th %						
1949	35.65	4%	-10.49	-13.16	72	26	4	2
1950	39.51	18%	-6.63	-9.30	81	25	8	3
1951	45.6	51%	-0.54	-3.21	79	34	11	5
1952	41.54	32%	-4.60	-7.27	75	25	12	5
1953	57.01	90%	10.87	8.20	76	39	21	10
1954	51.53	77%	5.39	2.72	82	34	13	8
1955	51.71	79%	5.57	2.90	74	29	13	10
1956	42.67	37%	-3.47	-6.14	84	33	7	1
1957	30.08	3%	-16.06	-18.73	65	19	6	2
1958	51.54	78%	5.40	2.73	89	33	16	5
1959	43.14	40%	-3.00	-5.67	80	29	11	4
1960	40.08	21%	-6.06	-8.73	64	28	13	5
1961	49.56	71%	3.42	0.75	75	31	13	7
1962	50.33	74%	4.19	1.52	66	33	14	8
1963	39.5	16%	-6.64	-9.31	71	26	13	3
1964	38.41	11%	-7.73	-10.40	69	27	11	3
1965	25.44	1%	-20.70	-23.37	59	19	3	1
1966	38.68	15%	-7.46	-10.13	64	23	13	6
1967	46.5	58%	0.36	-2.31	83	32	10	5
1968	41.36	30%	-4.78	-7.45	71	24	12	5
1969	44.59	41%	-1.55	-4.22	72	28	14	7
1970	45.42	48%	-0.72	-3.39	68	29	12	7
1971	38.42	12%	-7.72	-10.39	71	25	10	5
1972	65.06	97%	18.92	16.25	95	42	21	11
1973	48.24	64%	2.10	-0.57	73	34	12	6
1974	40.66	25%	-5.48	-8.15	76	27	10	5
1975	50.83	75%	4.69	2.02	79	33	19	7
1976	46.32	56%	0.18	-2.49	71	26	11	5

T.F. Green Airport - Providence, RI								
Year	Rainfall (in)	Percentile	Difference (in.)		Number of Rain Days per Year:			
		10th %	Last 20 Years	All Years	≥ 0.1in	≥ 0.5in	≥ 1.0in	≥1.5in
		Average						
		90th %						
1977	48.84	67%	2.70	0.03	84	30	14	8
1978	47.01	60%	0.87	-1.80	72	32	14	8
1979	58.19	95%	12.05	9.38	88	32	17	9
1980	36.11	5%	-10.03	-12.70	67	20	10	4
1981	36.37	7%	-9.77	-12.44	81	25	7	4
1982	49.26	70%	3.12	0.45	77	29	13	9
1983	67.52	99%	21.38	18.71	88	46	20	11
1984	48.74	66%	2.60	-0.07	84	33	10	3
1985	40.42	23%	-5.72	-8.39	74	25	8	6
1986	46.13	55%	-0.01	-2.68	77	31	12	5
1987	40.67	26%	-5.47	-8.14	77	28	8	4
1988	38.37	10%	-7.77	-10.44	66	23	11	6
1989	56.06	88%	9.92	7.25	89	42	19	6
1990	44.78	45%	-1.36	-4.03	83	29	13	3
1991	45.69	52%	-0.45	-3.12	81	32	10	6
1992	47.48	62%	1.34	-1.33	78	31	12	6
1993	42.16	33%	-3.98	-6.65	77	30	9	4
1994	44.69	42%	-1.45	-4.12	73	31	14	7
1995	38.58	14%	-7.56	-10.23	69	28	8	2
1996	48.06	63%	1.92	-0.75	84	27	12	5
1997	37.97	8%	-8.17	-10.84	74	29	9	1
1998	52.7	82%	6.56	3.89	86	33	14	8
1999	42.26	34%	-3.88	-6.55	68	26	12	7
2000	46	53%	-0.14	-2.81	74	29	12	6
2001	40.19	22%	-5.95	-8.62	61	26	11	9
2002	42.34	36%	-3.80	-6.47	76	33	11	1
2003	50.27	73%	4.13	1.46	91	34	18	5
2004	45.33	47%	-0.81	-3.48	76	32	12	7
2005	57.92	93%	11.78	9.11	86	38	14	9
2006	54.3	85%	8.16	5.49	86	32	13	6
2007	42.81	38%	-3.33	-6.00	70	26	13	7
2008	57.12	92%	10.98	8.31	88	32	15	10
2009	54.85	86%	8.71	6.04	85	41	18	6
2010	53.54	84%	7.40	4.73	66	31	15	6
2011	56.72	89%	10.58	7.91	92	39	17	11
2012	41.19	29%	-4.95	-7.62	75	29	10	6
2013	45.46	49%	-0.68	-3.35	75	30	10	4
2014	46.94	59%	0.80	-1.87	73	26	16	7

T.F. Green Airport - Providence, RI								
Year	Rainfall (in)	Percentile	Difference (in.)		Number of Rain Days per Year:			
		10th %	Last 20 Years	All Years	≥ 0.1in	≥ 0.5in	≥ 1.0in	≥1.5in
		Average						
		90th %						
2015	40.83	27%	-5.31	-7.98	75	26	9	4
2016	40	19%	-6.14	-8.81	77	30	8	3
2017	49	68%	2.86	0.19	82	35	16	6
2018	63.49	96%	17.35	14.68	91	46	22	8
2019	51.97	81%	5.83	3.16	101	34	13	4
2020	44.71	44%	-1.43	-4.10	74	25	10	5

Table 2-3. Precipitation summary for T.F. Green Airport

T.F. Green Airport - Providence, RI					
Period	Average Rainfall (in)	Average Number of Rain Days per Year			
		≥ 0.1in	≥ 0.5in	≥ 1.0in	≥1.5in
(1949-2020)	46.14	77	30	12	6
(2000-2020)	48.81	80	32	13	6

2.1.4.2 Other Climate Data

Other climate data parameters are required to run both hydrology and snow simulation modules in LSPC which include potential evapotranspiration, dew point temperature, wind speed shortwave solar radiation, and cloud cover. Observed values were obtained for these parameters from both the GHCN and LCD data sets used to compile precipitation the temperature data. Some records were available for both the Taunton and Providence airports but monitoring of these secondary parameters is generally more limited so records at the two gauges were combined to build a complete data set covering the full period of record. Short data gaps were filled using fill-forward techniques while longer data gaps were filled with the long-term daily average by month calculated from the available data. Observed potential evapotranspiration was not available and was therefore calculated from other parameters using the Penman-Monteith method available in the BASINS WDM Utility (EPA, 2020). Plots of potential evapotranspiration, dew point temperature, wind speed shortwave solar radiation, and cloud cover used for review and quality assurance are presented in Appendix A.

2.1.5 Streamflow Data

Three United States Geological Survey (USGS) streamflow gages were located within the Taunton basin (Figure 2-2). Based on its location and the period of record (1925-present) the Wading River gage was identified as well suited for this study. The Wading River is regulated to some extent by Lake Mirimichi and other lakes and reservoirs upstream. Upstream of the USGS gage is a diversion for municipal supply for Attleboro, MA, as well as small diversions to and from the basin for other municipal supplies. The gage drains a 43.3 square mile area and has a very high (98.4%) percentage of complete data.

Figure 2-3 presents the flow duration curve (FDC) for the Wading River for the entire period of record (1925-2020). Figure 2-4 presents FDCs for each decade of data available. Each of the nine FDCs represents all the flow data recorded for the associated decade. Figure 2-5 highlights the right-hand side of Figure 2-4, focusing on the low flows. While consistent trends are difficult to assess from the graph, data from the 1990s and the

2010s show a portion of low flows becoming even lower. The figure may also suggest increasing variability in observed flows. Figure 2-6 highlights the left-hand side of Figure 2-4, focusing on the high flows. Like low flows, trends in high flow trends are difficult to assess from the graph, although it appears that high flows have somewhat increased over the past several decades. The [Task 5 Memo](#) presents an analysis of meteorological and flows conditions that attempt to control for climate variability and isolate the impact of watershed development on the changes in FDCs over time. The results suggest that watershed development may have played a role in changing the Wading River FDC, although the results are complicated because of the confounding influence of climate as well as the prevalence of diversions and small dams in parts of the watershed.

To further analyze characteristics of the FDC over time, several metrics were calculated using the Wading River gage data and the Indicators of Hydrologic Alteration (IHA) parameters. Several of these results are presented in Appendix A. The IHA parameters are a suite of 33 parameters that provide an ecologically meaningful assessment of flow data to provide indicators of anthropogenic impacts to riverine systems (Richter et al., 1996; Swanson, 2002). The IHA parameters are categorized into five groups of metrics that provide information on the magnitude and timing (Group 1), magnitude and duration (Group 2), timing (Group 3), frequency and duration (Group 4), and the rate of change and frequency (Group 5) of flows. Additional discussion can be found in the [Task 5 Memo](#). Figure 2-7 presents an assessment of ecosurplus and ecodeficit. Ecosurpluses and ecodeficits are calculated from flow duration curves, providing a simplified assessment of hydrological impacts compared to IHA parameters. An ecosurplus and an ecodeficit represent the overall gain or loss, respectively, in streamflow of the period of analysis (Vogel et al., 2007). Figure 2-7 compares FDCs for the 2001-2019 period against the 1972-1990 period, which was found to have relatively similar climate conditions ([Task 5 Memo](#)). Relative to the 1972-1990 period, the current conditions have an ecosurplus of 5.8 cfs/day and an ecodeficit of 3.4 cfs/day. Table 2-4 presents a summary of IHA parameters for the two periods. A limitation of the analysis is that it does not currently account for natural variability and whether differences are statistically significant. Methods such as the Range of Variability Approach (RVA) may help account for variability and have been used to identify changes to IHA parameters due to dam construction (Richter et al., 1997). However, for this comparison, simple % differences are used to assess the impact that development may have had on the IHA parameters.

2.1.6 Existing Models

The FDC 1 Project builds upon previous modeling work performed in the Taunton basin (Barbaro and Sorenson, 2013b). The previously developed HSPF model subbasins for the Wading River are presented in Figure 2-8. Additional details for these areas are presented in Appendix A. The existing HSPF model accounted for surface and groundwater withdrawals, as well as wastewater return-flows, however, these were calculated only for select sub-watersheds and did not include the Wading River. A HEC-RAS model was also developed for the Wading River watershed. As of the time of this writing, HEC-RAS models for tributaries to the Wading River, including Hodges Brook, appear to have been developed but are not publicly available. HEC-RAS models can help facilitate future analyses of FDCs by quantifying changes to flooding, stream power, and shear stress that may result from changes to impervious and next-generation stormwater approaches.

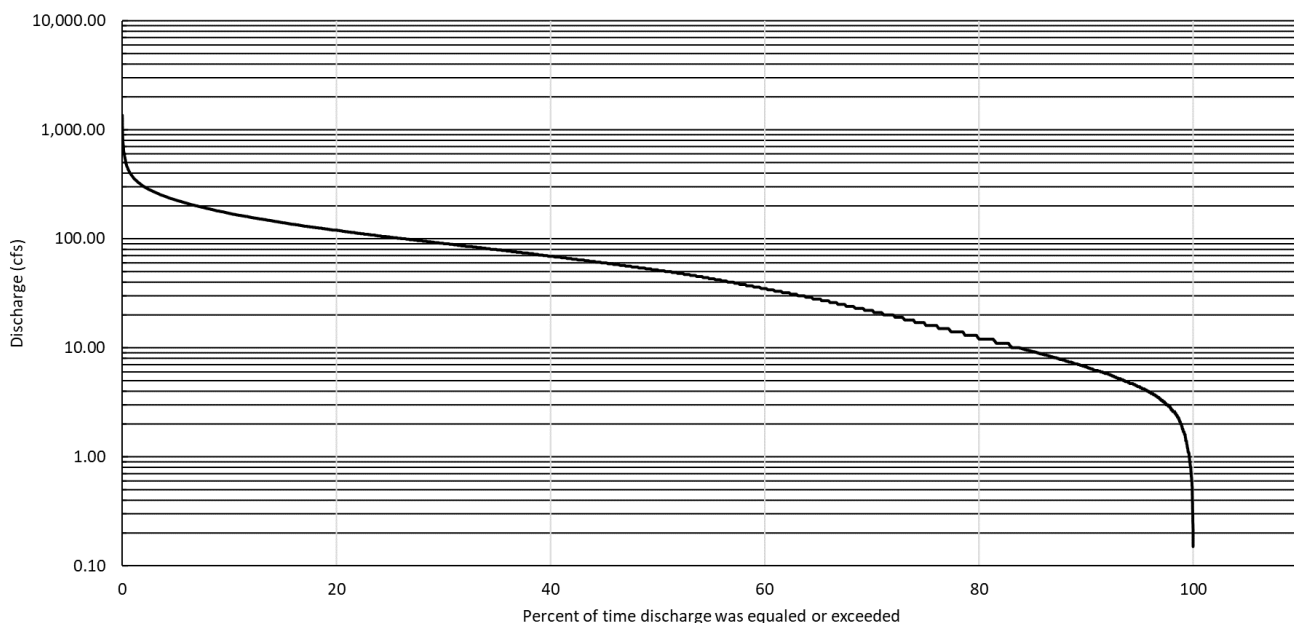


Figure 2-3. Flow duration curve 1925-2020. Wading River.

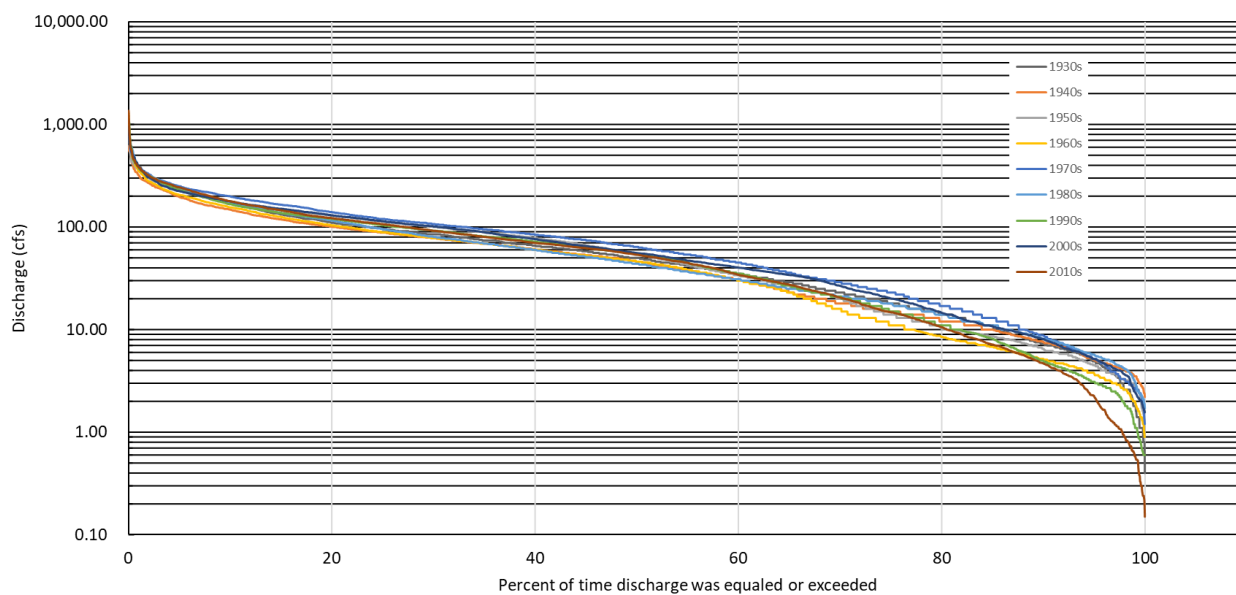


Figure 2-4. Flow duration curves by decade. Wading River.

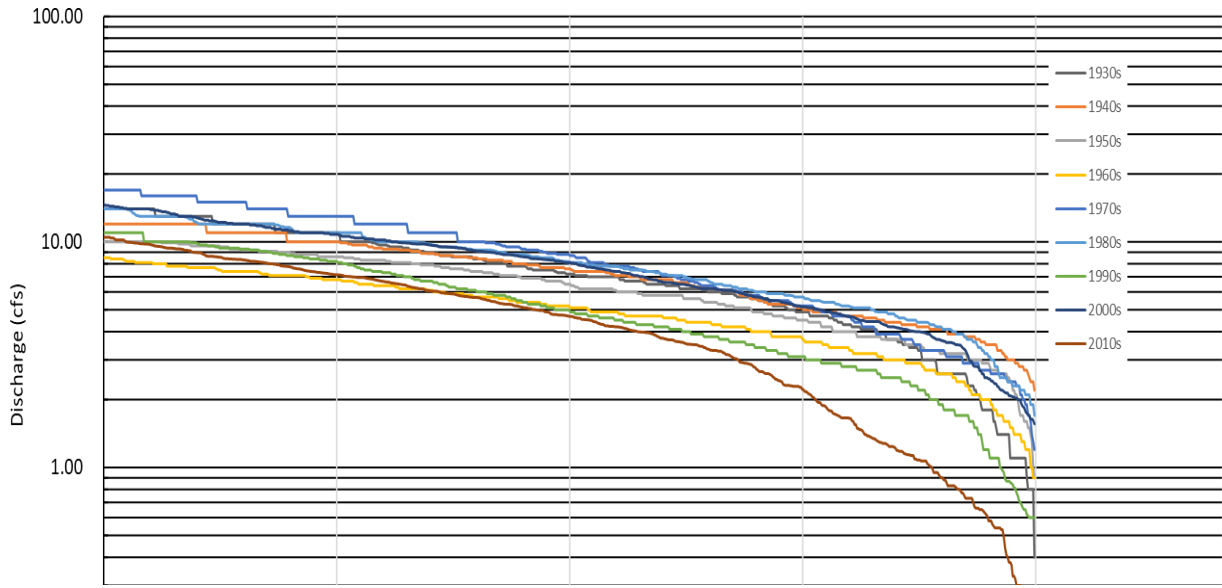


Figure 2-5. Enlarged section of Figure 2-4 showing the low flow portion of flow duration curves by decade. Wading River.

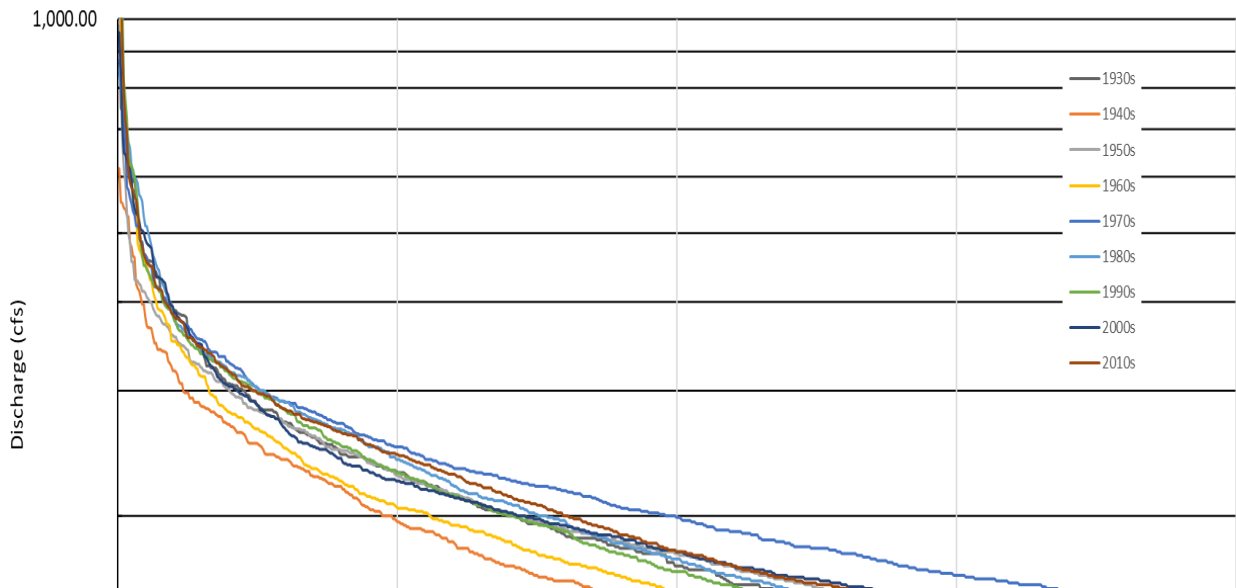


Figure 2-6. Enlarged section of Figure 2-4 showing the high flow portion of flow duration curves by decade. Wading River.

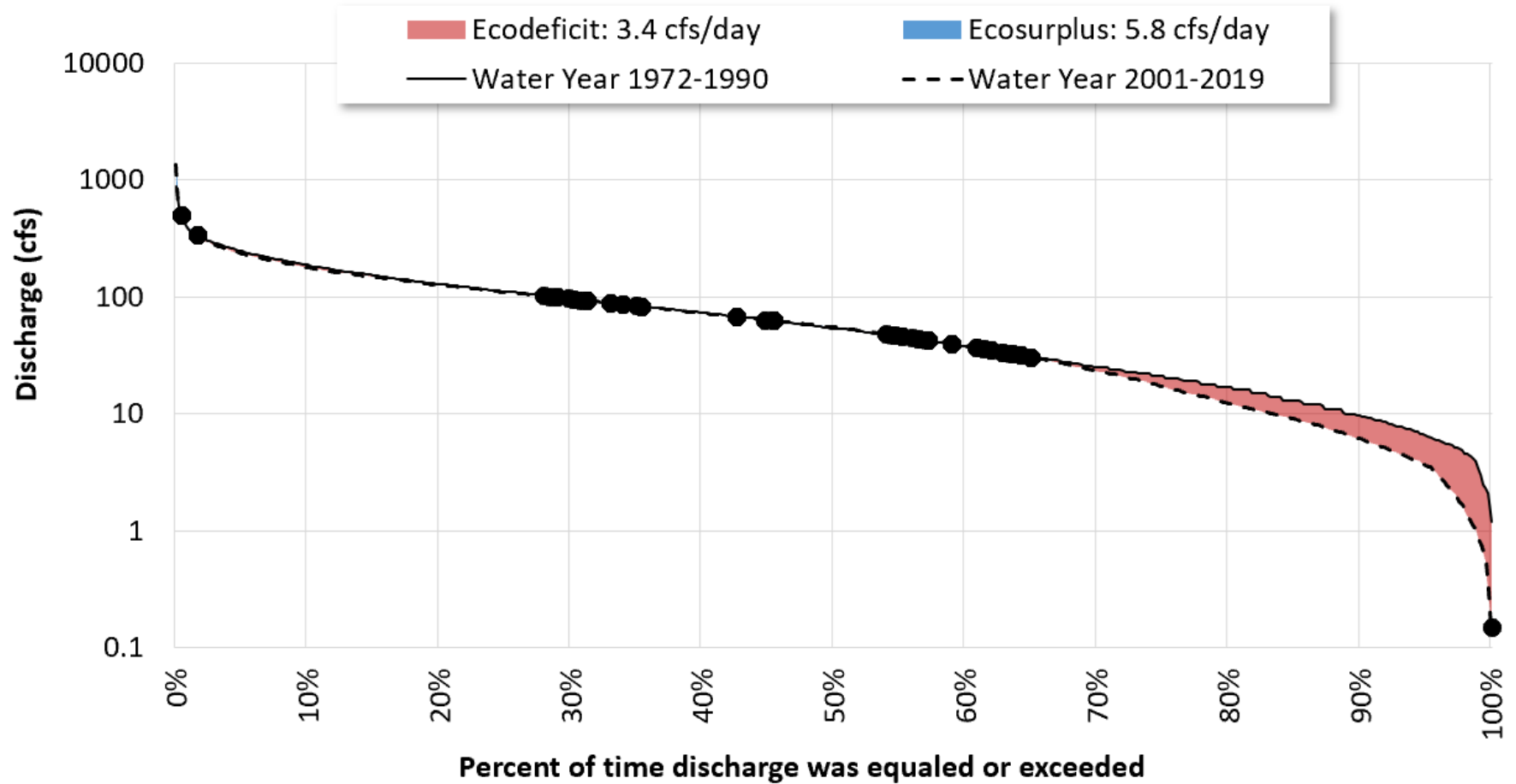


Figure 2-7. Ecosurplus and ecodeficit for the Wading River for 2001-2019 vs. 1972-1990. Black dots represent inflection points where the two curves change between surplus and a deficit.

Table 2-4. IHA parameter comparison for observed historical and current conditions

	1972-1990	2001-2019	% difference
Group 1. Magnitude and timing	Average (cfs)		
January	116.19	102.66	-11.65%
February	117.82	104.57	-11.25%
March	143.77	151.01	5.04%
April	140.82	147.19	4.52%
May	89.20	82.37	-7.66%
June	66.84	69.24	3.58%
July	23.91	28.51	19.22%
August	31.25	17.77	-43.15%
September	23.54	20.07	-14.77%
October	44.21	45.98	4.02%
November	75.90	74.35	-2.05%
December	107.81	105.47	-2.17%
Group 2. Magnitude and duration of annual extremes	Average (cfs)		% difference
1 day minimum	5.20	3.44	-34.0%
1 day maximum	501.32	544.25	8.6%
3 day minimum	5.98	3.54	-40.8%
3 day maximum	431.72	453.63	5.1%
7 day minimum	6.92	3.85	-44.4%
7 day maximum	351.07	361.91	3.1%
30 day minimum	11.32	7.48	-33.9%
30 day maximum	222.61	233.40	4.8%
90 day minimum	18.73	13.82	-26.2%
90 day maximum	159.32	156.19	-2.0%
Group 3. Timing of annual extremes	Average Julian Day		% difference
Julian date of annual minimum	230	249	8.30%
Julian date of annual maximum	511	529	3.51%
Group 4. Frequency and duration of high (90th percentile) and low (10th percentile) pulses	Average Count/ Average # Days		% difference
Low pulse count	453	771	70.20%
Low pulse duration (days)	7.95	12.44	56.47%
High pulse count	825	756	-8.36%
High Pulse duration (days)	6.11	5.77	-5.57%
Group 5 Rate and frequency of change	Average Count/ Average cfs		% difference
Fall rate (cfs)	4569	4826	5.62%
Fall count	22.58	22.69	0.48%
Rise rate(cfs)	1956	1982	1.33%
Rise count	4569	4826	5.62%

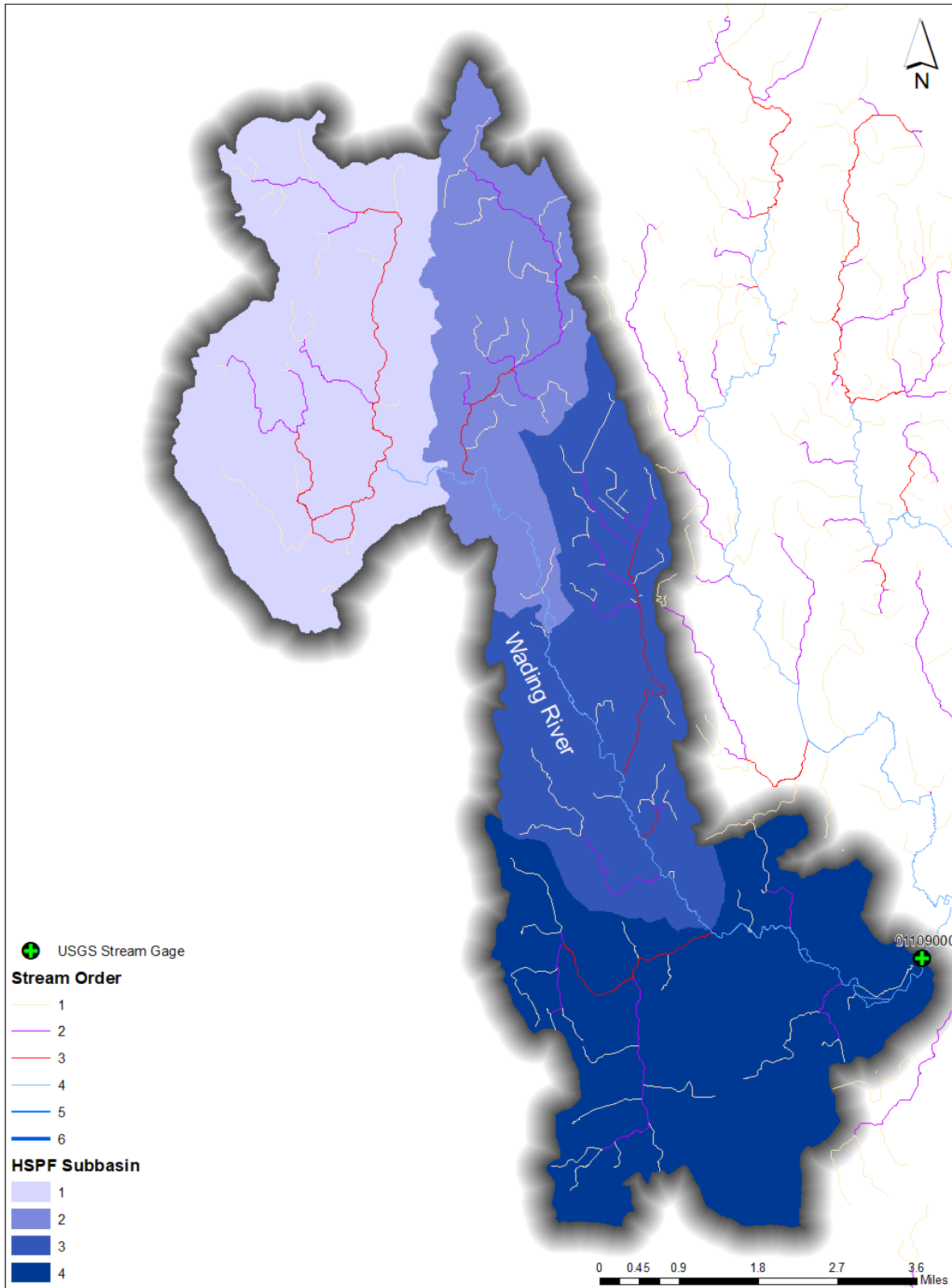


Figure 2-8. HSPF subbasins for the Wading River.

2.1.7 Study Sub-watersheds Identification and Prioritization

Wading River watershed (HUC12-010900040302) is 43.3 mi², contains 1st through 4th order streams, and is in the Taunton basin. The Wading River is 13.9 miles long and is a tributary to the Three Mile River. The watershed includes Chartley Brook, Meadow Brook, Henkes Brook, Hodges Brook, Cocasset River, Mirimichi Lake, and Turnpike Lake. The outlet of the sub-watershed has long-term, continuous monitoring data from USGS gage 01109000. Because of this long-term flow data, the Wading River watershed was selected to configure and calibrate the LSPC model.

Three sub-watersheds (Figure 2-9) were selected from the Wading River watershed for which modeling tasks, including baseline and management scenario simulations, were performed. The three sub-watersheds, Pilot Tributary, Lower Hodges Brook, and Upper Hodges Brook have second and third-order streams at their outlets. Pilot Tributary does not represent an actual stream name, it is an unnamed brook. Pilot Tributary, Lower Hodges Brook, and Upper Hodges Brook have impervious surface areas comprising 4%, 20%, and 32% of the total sub-watershed area, respectively (Figure 2-9). Note that Upper Hodges Brook is nested within Lower Hodges Brook. These three sub-watersheds were selected based on their drainage to low-order stream reaches (i.e., 2nd and 3rd) within the Wading River watershed and varying levels of development ranging from very rural to more highly developed with distinctly different amounts of impervious cover (IC) (e.g., very rural (less than 10% IC); rural/suburban (15%-25% IC); and suburban to urban (greater than 30%)), suitable for further assessment and modeling analysis.

Appendix B contains information, including maps, on the land use/land cover area distribution for the Wading River watershed and selected sub-watersheds. The forest land cover is dominant (31%) followed by wetlands (22%) and developed open space (11%) in the Wading River watershed. The total impervious cover is 10% in the Wading River watershed. Forest is also the dominant land cover in all three selected sub-watersheds. The Upper Hodges sub-watershed is more urban with 17% industrial impervious cover and 20% developed open space as compared to the more rural pilot tributary sub-watershed with only 4% total impervious cover.

Appendix B contains available SSURGO and STATSGO2 soil data. While SSURGO has a higher resolution dataset, STATSGO2 is more complete, therefore STATSGO2 was used to fill in data gaps present in SSURGO. One-third of the Wading River watershed has high infiltration soil (hydrologic soil group [HSG] type A). The selected sub-watersheds have similar proportions of soil types A, C, and D, roughly 20% each. Elevation and slope data are presented are also presented in Appendix B. The elevation ranges from 18m to 135m in the Wading River watershed. Overall, the Wading River watershed has a low slope (75% of the area) with only 6% of the high slope areas. More than 92% of the areas have a low slope and less than 1% of the areas have a high slope in the selected sub-watersheds.

2.2 Climate Data: Historic Trends and Future Conditions

The climate of Massachusetts is changing; the state has warmed by more than two degrees Fahrenheit in the last century and experiences heavier, more frequent rainstorms (EPA, 2016). Within the Taunton basin, both maximum and minimum temperatures are expected to continue to increase through the end of the century. Winters are expected to have more precipitation while summers may see an increase or decrease in precipitation (Northeast Climate Adaptation Science Center, 2018a). In response, the state has produced Climate Resilience Design Standards and Guidelines (Resilient Massachusetts Action Team, 2020) to incorporate climate resilience into the State's capital planning process. The design standards are intended to inform the climate resilience of assets and include design criteria for extreme precipitation. Best practice guidance from the Climate Resilience Design Standards includes embedding future capacity into projects and designing for uncertainty. The approach encourages that assets (such as stormwater SCMs) be implemented in locations that (1) reduce exposure to climate hazards, (2) mitigate adverse climate impacts and provide benefits and (3) protect, conserve, and restore critical natural resources on-site and off-site.

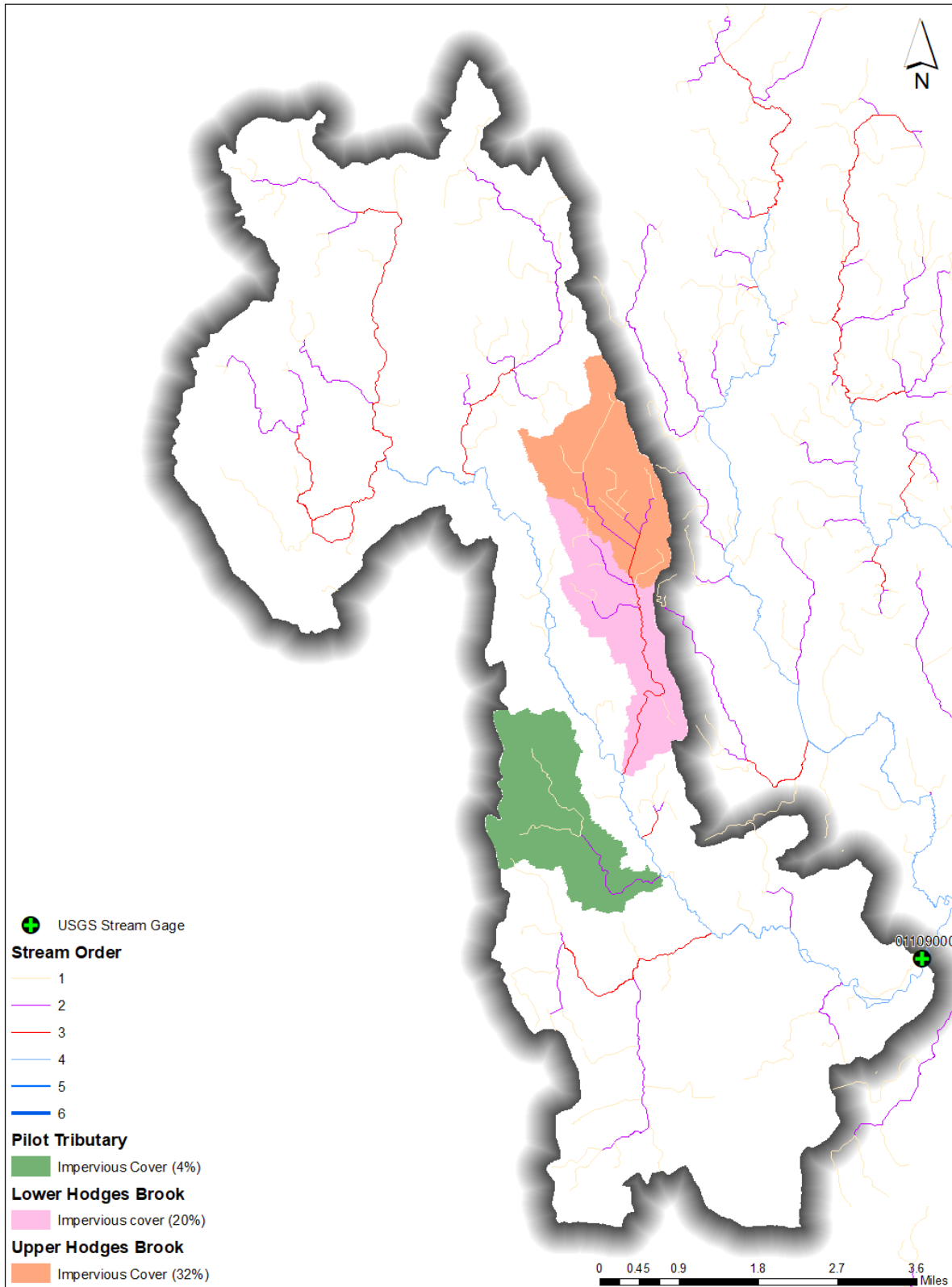


Figure 2-9. Selected sub-watersheds in the Wading River watershed.

Climate variability and changes to land use/land cover are two interwoven factors that impact hydrologic systems and improving the understanding of these two factors is the subject of research programs around the globe and an important part of sustainable water resource management.

2.2.1 Historic Trends

Appendix A presents several figures and tables assessing climate trends in the Taunton River Basin. Overall, there does not appear to be a strong increasing trend in terms of annual precipitation depths. However, there does appear to be a strong trend of increasing temperatures based on visual inspection of annual average and rolling 10 and 30-year averages. The additional analysis included using historic precipitation data to produce 24-hour rainfall depths for the 1, 2, 5, 10, 25, 50, 100, and 500-year storms. These storms correspond to approximately 100%, 50%, 20%, 10%, 4%, 2%, 1%, and 0.2% probability that at least that respective depth of rainfall will fall within 24 hours in any given year.

2.2.2 Future Conditions

The Massachusetts Climate Change Report (MA EOEE, 2011) presents estimates that annual precipitation will increase 5-8% in 2035-2064 and 7-14% in the period 2070-2099, with increased precipitation rates especially occurring during winter months (Hayhoe et al., 2006). These estimates are based on general circulation models (GCMs), which typically produce output at relatively coarse temporal and spatial resolutions. Temporal resolutions are often monthly timesteps and spatial resolutions are often grid cells of 1 or more degrees (~60-200 miles). However, most hydrological and water quality models require data at hourly timesteps or finer, and higher spatial resolutions depending on watershed size. Statistical downscaling allows modelers to create fine resolution climate time series using coarse resolution datasets by identifying statistical relationships between the coarse and fine resolution data. Raw climate model data has been downscaled from monthly resolution to daily resolution by a consortium of researchers (Northeast Climate Adaptation Science Center, 2018b) and is publicly available (<https://resilientma.org/>). However, further downscaling was necessary to generate the required hourly data.

The specific downscaling techniques used depend on the variable being downscaled. Precipitation data presents challenges in downscaling due to its high spatial and temporal variability. Fortunately, there are existing techniques developed to overcome these challenges (Hwang and Graham, 2014). Local Constructed Analogs (LOCA) has been shown to successfully downscale similarly variable climate data and was selected to downscale precipitation for the Taunton basin. While estimates of future precipitation are available at a daily timestep, the LSPC/Opti-Tool modeling requires hourly data. The LOCA approach examines historical hourly data to identify "analog days" that can be used to disaggregate represents of the future daily precipitation. The process iterates over each day in the modeled future precipitation. For each day of data, the process also extracts rainfall estimates for the preceding and following days to create a three-day time series of daily rainfall. Then, the LOCA approach searches through historical hourly rainfall data to find three-day periods with similar rainfall. It compares the hourly rainfall against the modeled daily rainfall and the historical three-day period with the most similar rainfall becomes the analog day. Thirty-two separate GCMs, each of which forecasted a future climate time series based on two Representative Concentration Pathways (RCPs), were selected as future scenarios. The RCP 4.5 predicts a stabilization of carbon emissions by 2100 while RCP 8.5 represents a scenario in which carbon emissions continue to climb at historical rates (Figure 2-10). However, current and pledged carbon emission reduction policies may mean that an RCP 8.5 scenario may be highly unlikely. The result of downscaling the selected GCMs was 64 hourly datasets (32 GCMs, 2 RCPs) of precipitation over the Wading River from 2005-2100, suitable for dynamic, continuous hydrologic modeling.

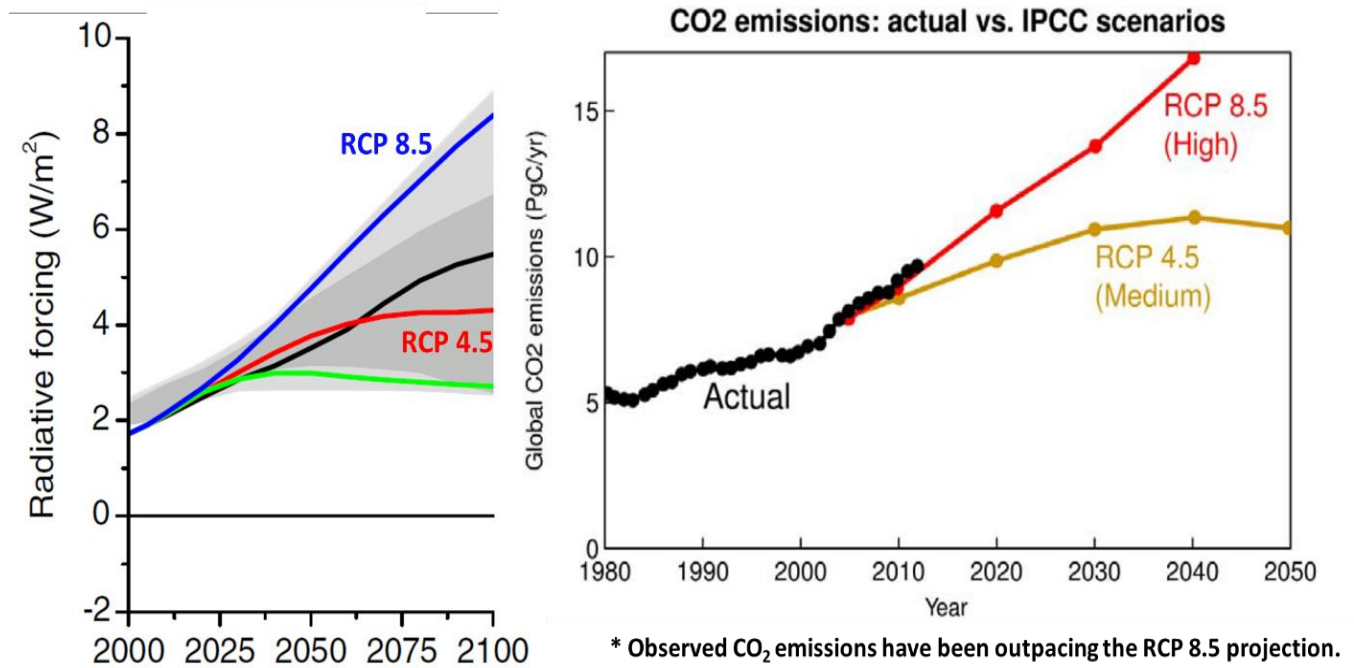


Figure 2-10. Representative Concentration Pathways for climate change analysis (International Institute for Applied Systems Analysis, 2009).

Similar downscaling techniques have been applied to other meteorological variables, including temperature, potential evapotranspiration, wind speed, solar radiation, and dew point. However, temperature, potential evapotranspiration, solar radiation, and dew point are all much less variable temporally than precipitation, and thus could be downscaled with simpler algorithms. For each future day, the daily average or daily total value for each variable was calculated, and then a historical diurnal cycle was fit to the daily value to create an hourly time series. To downscale air temperature, an hourly diurnal temperature cycle was derived for each season using observed temperature data. This cycle was scaled to the daily temperature values to generate hourly air temperature. To downscale evapotranspiration, the Penman-Monteith equation was used to calculate daily evapotranspiration using the daily resolution climate data. Then, an hourly diurnal evapotranspiration cycle was derived for each season using observed data. This cycle was scaled to the daily evapotranspiration values to generate hourly evapotranspiration. While wind speed is temporally variable, the model is less sensitive to its impacts, which meant that a simple downscaling technique could be applied to the wind as well. To create an hourly wind time series, the hourly average wind was assumed to be equal to the daily average wind. To downscale solar radiation, an hourly diurnal temperature cycle was derived for each season using observed radiation data. This cycle was scaled to the daily solar radiation values to generate hourly solar radiation. Hourly dew point data were calculated by scaling the hourly downscaled air temperature.

3. MODEL APPLICATION

The FDC modeling approach required a coupled watershed/SCM modeling framework that accounts for the full water balance associated with precipitation, runoff, evapotranspiration, runoff, groundwater interflow, and deep groundwater recharge. This section describes the watershed and SCM modeling approaches. This section presents a review of the configuration and calibration of the LSPC model as well as updates to the Opti-Tool that were performed as part of this study. While this section provides an overview, the [Task 6 Memo](#) provides a more detailed discussion. Appendices C and D also provide several supplementary tables and graphs.

3.1 Watershed Modeling Approach

The watershed modeling approach followed a top-down weight-of-evidence-based methodology. The approach leverages high-resolution HRU and meteorological data for model configuration. Figure 3-1 provides a schematic of the adaptive model development approach for assessing and integrating the required datasets for simulation, and how they relate to the overall model calibration and validation process. The gray arrows show the connections between the various stages of model development. The cycle can be summarized in six interrelated steps:

1. **Assess Data/Information.** Assess data to be used for land representation, source characterization, meteorological boundary conditions, etc.
2. **Define Model Domain.** Determine model segmentation and discretization needed to simulate hydrology and water quality at temporal and spatial scales appropriate for supporting decisions across the watershed.
3. **Set Boundary Conditions.** Set spatial and temporal model inputs, especially meteorological data, for establishing the conditions that drive variation in hydrology and water quality.
4. **Represent Processes.** Select the processes to be represented by the algorithms in the model based on the intended application (e.g., which pollutants to simulate).
5. **Confirm Predictions.** Adjust model rates and constants to mimic observed physical processes of the natural system, mostly through comparison to observational data.
6. **Assess Data Gaps.** Modeled responses and/or poor model performance can indicate the influence of unrepresented physical processes in the modeled system. A well-designed model can be adapted for future applications as new information about the system becomes available. Depending on the study objectives, data gaps sometimes provide a sound basis for further data collection efforts to refine the model, which cycles back to Step 1.

These steps are organized into two primary efforts: model configuration (green boxes) and model calibration and validation (blue), as described in Figure 3-1 below. The LSPC model is an open-source, process-based watershed modeling system developed by the EPA for simulating watershed hydrology, sediment erosion and transport, and water quality processes from both upland contributing areas and receiving streams (EPA 2009b). The LSPC model simulates flow accumulation in stream networks and the transport of pollutants, which may be deposited or scoured from the stream bed, sorbed, or transformed due to various chemical and biological processes. LSPC is capable of dynamically simulating flow, sediments, nutrients, metals, dissolved oxygen, temperature, and other pollutants for pervious and impervious lands and water bodies of varying order. LSPC algorithms were developed from a subset of those in HSPF (Bicknell et al. 1997) but designed to overcome some of the structural attributes that limit the size, resolution, and complexity associated with HSPF model configuration (Shen et al. 2004). The hydrologic portion of HSPF is based on the Stanford Watershed Model (Crawford & Linsley 1966), one of the pioneering watershed models. LSPC

is built upon a relational database platform, enabling the collation of diverse datasets to produce robust representations of natural systems. LSPC integrates GIS outputs, comprehensive data storage, and management capabilities, the original HSPF algorithms, and a data analysis/post-processing system into a PC-based Windows environment. Figure 3-2 is a generalized schematic of the underlying hydrology model (Stanford Watershed Model) used in LSPC. The schematic represents land-based processes for a single land unit in the model. The schematic shows the major processes that influence hydrology in a land segment. The baseline hydrological condition was calibrated for the most recent period using various graphical and tabular statistical assessments of model goodness of fit.

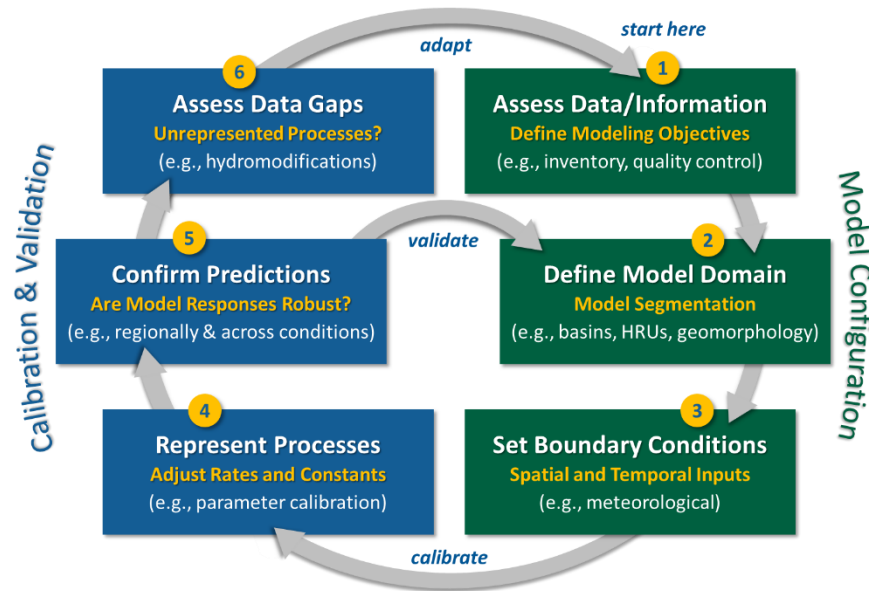


Figure 3-1. Conceptual representation of the LSPC model development cycle.

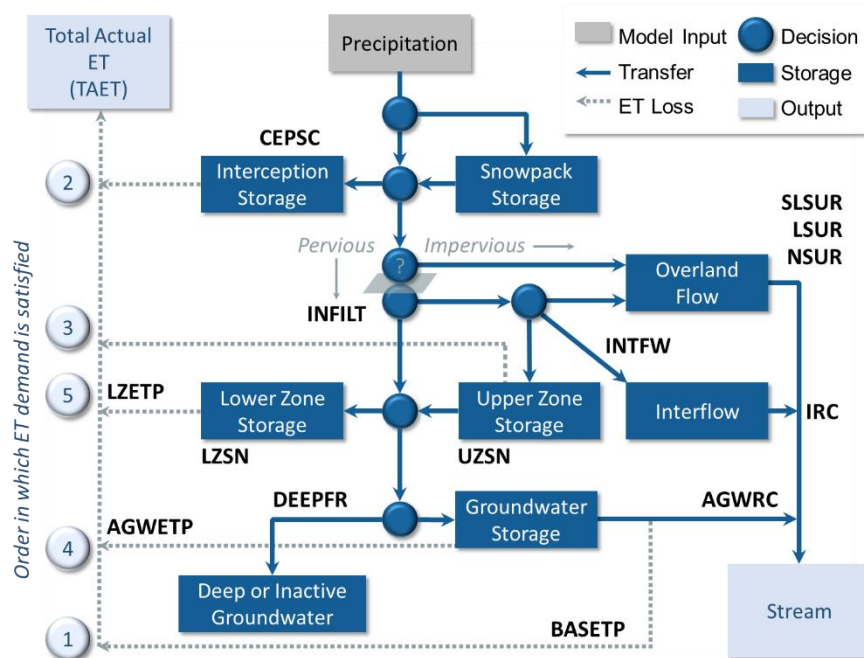


Figure 3-2. Hydrology model schematic for LSPC (based on Stanford Watershed Model).

3.2 SCM Modeling Approach with FDC Attenuation Objective

A coupled watershed-SCM modeling framework provides an integrated platform for representing the impact of stormwater management on watershed-scale hydrology and water quality. LSPC is designed for direct linkage to the Opti-Tool. LSPC outputs unit-area HRU time series in the format that can be linked directly to the Opti-Tool. Figure 3-3 shows how the two models were linked in this study. The baseline watershed model routes surface, interflow, and groundwater outflow directly to the stream network. When LSPC is linked to the Opti-Tool, overland flow (SURO) from managed areas is intercepted and routed to SCMs, where it is either treated, bypassed, or overflows when inflow exceeds treatment capacity. Infiltrated water from SCMs is stored in an aquifer segment for attenuated routing back to the Opti-Tool reach network. For the managed areas, the stormwater outflow from SCM routes to the downstream reach in the Opti-Tool, while other components of the water balance, along with unmanaged areas, are routed directly to the reach network in the Opti-Tool. Reach geometry can be configured as pipes or open channels in the Opti-Tool. The optimization run requires several thousand iterations to find an optimal solution and in such case, the reach routing simulation could become very expensive in terms of model run time. Alternatively, F-tables (functional tables) representing the stage-volume-discharge relationships of the reach geometry from the LSPC baseline model are directly used in the Opti-Tool.

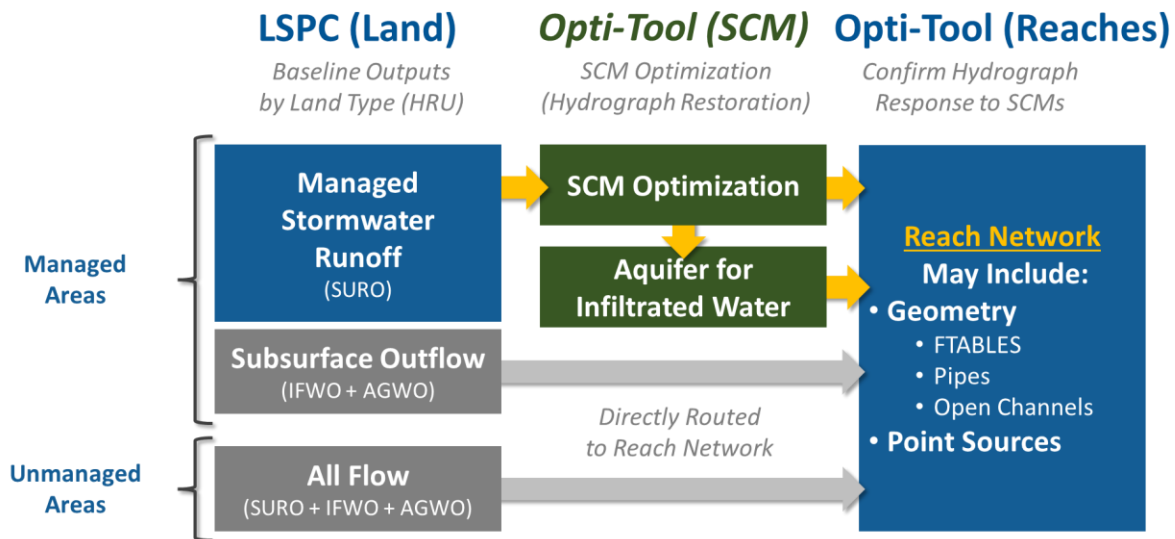


Figure 3-3. LSPC and Opti-Tool linkage schematic for integrated watershed-SCM hydrology modeling.

3.3 LSPC Model Configuration, Calibration, and Validation

3.3.1 Model Configuration

The goal of model calibration is to adjust model parameters to improve the predictive performance of the model based on comparisons to observed data. The desired outcome of the calibration process is a set of representative parameters for all processes in LSPC, modeled by HRU type on the land and reach segment, which represents the baseline existing condition. Figure 3-4 shows how the model configuration and calibration components are layered in the model. LSPC makes clear distinctions between inputs that are physical characteristics and process parameters. The term “parameters” refers to the rates and constants used to represent physical processes in the model. All other model inputs such as weather data, watershed elevation, HRU distribution, and the length and slope of overland flow for individual HRUs are generally considered physical characteristics of the watershed because they can be directly measured, assigned, or

reasonably estimated. Those terms are set during model configuration and not varied during model calibration unless new information is received that justifies a systemwide change to those terms.

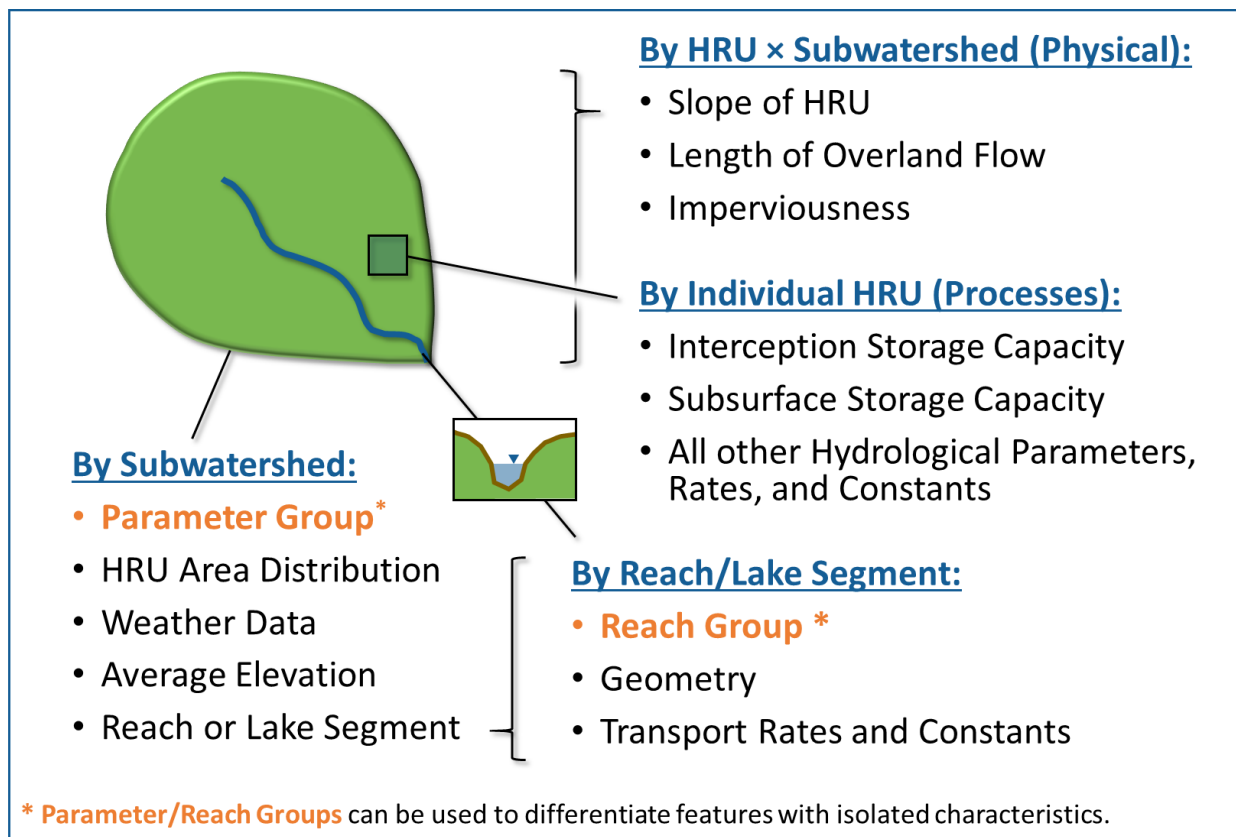


Figure 3-4. LSPC model configuration and calibration components.

3.3.1.1 Hydrological Response Unit Development

This section describes the methodology to develop a set of unique hydrologic response units (HRUs) representing the land use, land cover, soil, and slope characteristics in the Taunton basin. Each HRU represents areas of similar physical characteristics attributable to core processes identified through GIS overlays. The HRU layer combines spatial information into a single raster layer with identified 36 unique categories. The unit-area HRU time series for the baseline conditions was developed using the most recent 20-year period of observed meteorological boundary conditions and calibrating the rainfall-runoff response on each HRU along with reach routing processes in the LSPC model.

Within LSPC, the land is categorized into HRUs, which are the core hydrologic modeling land units in the watershed model. Each HRU represents areas of similar physical characteristics attributable to certain processes. The HRU development process uses these three primary data types that are typically closely associated with hydrology in the watershed.

- **Land Use – Land Cover:** *Land use describes the principal programmatic use and/or vegetation type. The programmatic, or zoning, element of this attribute is critical for water quality simulation. The land cover defines landscape as having either pervious or impervious cover.*
- **Hydrologic Soil Group:** *Represents one of four soil classes (i.e., A, B, C, and D) commonly associated with a spectrum of infiltration rates with HSG-A having the highest and HSG-D having the lowest.*
- **Landscape Slope:** *Represents the overland flow slope derived from a digital elevation model. The percent slope was categorized into three groups: low (<5%), medium (5% - 15%), and high (>15%).*

The HRU-based approach reflects the key physical features that influence runoff and pollutant loadings such as land use, slope, soils, and impervious cover and is based on the best available local datasets characterizing existing conditions for the Taunton basin. The raster combination of these dataset characteristics determined the number of possible HRU categories considered for the model. Ultimately, some consolidation of HRUs was implemented to balance the need for spatial resolution with model simulation efficiency, resulting in a set of meaningful HRUs for model configuration. Figure 3-5 shows the three spatial layers used to create the mapped HRU raster.

Land Use – Land Cover Reclassification

Land use categories indicate activities taking place at the parcel scale (e.g., industrial use) and are important for characterizing the hydrologic and water quality responses from those areas (Huang et al., 2013; Tong and Chen, 2002; Tunsaker and Levine, 1995). Land cover designations supplement land use categories by providing additional texture to parcel descriptions, enabling their hydrologic and water quality responses to be further characterized (Wilson, 2015). The MassGIS (Bureau of Geographic Information) 2016 land use – land cover layer contains both land use and land cover information as separate attributes and can be accessed independently or in a useful combination with one another. For example, it is possible to measure the portions of pervious and impervious surfaces for a commercial parcel. The land cover information in this layer is consistent with Coastal Change Analysis Program (C-CAP)'s high-resolution land cover classification scheme. For more information on the data development process and data accuracy reporting, see the [full detailed description \(PDF\)](#) document. For HRU development, the MassGIS 2016 land use – land cover attributes were reclassified to 15 unique either pervious or impervious land segments (See Appendix C)

Hydrologic Soil Group Reclassification

HSGs characterize the propensity for precipitation to saturate and percolate through the subsurface or contribute to runoff. Soils with similar hydrologic and physical properties (e.g., texture, permeability) are grouped by HSGs (USDA, 2003, Table 23). HSG-A generally has the highest infiltration and lowest runoff potential whereas HSG-D has the lowest infiltration and highest runoff potential. HSG classifications are used within the model as a basis for setting certain hydrologic parameters including infiltration rates.

HSG designations for the Taunton basin were obtained from the Natural Resources Conservation Service (NRCS) Soil Survey Geographic Database (USDA, 2019) and the State Soil Geographic (STATSGO2) Database. Some HSG designations were unspecified in the SSURGO database which were assigned a HSG from the STATSGO2 database or contained dual HSG assignments, therefore a conservative assumption to assign all as HSG-D was applied.

Slope Group Reclassification

A DEM is a raster-based dataset describing the elevation of the landscape across a regular grid. DEMs are useful for determining flow direction and drainage and are used to derive the landscape slope, defined as the change in elevation over a set distance. The slope was calculated from the USGS National Elevation Dataset (NED) product for the contiguous United States and clipped to the Taunton basin (USGS, 2002). Slopes were categorized as low (< 5%), medium (5% - 15%) and high (> 15%).

3.3.1.2 Mapped HRU Categories

Each of the three spatial datasets described above (land use - land cover, HSG, and slope) were spatially joined in GIS to derive a composite raster. The resulting raster and attribute table were reclassified into 36 unique mapped HRUs (Table 3-1). The spatial distribution of mapped HRUs for the Taunton basin is shown in Figure 3-6. The spatial distribution of mapped HRUs for Lower Hodges Brook, Upper Hodges Brook, Pilot Tributary, and Wading River are shown in Figure 3-7.

3.3.1.3 Directly Connected Impervious Area

Mapped impervious area (MIA) represents the mapped portion of impervious cover over the landscape, as represented by available spatial layers. However, the Effective Impervious Area (EIA) is the portion of the MIA that contributes to runoff, or which is directly connected to the conveyance network within the LSPC model. Estimates of Directly Connected Impervious Area (DCIA) are rarely available locally and, thus, empirical algorithms are typically used to convert MIA to DCIA for input to LSPC (Said, 2014).

EIA is derived as a function of DCIA, with other adjustments as needed to account for other structural and non-structural management practices in the flow network. Figure 3-8 illustrates the transitional sequence from MIA to DCIA. Runoff from impervious areas that are not connected to the drainage network may flow onto pervious surfaces, infiltrate, and become part of pervious subsurface and overland flow. Because segments are modeled as being parallel to one another in LSPC, this process can be approximated using a conversion of a portion of impervious land to pervious land. On the open landscape, runoff from disconnected impervious surfaces can overwhelm the infiltration capacity of adjacent pervious surfaces during large rainfall/runoff events creating sheet flow over the landscape—therefore, the MIA-EIA translation is not a direct linear conversion. Finding the right balance between MIA and EIA can be an important part of the hydrology calibration effort.

The Sutherland Equations were the empirical relationships used for DCIA estimates in the LSPC model. This refinement is necessary to avoid an initial overestimation of impervious surfaces contributing to runoff before initiating process-based model calibration (Sutherland, 2000). The Sutherland Equations, presented in Figure 3-9, show a strong correlation between the density of the developed area and DCIA. The curve for high-density developed land trends closer to the line of equal value than the curve for less developed areas. Similarly, as the density of mapped impervious areas approaches 1.0, the translation to DCIA also approaches 1.0. An estimate of EIA equal to $MIA \times DCIA$ fraction based on the Sutherland Equations was used to adjust the MIA from the MassGIS land use – land cover layer into EIA for use in the LSPC watershed model. Impervious area summary comparing the MIA and EIA in the Wading River watershed is shown in Table 3-2 and the EIA from this analysis was compared with the USGS published HSPF models for the Wading River watershed (Table 3-3).

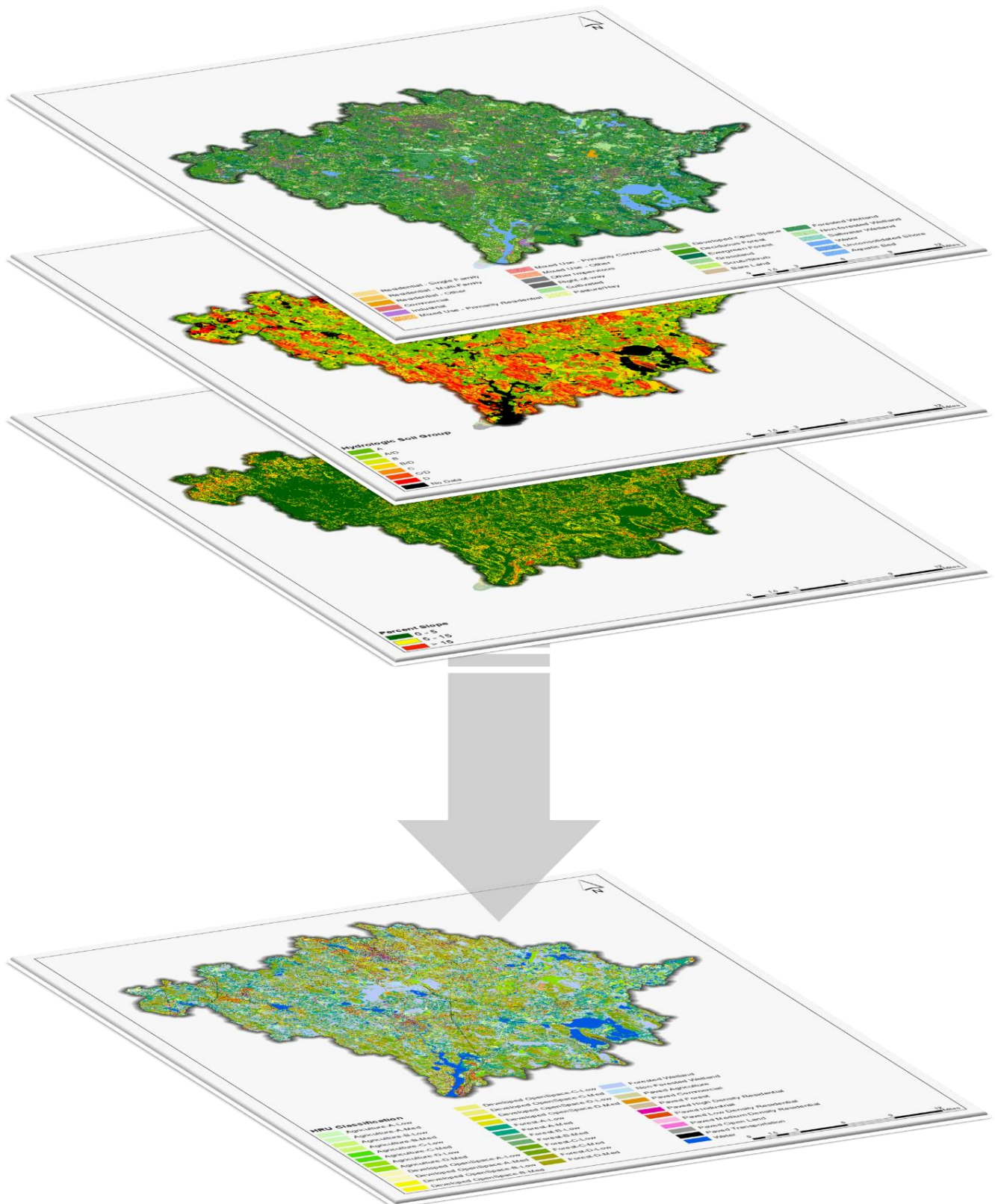


Figure 3-5. Mapped HRUs process (spatial overlay of land use – land cover, soil, and slope layers).

Table 3-1. Final HRU categories

HRU Code	HRU Description	Land Use	Soil	Slope	Land Cover
1001	Paved Forest	Paved Forest	N/A	N/A	Impervious
2001	Paved Agriculture	Paved Agriculture	N/A	N/A	Impervious
3001	Paved Commercial	Paved Commercial	N/A	N/A	Impervious
4001	Paved Industrial	Paved Industrial	N/A	N/A	Impervious
5001	Paved Low Density Residential	Paved Low Density Residential	N/A	N/A	Impervious
6001	Paved Medium Density Residential	Paved Medium Density Residential	N/A	N/A	Impervious
7001	Paved High Density Residential	Paved High Density Residential	N/A	N/A	Impervious
8001	Paved Transportation	Paved Transportation	N/A	N/A	Impervious
9001	Paved Open Land	Paved Open Land	N/A	N/A	Impervious
10110	Developed OpenSpace-A-Low	Developed OpenSpace	A	Low	Pervious
10120	Developed OpenSpace-A-Med	Developed OpenSpace	A	Med	Pervious
10210	Developed OpenSpace-B-Low	Developed OpenSpace	B	Low	Pervious
10220	Developed OpenSpace-B-Med	Developed OpenSpace	B	Med	Pervious
10310	Developed OpenSpace-C-Low	Developed OpenSpace	C	Low	Pervious
10320	Developed OpenSpace-C-Med	Developed OpenSpace	C	Med	Pervious
10410	Developed OpenSpace-D-Low	Developed OpenSpace	D	Low	Pervious
10420	Developed OpenSpace-D-Med	Developed OpenSpace	D	Med	Pervious
11000	Forested Wetland	Forested Wetland	N/A	N/A	Pervious
12000	Non-Forested Wetland	Non-Forested Wetland	N/A	N/A	Pervious
13110	Forest-A-Low	Forest	A	Low	Pervious
13120	Forest-A-Med	Forest	A	Med	Pervious
13210	Forest-B-Low	Forest	B	Low	Pervious
13220	Forest-B-Med	Forest	B	Med	Pervious
13310	Forest-C-Low	Forest	C	Low	Pervious
13320	Forest-C-Med	Forest	C	Med	Pervious
13410	Forest-D-Low	Forest	D	Low	Pervious
13420	Forest-D-Med	Forest	D	Med	Pervious
14110	Agriculture-A-Low	Agriculture	A	Low	Pervious
14120	Agriculture-A-Med	Agriculture	A	Med	Pervious
14210	Agriculture-B-Low	Agriculture	B	Low	Pervious
14220	Agriculture-B-Med	Agriculture	B	Med	Pervious
14310	Agriculture-C-Low	Agriculture	C	Low	Pervious
14320	Agriculture-C-Med	Agriculture	C	Med	Pervious
14410	Agriculture-D-Low	Agriculture	D	Low	Pervious
14420	Agriculture-D-Med	Agriculture	D	Med	Pervious
15000	Water	Water	N/A	N/A	Pervious

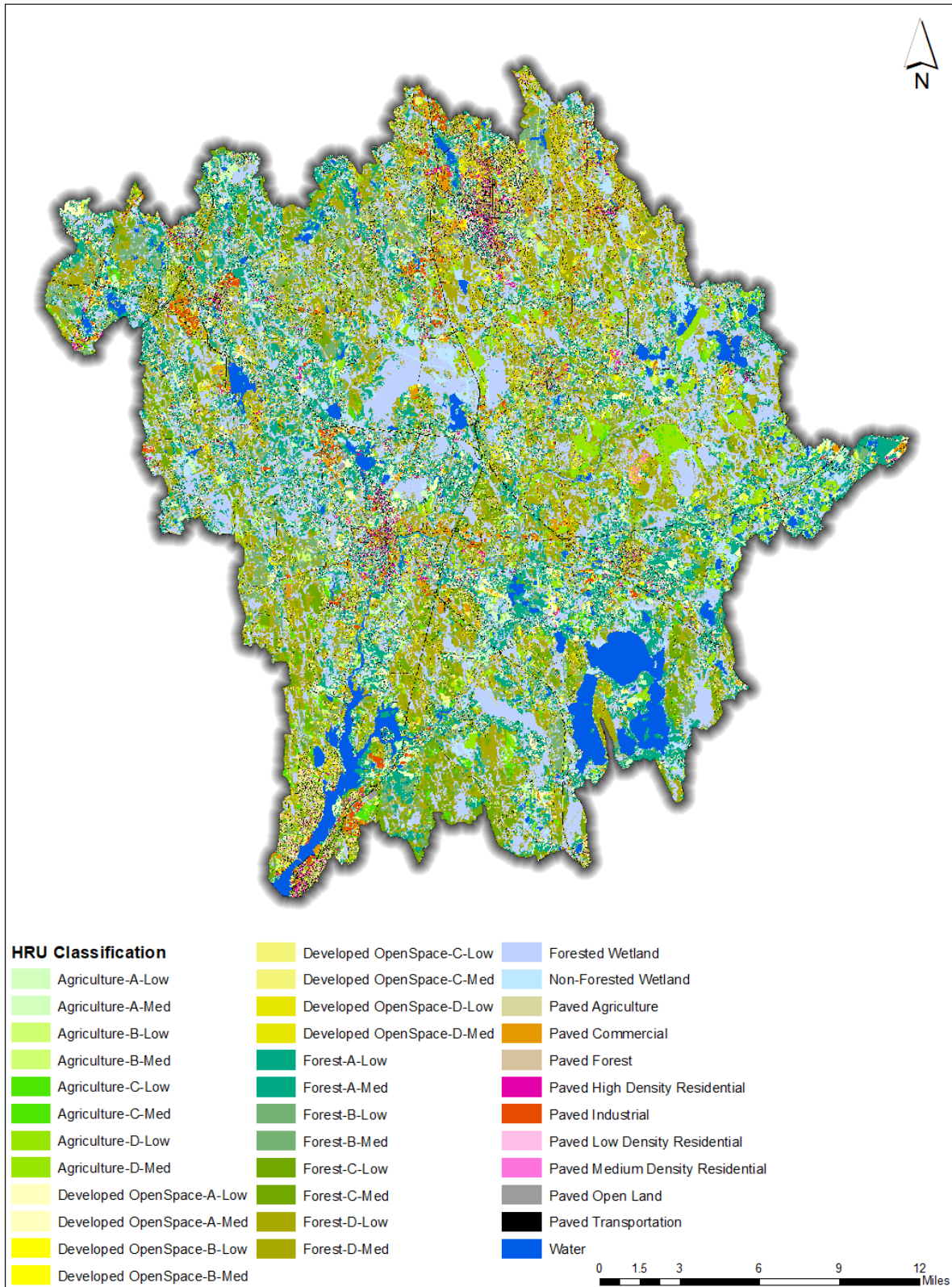


Figure 3-6. Mapped HRUs for the Taunton basin.

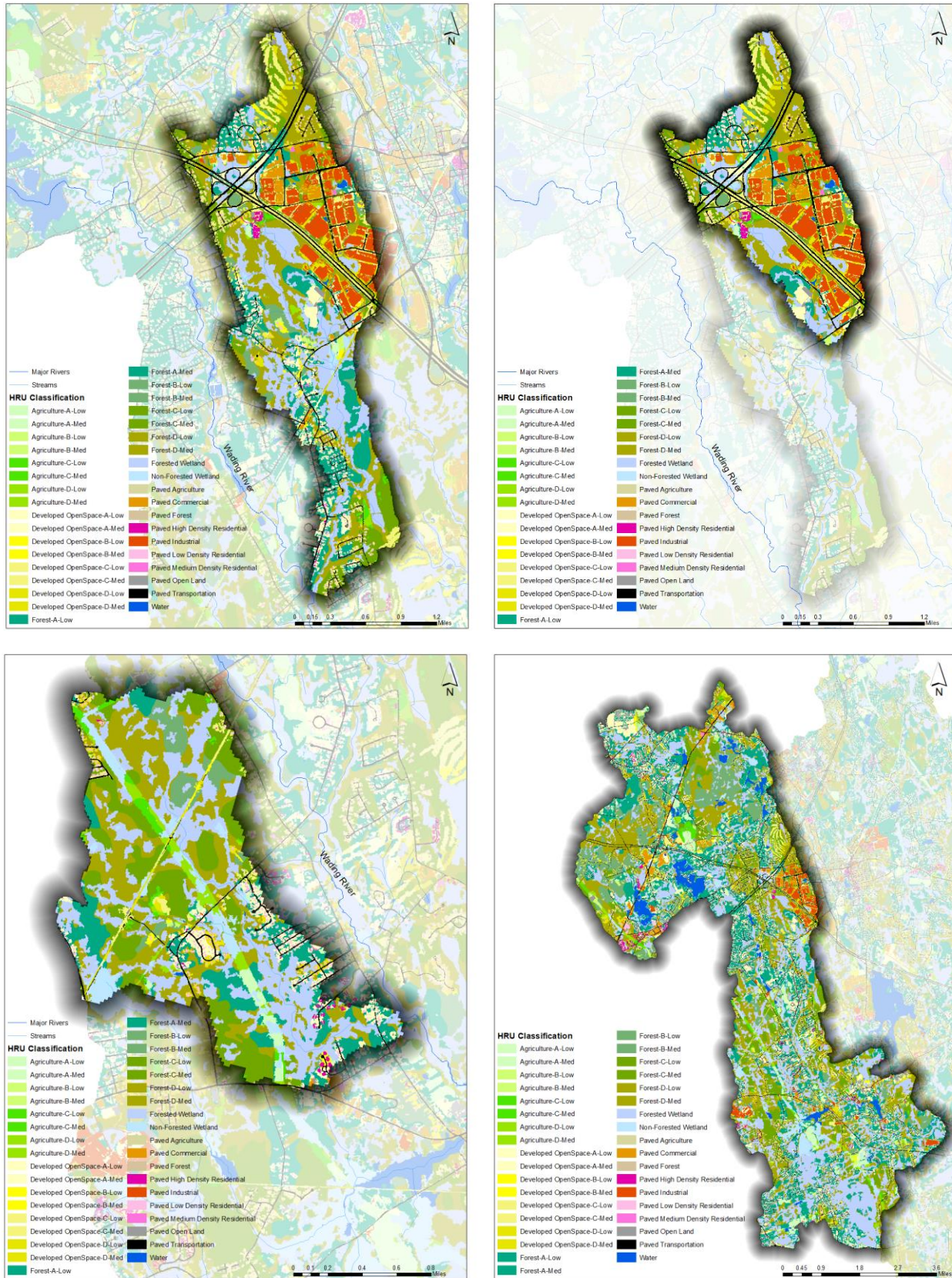


Figure 3-7. Mapped HRUs for Lower Hodges Brook (top left), Upper Hodges Brook (top right), Pilot Tributary (bottom left), and Wading River (bottom right).

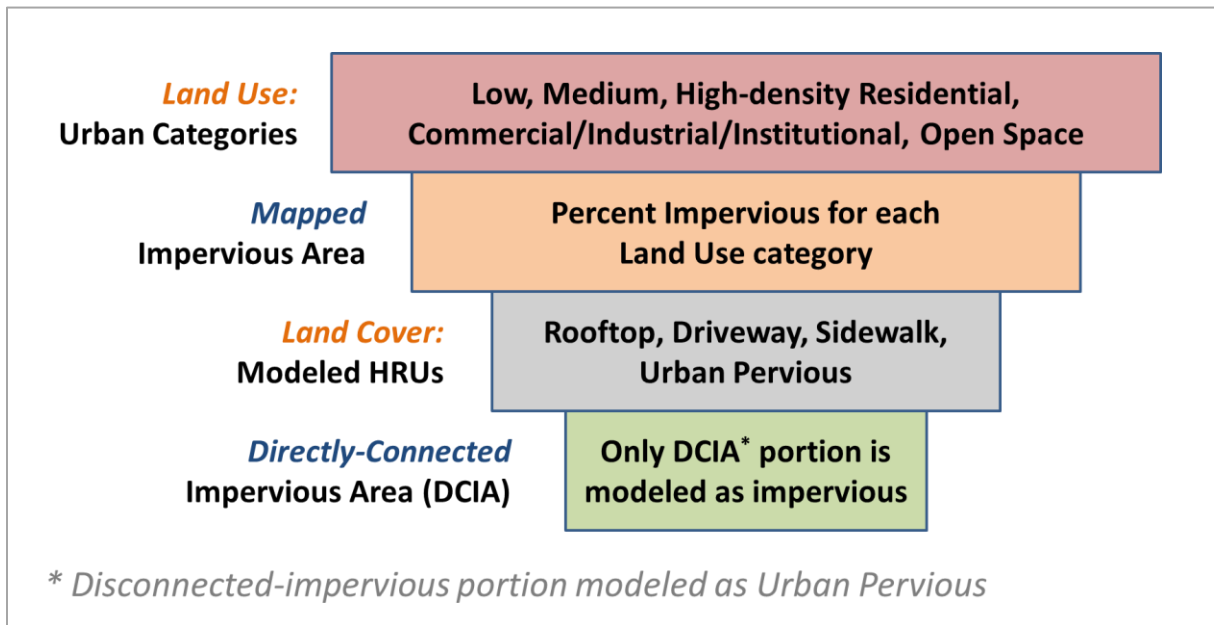


Figure 3-8. Translation sequence from MIA to DCIA.

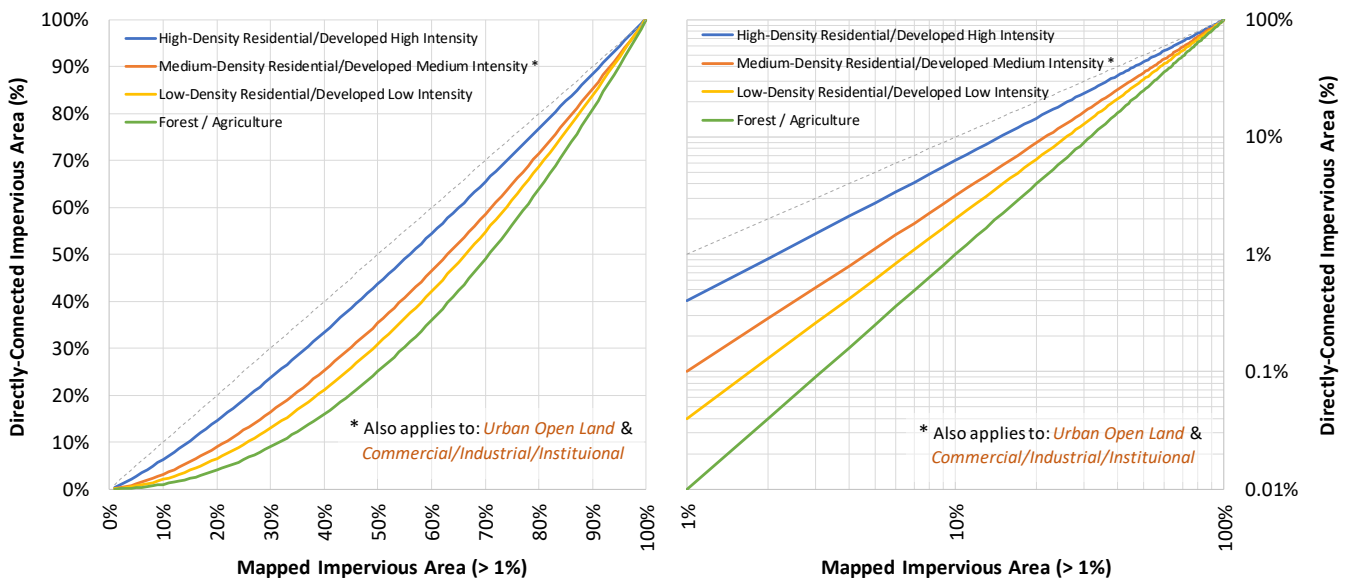


Figure 3-9. Relationships between Mapped and Directly Connected Impervious Area (Sutherland 2000).

Table 3-2. Mapped Impervious Area (MIA) and Effective Impervious Area (EIA) distribution in Wading River watershed

HRU Description	Total Impervious Area (acre)	Effective Impervious Area (acre)	EIA (%)
Paved Forest	0.3	0.0	0%
Paved Agriculture	3.4	0.0	0%
Paved Commercial	375.8	96.5	26%
Paved Industrial	366.2	103.5	28%
Paved Low Density Residential	778.4	147.4	19%
Paved Medium Density Residential	20.5	5.6	27%
Paved High Density Residential	147.4	122.3	83%
Paved Transportation	956.5	793.7	83%
Paved Open Land	245.7	61.9	25%
Total	2,894.2	1,330.9	46%

Table 3-3. HSPF and LSPC Model area comparison for Wading River watershed

Wading River Model	HSPF Model* (acre)	LSPC Model (acre)	Difference (%)
Total Impervious Area	1,367.2	1,330.9	-2.65%
Total Pervious Area	26,231.4	26,270.3	0.15%
Total	27,598.6	27,601.2	0.01%

* USGS published HSPF models for the Taunton basin (Barbaro and Sorenson, 2013b)

The effective impervious areas have no spatial representation in GIS. For example, a commercial parcel has mapped impervious areas with no spatial reference of directly connected impervious areas. A peppering approach was developed to assign a pervious HRU category to the disconnected impervious areas (MIA – EIA) within the same commercial parcel. The approach uses a probabilistic raster reclassification algorithm to modify an existing HRU raster and replace individual HRU cells with new ones. The result of the probabilistic reclassification is a raster that has reclassified pixels scattered throughout it. Figure 3-10 shows the comparison between mapped HRUs and peppered HRUs for the Upper Hodges Brook sub-watershed.

3.3.1.4 Sub-watersheds

The domain of the Wading River LSPC model consisted of 43 square miles of watershed area and 27.6 miles of modeled stream reaches. The watersheds used in calibration were previously delineated for a previous modeling effort (Barbaro and Sorenson, 2013b) in the Taunton watershed (Figure 2-8). The original HSPF model configuration, including hydrology parameter values, was transferred to the LSPC model. LSPC is based on HSPF algorithms but includes additional functionality, including easy linkage to the Opti-Tool.

The original HSPF model included virtual reaches to represent the presence of wetlands in specific drainage areas. Generally, virtual wetland reaches were developed for watersheds in which wetlands composed 20 percent or more of the area (Barbaro and Sorenson, 2013b). The Wading River LSPC model included one virtual reach for the representation of wetlands. The virtual reach represents the combined storage of all the non-forested wetlands in watershed 4 (Figure 2-8). Compared to stream reaches, discharge in virtual reaches was configured to be low and increased substantially less as storage increased.

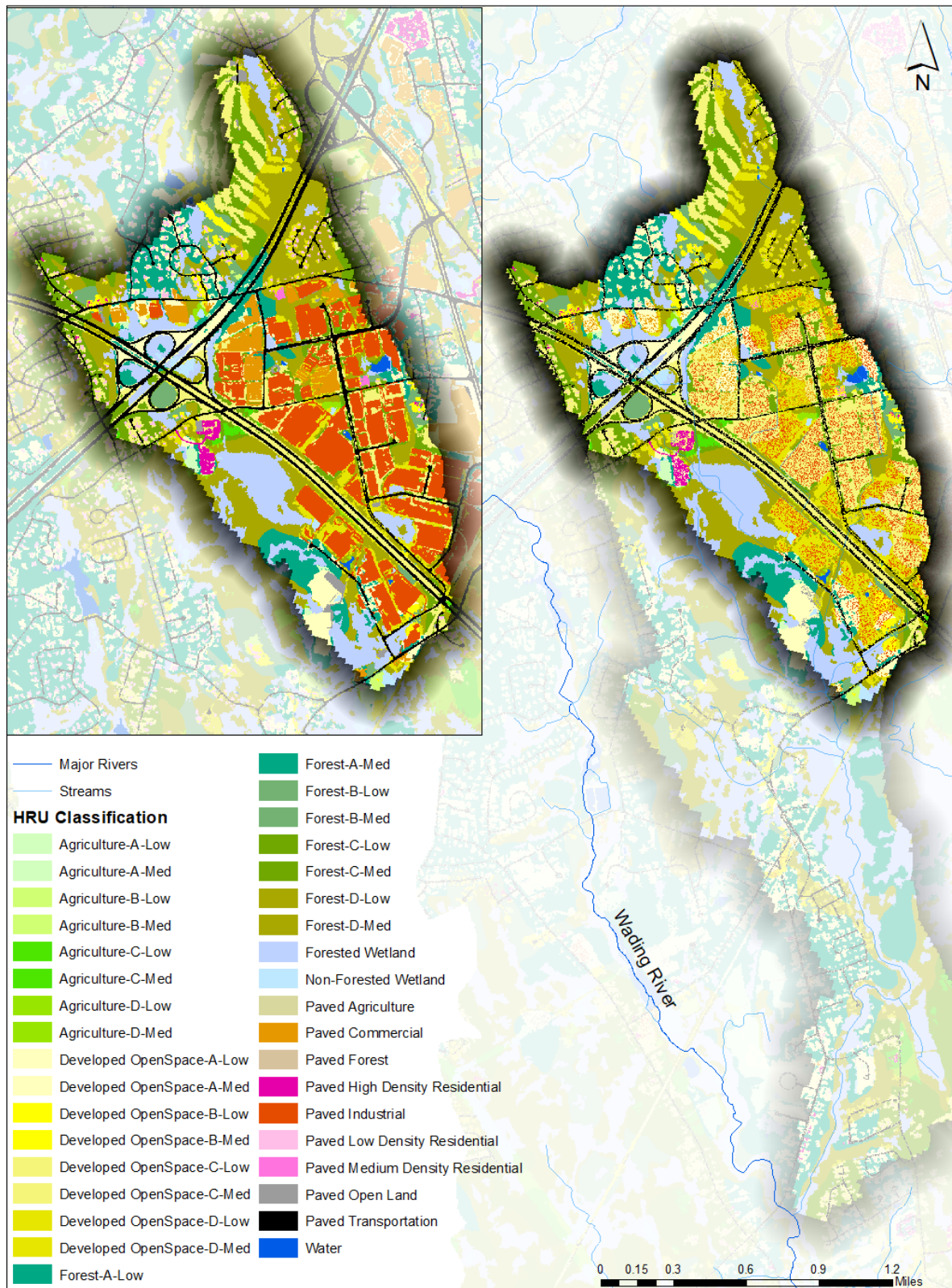


Figure 3-10. Peppered HRUs representing the effective impervious areas for Upper Hodges Brook (MIA on left and EIA on right).

While the Wading River watersheds were included in the Taunton model calibrated by Barbaro and Sorenson, (Barbaro and Sorenson, 2013b), no Wading River gages were used during the calibration of that model. Therefore, while the calibrated HSPF model was obtained and converted to LSPC, additional calibration occurred to improve agreement between observed and predicted flows at the Wading River gage (0110900), calibration and validation are discussed in Section 3.3.2.

After calibration and validation, a set of three smaller sub-watersheds (Figure 2-9) were used to quantify the impact of impervious surfaces and climate change on flow characteristics. The sub-watersheds were delineated using National Hydrography Dataset (NHD) watershed boundaries. As discussed in Section 2.1.7, the sub-watersheds were selected based on their representation of a range of watershed imperviousness. Pilot Tributary, Lower Hodges Brook, and Upper Hodges Brook have impervious surface areas comprising 4%, 20%, and 32% of the total sub-watershed area, respectively.

3.3.1.5 Channel Geometry

LSPC routes streamflow and contaminants downstream using stage-storage-discharge relationships defined using an F-table (functional table). The basic channel geometry is a trapezoid, an example cross-section from the LSPC model is presented in Appendix C. By altering the stage, the cross-sectional geometry of the mainstem segments represented in LSPC affects the shape of the hydrograph through each sub-catchment. The majority of the original HSPF F-tables were based on relationships between drainage areas, bankfull width, and bankfull depth (Leopold, 1994). The LSPC F-tables were updated using more recent channel geometry equations (Bent and Waite, 2013) as follows:

$$\text{Bankfull width (ft)} = 10.6640 [\text{Drainage area (mi}^2)]^{0.3935} [\text{Mean basin slope (\%)}]^{0.1751} \quad (1)$$

$$\text{Bankfull mean depth (ft)} = 0.7295 [\text{Drainage area (mi}^2)]^{0.2880} [\text{Mean basin slope (\%)}]^{0.1346} \quad (2)$$

During calibration (Section 3.3.2), the F-tables were revised to reflect the observed attenuation in the system, likely due in part to the proliferation of small dams and ponds in the area. However, Equations 1 and 2 were still used for the smaller study sub-watersheds given the lack of dams in those areas.

3.3.1.6 Baseline Boundary Conditions

Precipitation is the primary input to the LSPC water budget. Precipitation discharges to modeled reaches through overland flow, interflow, and active groundwater. The water budget in LSPC resolves the partitioning of rainfall to total actual evapotranspiration (TAET), interflow, groundwater, and overland flow determined for each watershed on an HRU-basis. The amount of TAET is in part determined by potential evapotranspiration (PET), a user input. The interaction of model parameters ultimately determines how much PEVT becomes TAET. Sources of evapotranspiration include groundwater outflow, interception storage, and soil moisture storage. Interflow and overland flow are then determined based on HRU characteristics, including soil infiltration rate, surface roughness, and slope. Precipitation and potential evapotranspiration drive the water balance for the snow accumulation/melt module. Table 3-4 presents a summary of the LSPC modules activated for the Wading River model. Section 2.1.4 presents a detailed review of meteorological inputs.

Table 3-4. Summary of climate data input requirements by LSPC module

LSPC Module	Precipitation	Potential Evapotranspiration	Temperature	Dew Point	Wind Speed	Solar Radiation	Cloud Cover
Snow Accumulation/Melt	●	●	●	●	●	●	●
Hydrology	●	●	--	--	--	--	--
Water Quality (GQUAL)	●	●	--	--	--	--	--

3.3.1.7 Climate Change Scenarios

The downscaling processes and algorithms described in Section 2.2.2 were implemented in Python and converted to LSPC format for use as weather files. The Wading River LSPC model was ran using each of these 62 climate change datasets for the years 2005-2100, a total of 5,890 years of simulated rainfall and streamflow at a daily timestep.

3.3.1.8 Point Source Withdrawals

Appendix C includes information on available water supply and permitted groundwater discharge information that was incorporated into the LSPC model as daily time series. To quantify the impact of water withdrawals and groundwater discharge on the water balance, 5 years from 10/1/2015 – 9/30/2020 were assessed. During this time, the amount of water withdrawn for both Public Water Supply and Non-Public Water Supply purposes was approximately 0.25% of the water budget while water returned to the system via permitted groundwater discharge was approximately 0.05% of the water budget.

3.3.2 Hydrology Calibration and Validation

The study design for this modeling project used 20 years of observed precipitation and streamflow, separated into a 10-year calibration and a 10-year validation period (Table 3-5). Hydrological modeling studies often split measured data into two datasets, one used for calibration, and one used for validation. Generally, model calibration involves minimizing the deviation between model output and corresponding measured data by adjusting model parameter values (Jewell et al., 1978). The model was calibrated manually whereby parameters were adjusted individually to improve the performance. Calibrated parameters were adjusted to maintain consistency with watershed characteristics that they describe and kept within the ranges reported in the literature. Manual calibration contrasts with automatic calibration which uses optimization routines to estimate “best” values for parameters within user-defined upper and lower bounds.

Table 3-5. Calibration and Validation Simulation Periods for the LSPC Wading River Model

Period	Observed data
Calibration	10/01/2010 – 09/30/2020
Validation	10/01/2000 – 09/30/2010

Appendix C presents visual and statistical assessments of observed versus predicted results for the calibration and validation periods, as well as the full 20-year baseline period. These results include hydrographs for daily flows and monthly flows, flow duration curves, and statistical evaluation using a suite of metrics. Below is a summary of the calibration and validation:

- Every metric achieved a Satisfactory or better for the All category. The “All” category assesses performance for the full simulation period, including all flow regimes and seasons. The results suggest the LSPC model is reasonably calibrated for flows and can provide a reliable baseline for scenario simulations.
- Most assessments for flow regimes using PBIAS were satisfactory or higher, suggesting that the model does not tend towards a systematic bias towards over- or under-prediction.
- Results for R^2 also suggest that the model performed reasonably well in establishing a linear relationship between model results and observations.
- There appear to be some limitations in seasonal performance. Spring flows appear to be somewhat under-predicted (positive PBIAS) while summer flows are over-predicted (negative PBIAS). However, satisfactory results for spring flow PBIAS was still achieved in the validation and full baseline periods. Fluctuations in low flows are likely in response to processes that are not well captured by LSPC. Causes of low flow fluctuations may include minor discharges and groundwater dynamics. Water use and discharge data were included in the model, but the available data did not cover the entire period used for calibration and validation (Table 3-5). Additionally, LSPC was not coupled to a groundwater model, and spatial variations in groundwater are not well characterized by available data.
- The NSE metric, in particular the top 10% and low 50% flow regimes, show the poorest performance grading. During periods of unsatisfactory NSE results, the residual variance (the variance in the differences between observations and predictions) is larger than the variance of the observed data. NSE is very sensitive to extreme values and reflects the timing of simulated versus observed values. There is potential that using a single rain gauge for the entire watershed affected the predicted timing of flows. Satisfactory results for NSE were achieved for the All-conditions category in the calibration and the validation period.

3.3.3 HRU Based Water Quality Calibration

For water quality, the default option in the Opti-Tool is to utilize the embedded HRU-SWMM models, calibrated to nine major land use categories for the New England Region. These SWMM models were calibrated using observed stormwater data from National Stormwater Quality Database (NSQD) and collected locally at the University of New Hampshire for a wide range of storm sizes. Additionally, the models were further calibrated to the long-term annual average pollutant loading rates consistent with the pollutant export rates reported in the small MS4 permits for Massachusetts and New Hampshire. For this project, instead of using the SWMM models directly, the hydrology model for the Wading River watershed was calibrated for four pollutants: Total Suspended Solids (TSS), Total Nitrogen (TN), Total Phosphorus (TP), and Zinc (Zn). The pollutant build-up and wash-off parameters from the SWMM models were used as a starting point and were adjusted to calibrate the long-term annual average loading rates reported in the Opti-Tool. The model was simulated for 20 years (October 2000 – September 2020) and annual average loading rates from the model prediction were compared against the pollutant export rates for the similar HRU type in the Opti-Tool. This approach provided a more detailed, locally specific calibration compared to simply using the SWMM models; the loading results match the regional export rates but the buildup and washoff processes that produce those rates are tailored to the hydrology of the Wading River. Table 3-6 presents the summary of unit-area annual average pollutant loading rates from the calibrated Wading River model. Note that fate and transport of pollutants in the stream were not modeled and no instream water quality calibration was performed under this effort. The objective was to estimate the source loads from the modeled HRU types and quantify the water quality benefits that SCM provides for the source load reductions.

Table 3-6. Summary of annual average pollutant loading rate calibrated to HRU type for the study area

HRU Category	TSS (lb/ac/year)	TN (lb/ac/year)	TP (lb/ac/year)	Zn (lb/ac/year)
Paved Forest	649.15	11.48	1.502	0.714
Paved Agriculture	649.29	11.48	1.502	0.714
Paved Commercial	377.59	15.24	1.794	1.377
Paved Industrial	377.59	15.24	1.794	1.377
Paved Low Density Residential	438.25	14.27	1.503	0.714
Paved Medium Density Residential	438.25	14.27	1.970	0.714
Paved High Density Residential	438.29	14.26	2.381	0.714
Paved Transportation	1,480.46	10.26	1.532	1.760
Paved Open Land	649.29	11.48	1.568	0.987
Developed OpenSpace-A-Low	5.75	0.23	0.020	0.002
Developed OpenSpace-A-Med	6.89	0.25	0.022	0.002
Developed OpenSpace-B-Low	24.73	0.93	0.097	0.016
Developed OpenSpace-B-Med	30.48	1.21	0.126	0.020
Developed OpenSpace-C-Low	57.33	2.26	0.209	0.046
Developed OpenSpace-C-Med	60.04	2.39	0.220	0.049
Developed OpenSpace-D-Low	86.17	3.30	0.305	0.058
Developed OpenSpace-D-Med	100.83	4.04	0.374	0.071
Forested Wetland	27.60	0.52	0.109	0.039
Non-Forested Wetland	27.69	0.52	0.109	0.039
Forest-A-Low	5.97	0.12	0.023	0.009
Forest-A-Med	6.81	0.12	0.025	0.010
Forest-B-Low	26.66	0.52	0.102	0.034
Forest-B-Med	28.60	0.55	0.109	0.036
Forest-C-Low	57.07	1.10	0.204	0.089
Forest-C-Med	59.99	1.17	0.217	0.095
Forest-D-Low	92.09	1.78	0.360	0.133
Forest-D-Med	95.00	1.84	0.373	0.138
Agriculture-A-Low	5.86	0.51	0.088	0.005
Agriculture-A-Med	6.78	0.54	0.093	0.005
Agriculture-B-Low	26.24	2.32	0.409	0.017
Agriculture-B-Med	28.14	2.49	0.439	0.018
Agriculture-C-Low	57.03	5.04	0.773	0.043
Agriculture-C-Med	60.39	5.41	0.829	0.047
Agriculture-D-Low	91.12	8.02	1.366	0.069
Agriculture-D-Med	95.67	8.49	1.447	0.073

3.4 Opti-Tool Background and Updates

The Opti-Tool provides the ability to evaluate options for determining the best mix of structural BMPs to achieve specific water resource goals, such as improving water quality or reducing runoff. As part of this study, several updates to the user interface and source code of the Opti-Tool were implemented. These updates provide the functionality of groundwater/aquifer and FDC evaluation needed to meet the project goals. The aquifer function uses an aquifer release coefficient to govern how quickly water that has been infiltrated into SCMs is released back to the stream. Functionally, the coefficient is the inverse of the LSPC groundwater recession rate parameter AGWRC. Laroche et al (1996) reported an optimized AGWRC value of 0.99, which is also reported in [BASINS Technical Note 6](#). Therefore, a value of 0.01 was used for the aquifer release coefficient. Appendix E provides a detailed discussion of these updates. The Opti-Tool explicitly represents structural BMPs, their performance is largely governed by the parameters representing stormwater storage capacity as well as associated vegetation and soil processes. Structural controls simulated by the tool include low impact development (LID) and green infrastructure (GI) practices, such as surface infiltration systems, bio-filtration systems, and sub-surface infiltration systems.

4. HYDROLOGIC STREAMFLOW MODELING ANALYSES

4.1 LSPC Streamflow Modeling Results

4.1.1 *Baseline Unit–Area Analysis*

After calibration and validation, the 20-year baseline model time series was used to assess the water balance for various land uses (Figure 4-1) and soil groups (Figure 4-2). Unsurprisingly, impervious surfaces demonstrate the most substantial deviation from natural watershed conditions such as forests and wetlands. Over 90% of the water balance for impervious surfaces is overland flow. The runoff generated from impervious surfaces is often conveyed to receiving waters including streams, rivers, and lakes where both the quantity and quality of stormwater can impact the health of the systems. Combined, groundwater and interflow represent the portion of the water balance that has been infiltrated into the ground and not removed by ET. Impervious surfaces provide no opportunity for infiltration. Interestingly, the water balance suggests that developed open space has a higher proportion of the water balance that is attributed to interflow and groundwater than forests. While infiltration occurs on both land types, a greater proportion in forests is returned to the atmosphere via ET.

Wetlands produce the most (~64%) ET and relatively little groundwater recharge. This is intuitive as many wetlands are locations of groundwater discharge rather than recharge. After wetlands, forests provide the most evapotranspiration, followed by agriculture, and developed open space. Evapotranspiration differences in soil groups are less pronounced, soils with lower infiltration rates (C, D) have less groundwater recharge than high infiltration soils (A, B).

4.1.2 *Relationships Between Impervious Cover and Watershed Function*

Modeling results from the three study sub-watersheds were assessed to improve the understanding between impervious cover and watershed function. Figure 4-3 presents the water balance and Figure 4-4 presents the FDCs for the three sub-watersheds. Since discharge (cubic feet per second [cfs]) is associated with watershed size, a standard FDC and one normalized by watershed area ($\frac{\text{daily flow in } ft^3}{\text{watershed area in } ft^2}$) are presented. The normalized FDC suggests that flows across the FDC tend to increase with imperviousness. Both Upper and Lower Hodges have higher normalized flows compared to Pilot Tributary. However, the high impervious watershed (Upper Hodges) FDC does appear to dip below the medium impervious watershed (Lower Hodges) at lower flows. Figure 4-5 shows that although slight, the two normalized FDCs for Upper and Lower Hodges cross each other, producing an ecosurplus and ecodeficit. The results suggest that initially, as development begins in a watershed, increases across the flow regime may be expected. However as impervious surfaces continue to increase, high flows will continue higher but low flows may begin to become lower. This relationship was further investigated using the Upper Hodges sub-watershed to study the effect of various land use scenarios.

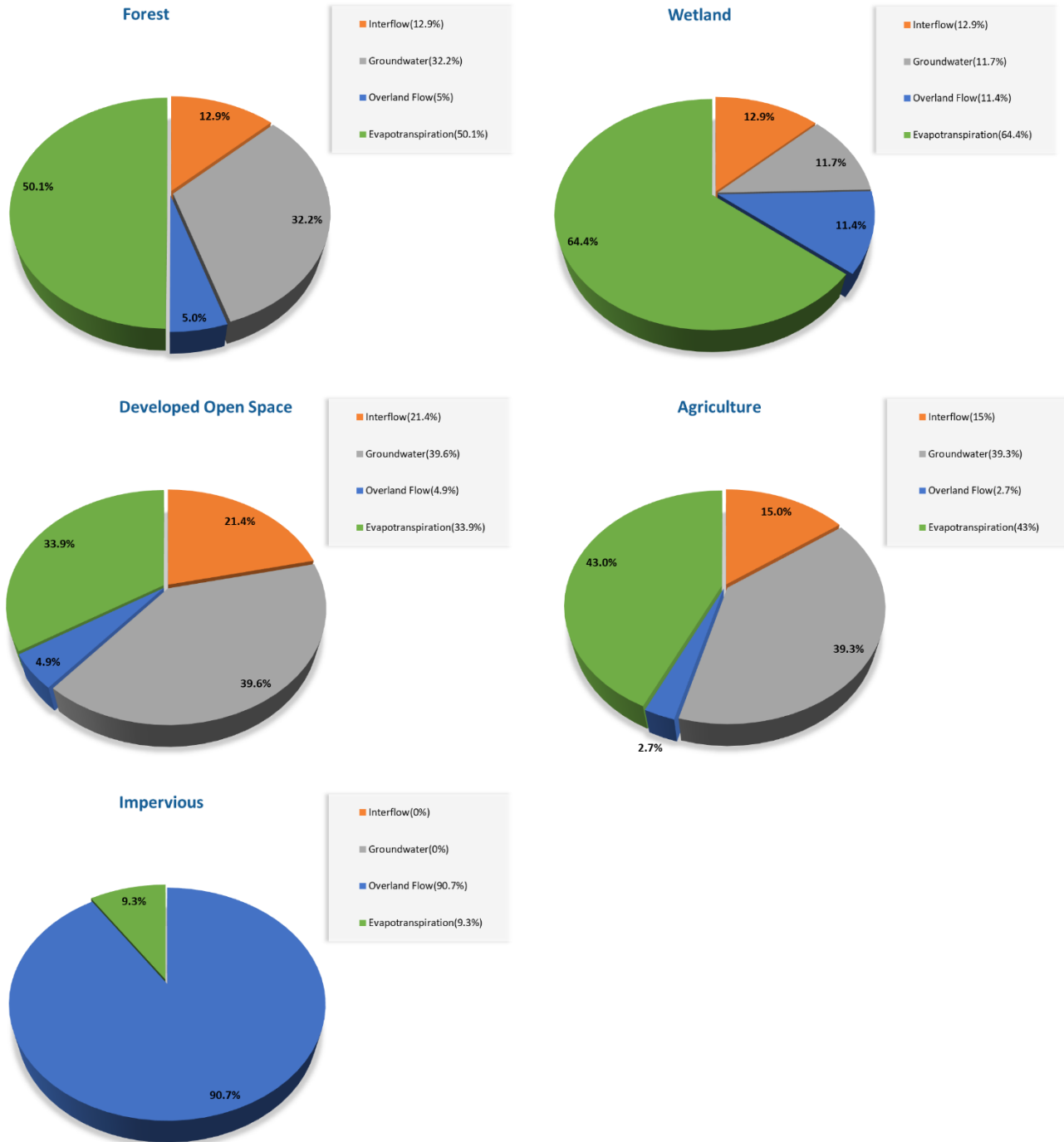


Figure 4-1. Water Balance for LSPC Hydrological Response Units, Summarized by Land Use. Baseline Simulation 2000-2020.

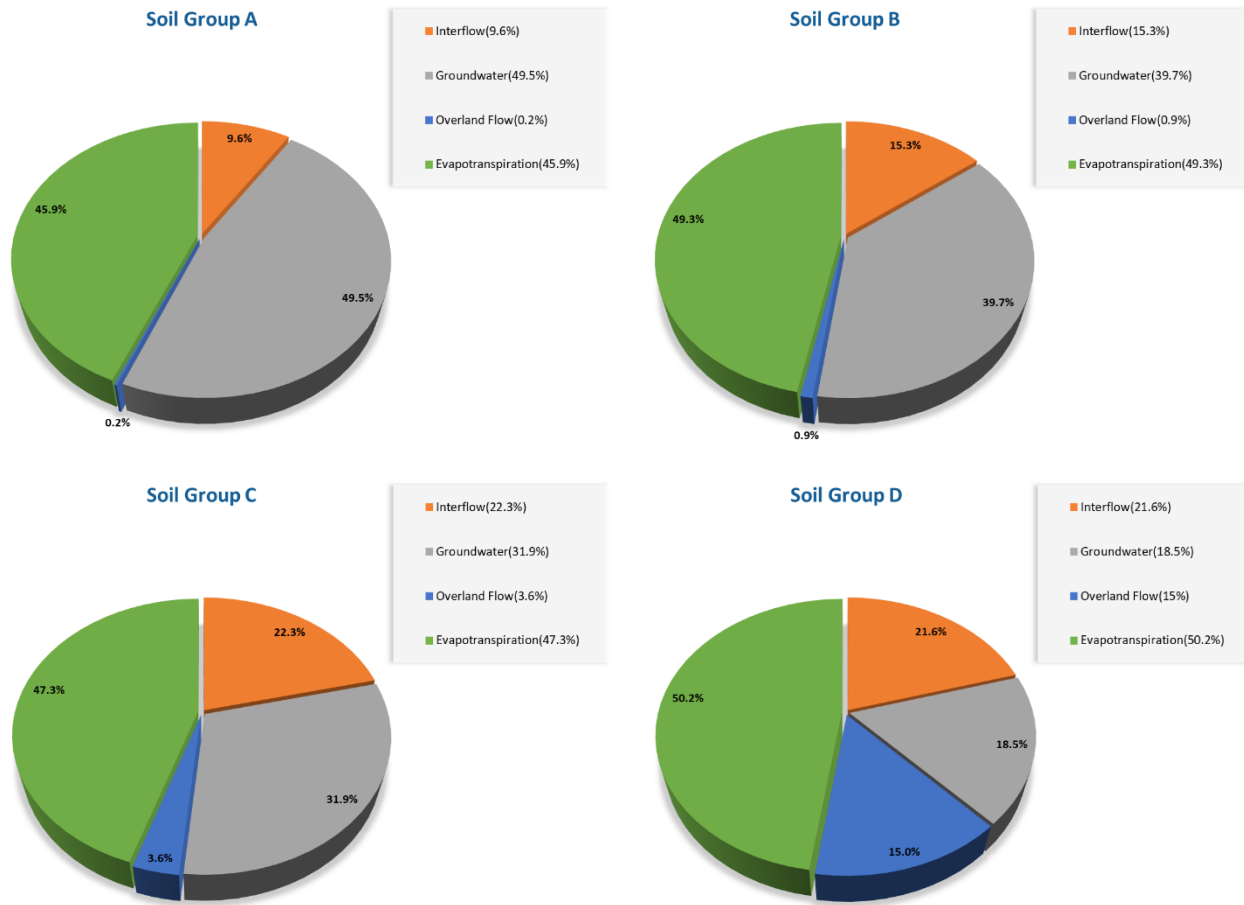


Figure 4-2. Water Balance for LSPC Hydrological Response Units, Summarized by Soil Group. Baseline Simulation 2000-2020.

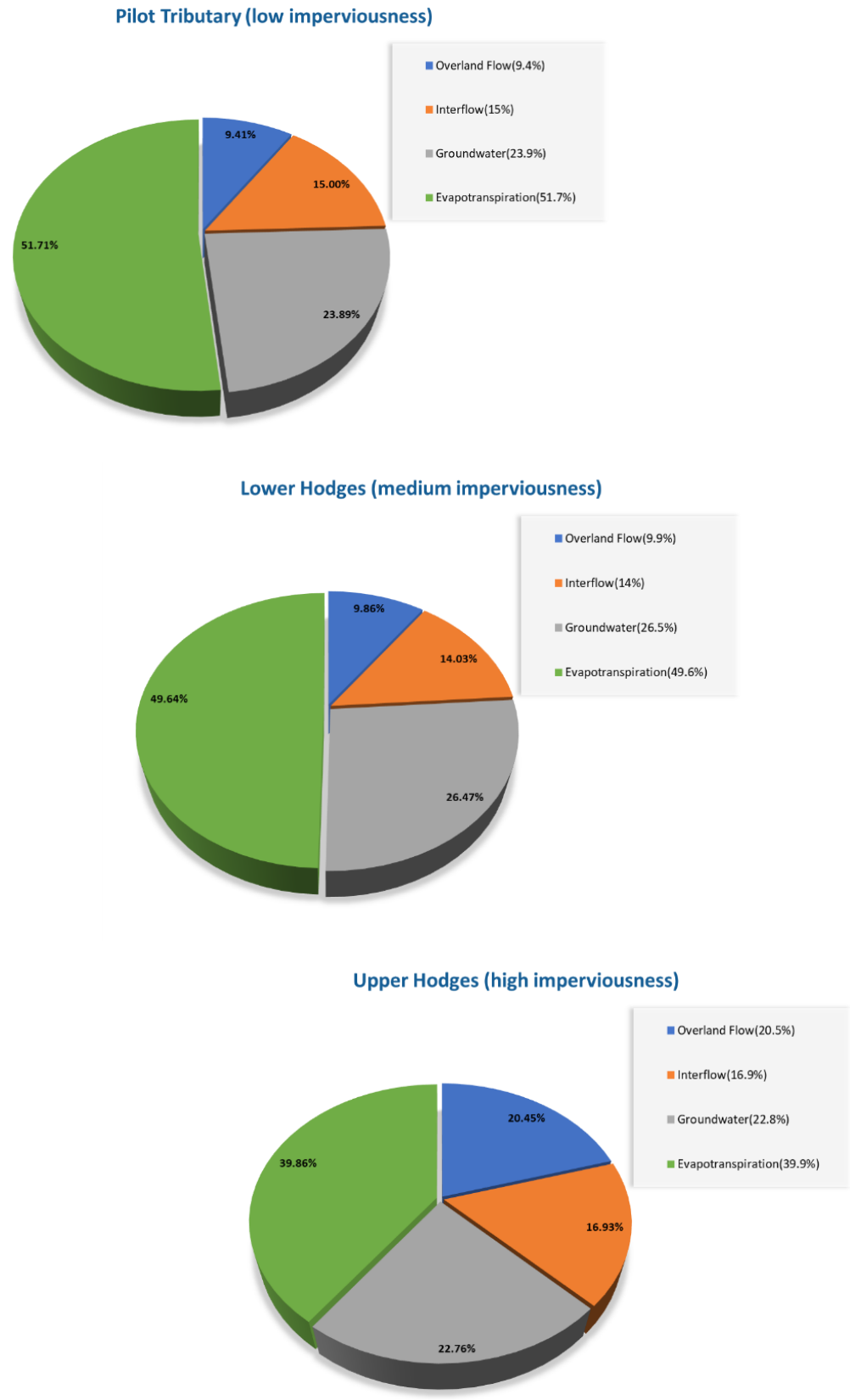


Figure 4-3. Water Balance for LSPC sub-watersheds.

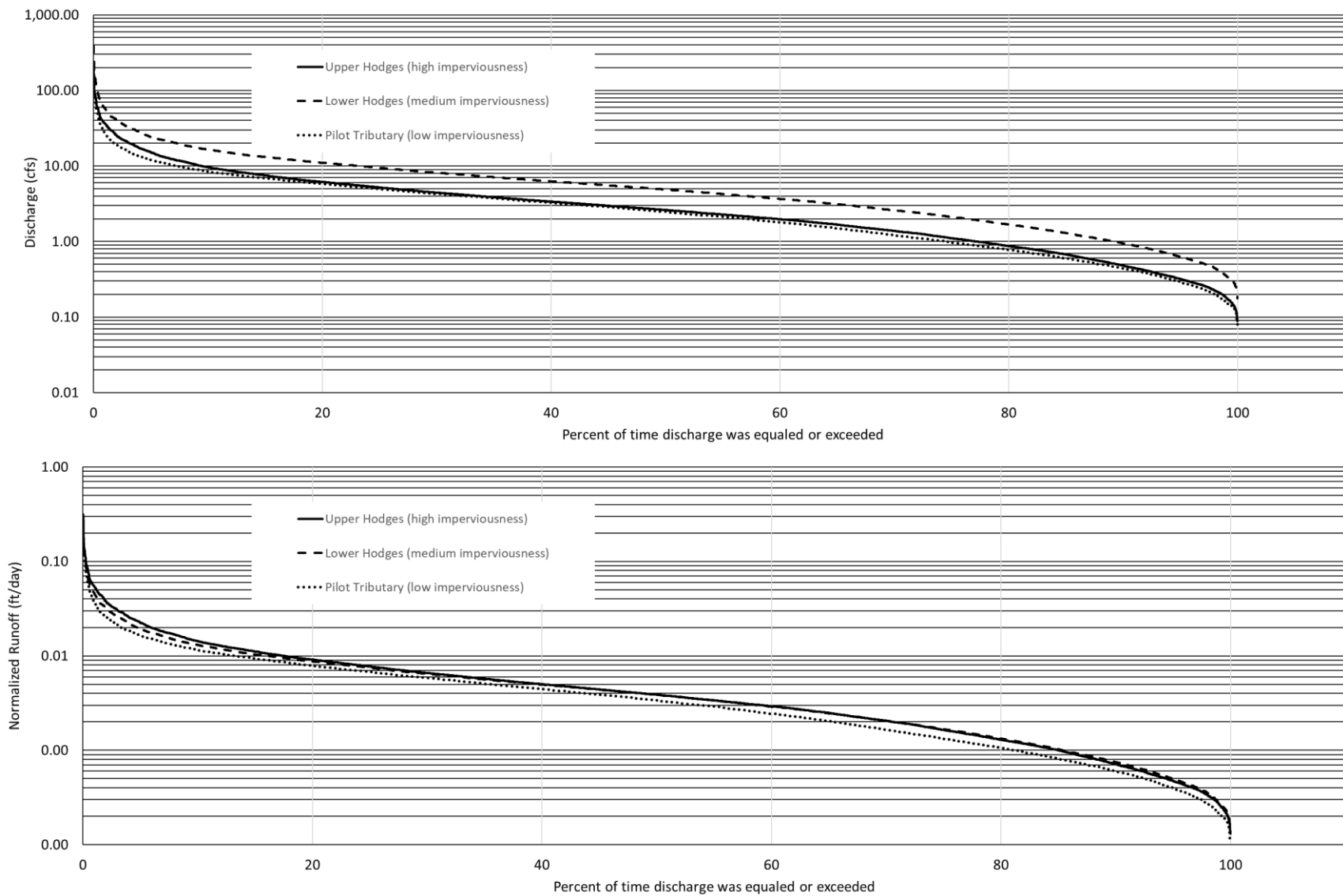


Figure 4-4. Standard FDC (top) and Normalized FDCs (bottom) for the three study watersheds.

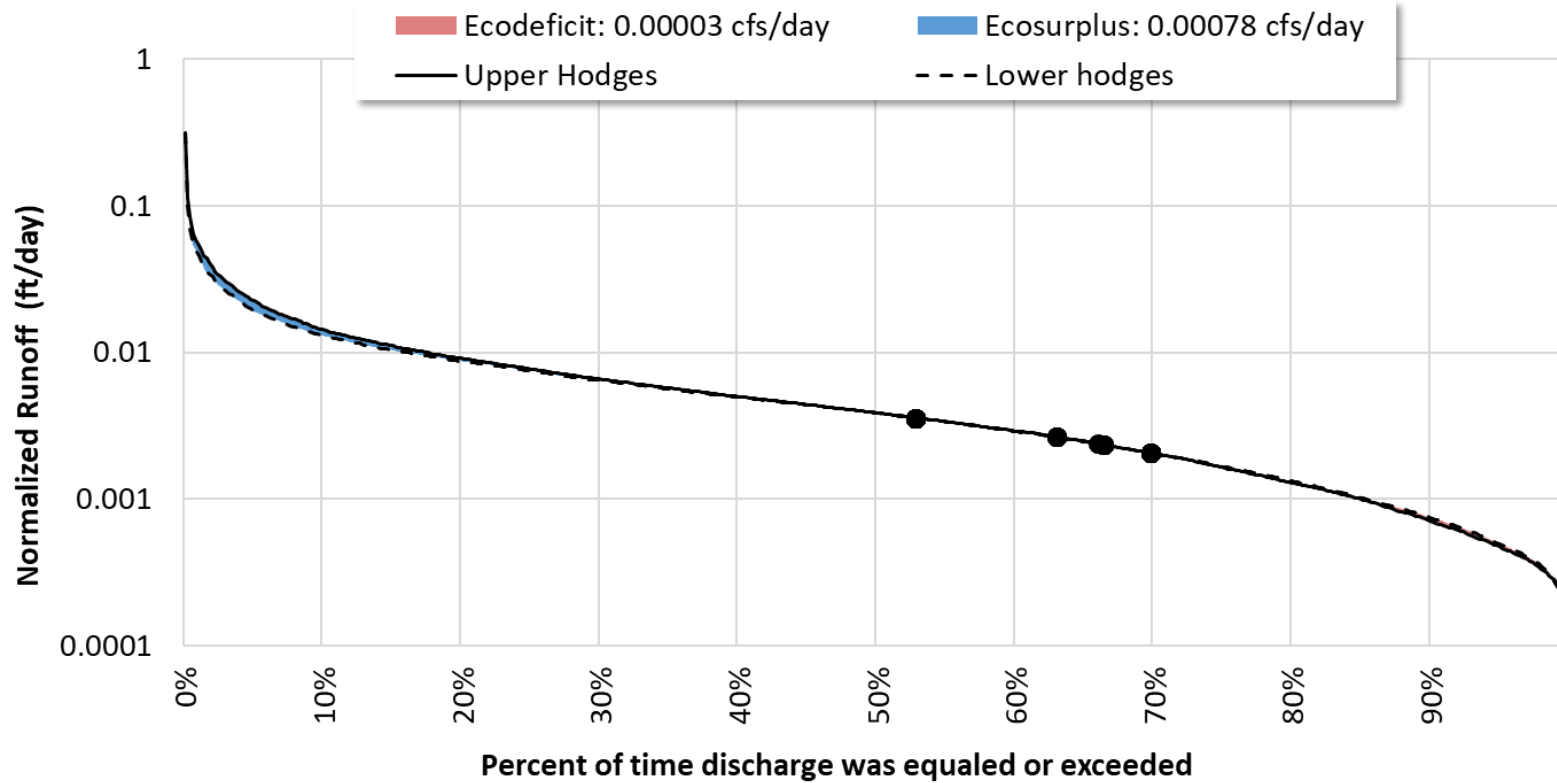


Figure 4-5. Ecosurplus and Ecodeficit for Upper Hodges compared to Lower Hodges.

Figure 4-7 presents the average monthly discharge for the three study sub-watersheds. When normalized by sub-watershed area, the differences between the most undeveloped sub-watershed (Pilot Tributary) and the more developed sub-watershed appear to increase in the summer months. The differences in ET between in Pilot Tributary and Upper Hodges Book in the overall water balance (Figure 4-3) are driven by a pronounced increase in ET from the Pilot Tributary in the summer months.

While increases in impervious surfaces have been shown to consistently increase the volume and flashiness of stormflows, studies have found diverse, sometimes contrasting responses to base flow (Hopkins et al., 2015). Bhaskar et al. (2016) found that total streamflow and baseflow increased in a watershed with LID practices during urbanization compared to control watersheds. The authors suggest that the flow regime changes may be due to a reduction in evapotranspiration associated with decreased vegetative cover as urbanization occurred and an increase in the point source of recharge. Both increases and decreases to flow regimes can have deleterious effects on both the ecology of a watershed as well as human health (See Appendix F). It is noted that the impact of SCMs on baseflow is a field of ongoing research, often relying on modeling approaches given the difficulty of monitoring baseflows at the local scale (Li et al., 2017).

Land Use Scenarios

To further investigate relationships between impervious cover and watershed functions, three land use scenarios were simulated using the Upper Hodges Brook sub-watershed. The Upper Hodges Brook was chosen as it had the most impervious cover of the three study sub-watersheds. Four scenarios were simulated for the sub-watershed (Table 4-1). Figure 4-7 and Figure 4-8 present flow duration curves for the four scenarios and present the high and low flow sections of those curves. Results support conclusions from others (Bhaskar et al., 2016) that watershed development and associated stormwater management, including disconnecting all impervious surfaces ($EIA = 0$) can result in consistently higher flows across the flow regime compared to pre-development conditions. Figure 4-9, Figure 4-10, and Figure 4-11 present water balance and FDCs for baseline conditions compared to $EIA = TIA$, pre-developed/forested, and $EIA = 0$, respectively. The figures present ecosurplus and ecodeficit in cfs/day as well as millions of gallons/year. Figure 4-12 presents average and minimum monthly flows for each land use scenario. As ET increases, average flows decrease for all scenarios. The pre-development scenario has the highest ET and the lowest average flows while the $EIA=TIA$ scenario has the lowest ET and the highest average flows. Interestingly, this relationship changes for low flows, where the most developed scenario ($EIA=TIA$) has the lowest low flows, and the disconnected scenario ($EIA = 0$) has the highest low flows. Figure 4-13 presents three-day minimum and maximum flows by land use scenario. The $EIA=TIA$ scenario consistently had the lowest minimum flows while the $EIA = 0$ scenario (all impervious surfaces disconnected) had the highest low flows. Furthermore, the $EIA=TIA$ scenario had the highest maximum three-day flows while pre-developed conditions had the lowest. Table 4-2 further supports these conclusions but is based on the average of flows over the simulation period. Table 4-3 presents a summary of average flows. Care should be taken in making conclusions only from average flows. While it would appear that the pre-development condition has consistently lower flows, Figure 4-8 and Figure 4-13 provide evidence that the $EIA=TIA$ scenario results in the lowest of low flow conditions.

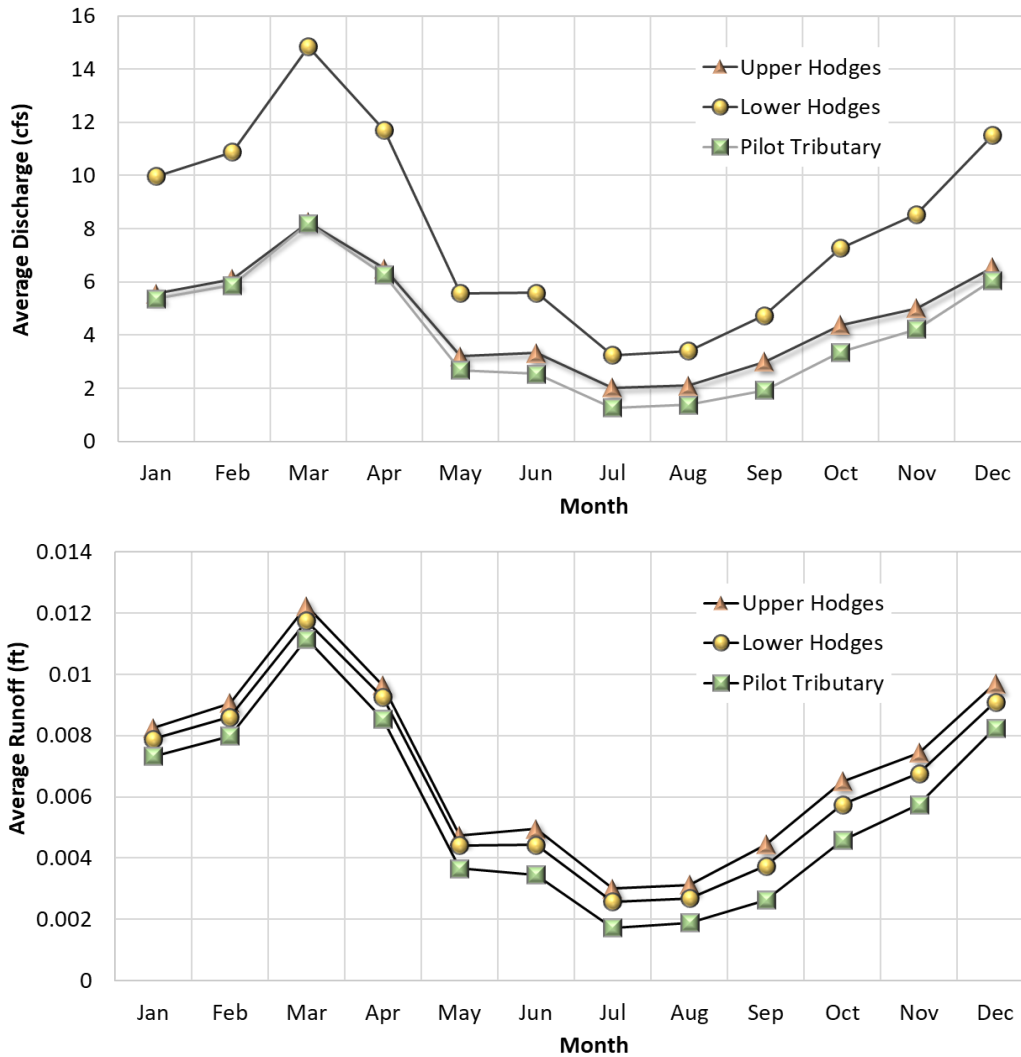


Figure 4-6. Average monthly discharge and runoff depth for the three study watersheds.

Table 4-1. Land Use Scenarios simulated using Upper Hodges Brook sub-watershed

Scenario	Description
Baseline/ Existing conditions	Existing land use and effective impervious surfaces as described in Section 2.
Pre-development/ forested	All land not classified as forest or wetland in the baseline conditions, including impervious surfaces, developed open space, and agriculture was converted to forested land cover but maintained their soil and slope classifications
EIA=TIA	Baseline Effective Impervious Area was increased to the Total Impervious Area. Therefore, the effect of the Sutherland Equations discussed in Section 3.3.1 was removed, and all mapped impervious surfaces were assumed to be directly connected to the stream channel. This resulted in an increase of EIA from 15% to 32%.
EIA=0	Effective Impervious Area was converted to pervious developed open space. This represents a scenario where all existing impervious surfaces have been disconnected.

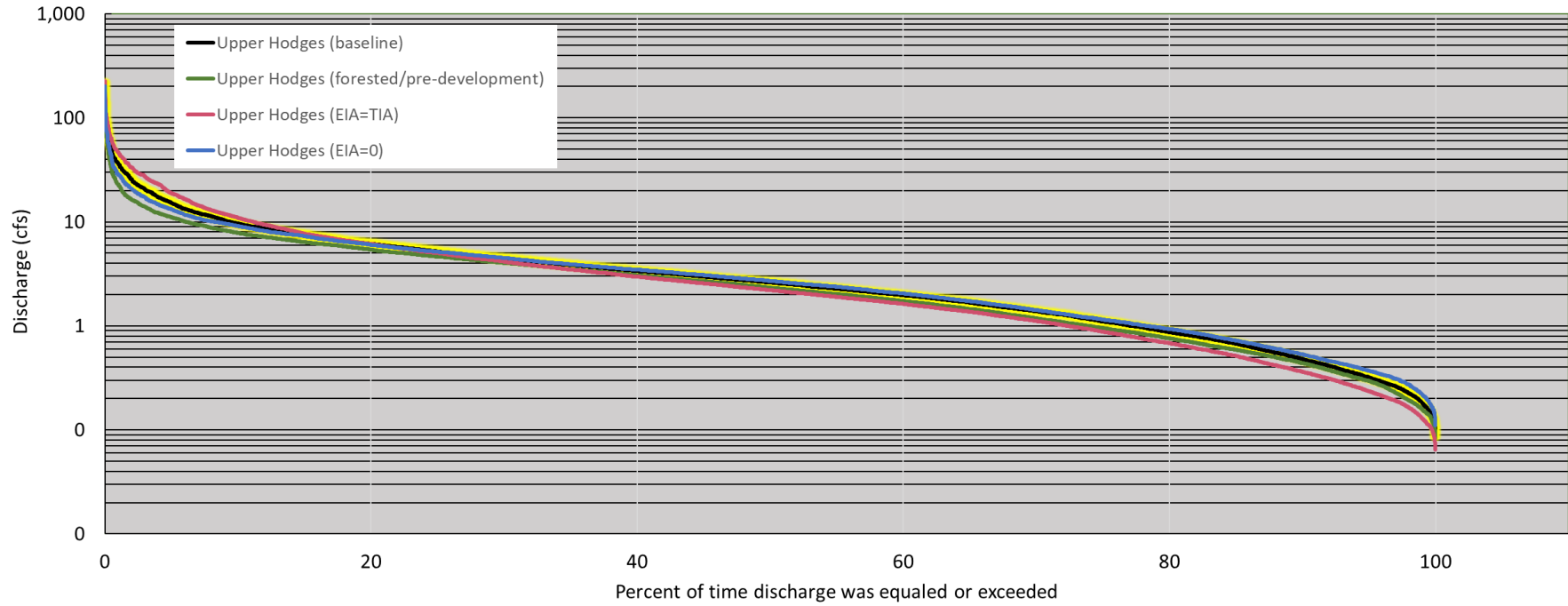


Figure 4-7. Flow Duration Curves for Upper Hodges Brook watershed for baseline, predevelopment, EIA=TIA, and EIA=0 conditions. Baseline FDC is black with a yellow highlight.,

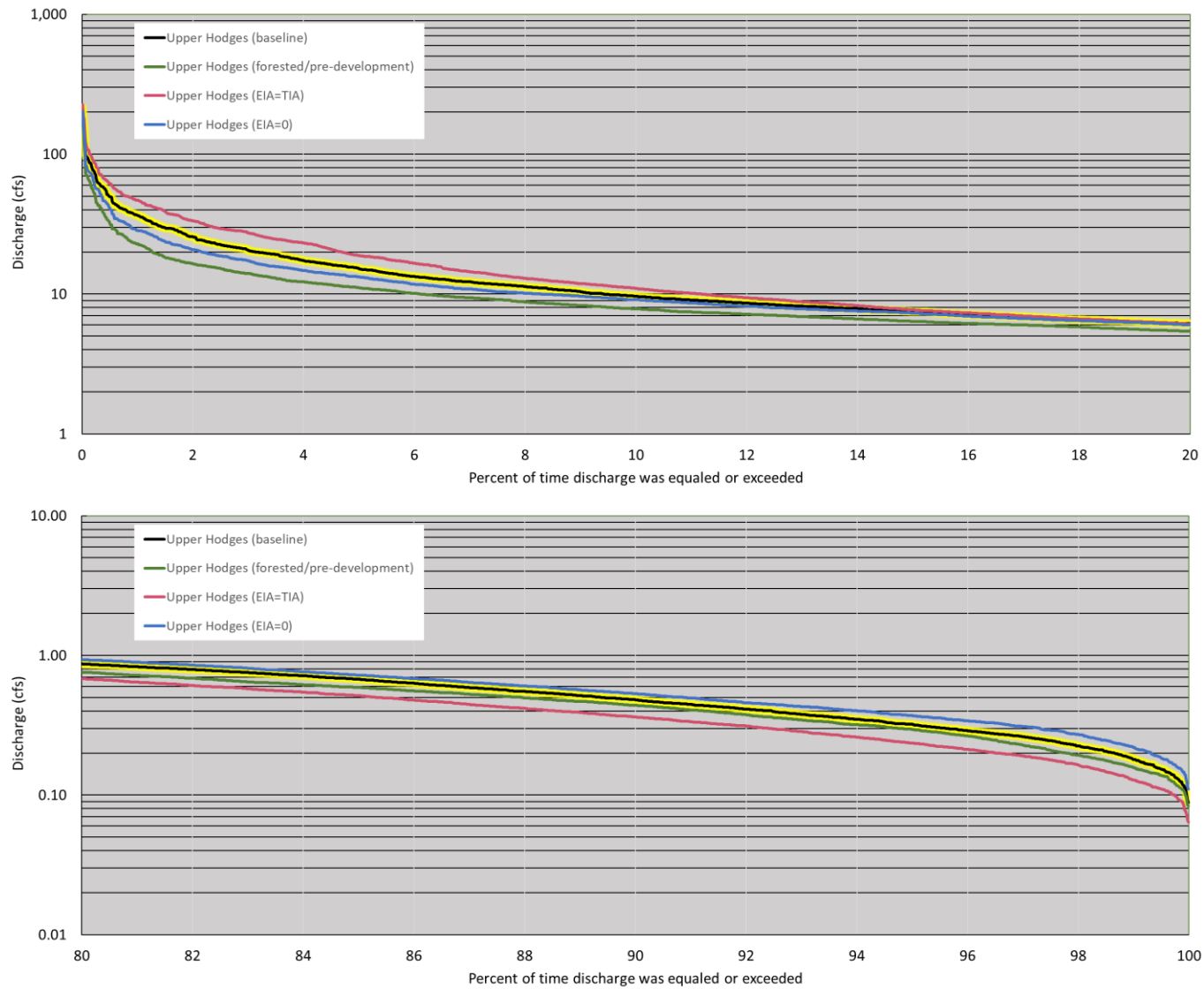


Figure 4-8. High flow (top) and low flow (bottom) sections of the FDC-presented in Figure 4-7 Baseline FDC is black with a yellow highlight.

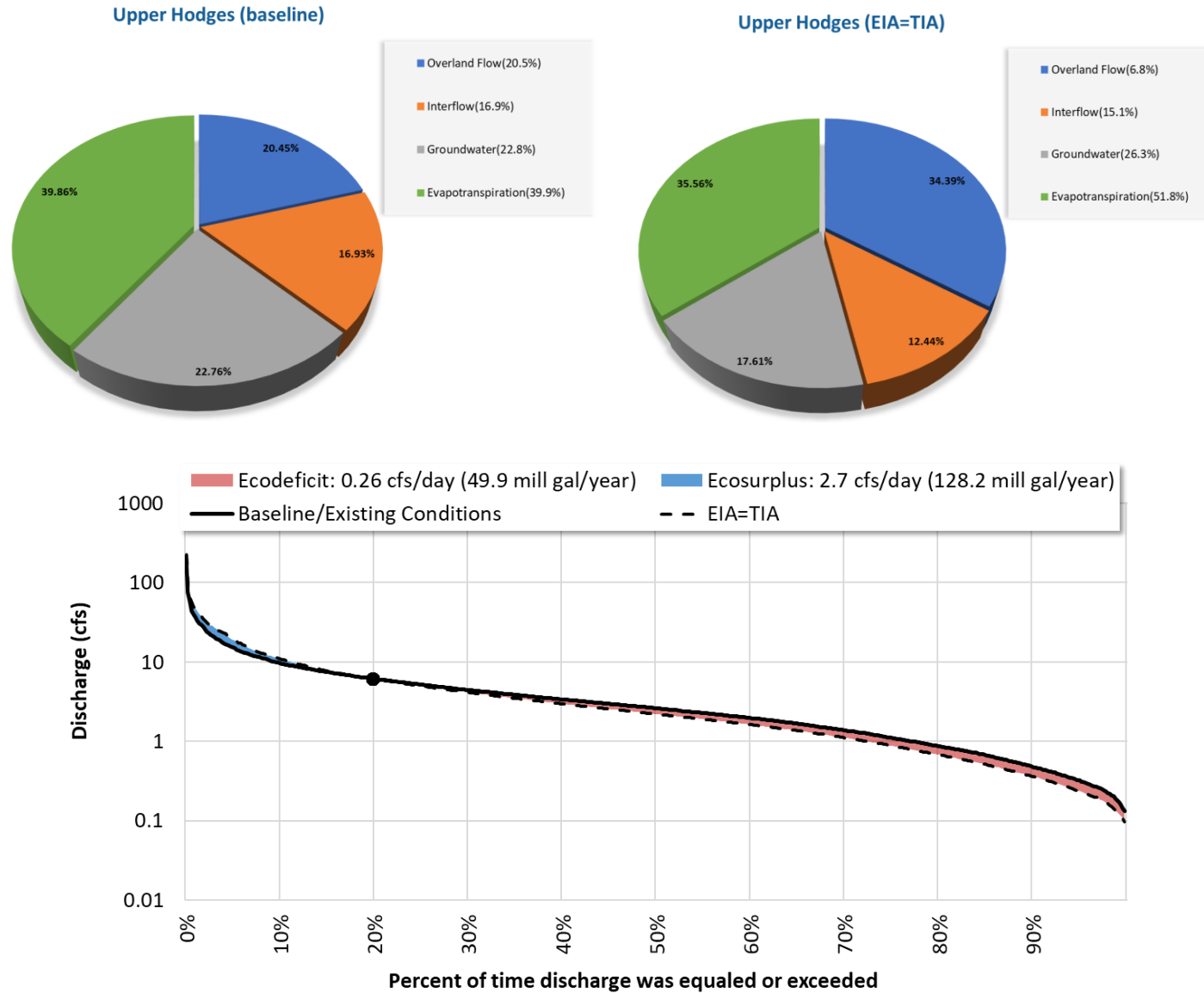


Figure 4-9. Water balances and Ecosurplus and Ecodeficit for Upper Hodges Brook watershed for baseline and EIA=TIA conditions. EIA=TIA reflects an increase in directly connected impervious surfaces. Black dots indicate places where FDCs cross.

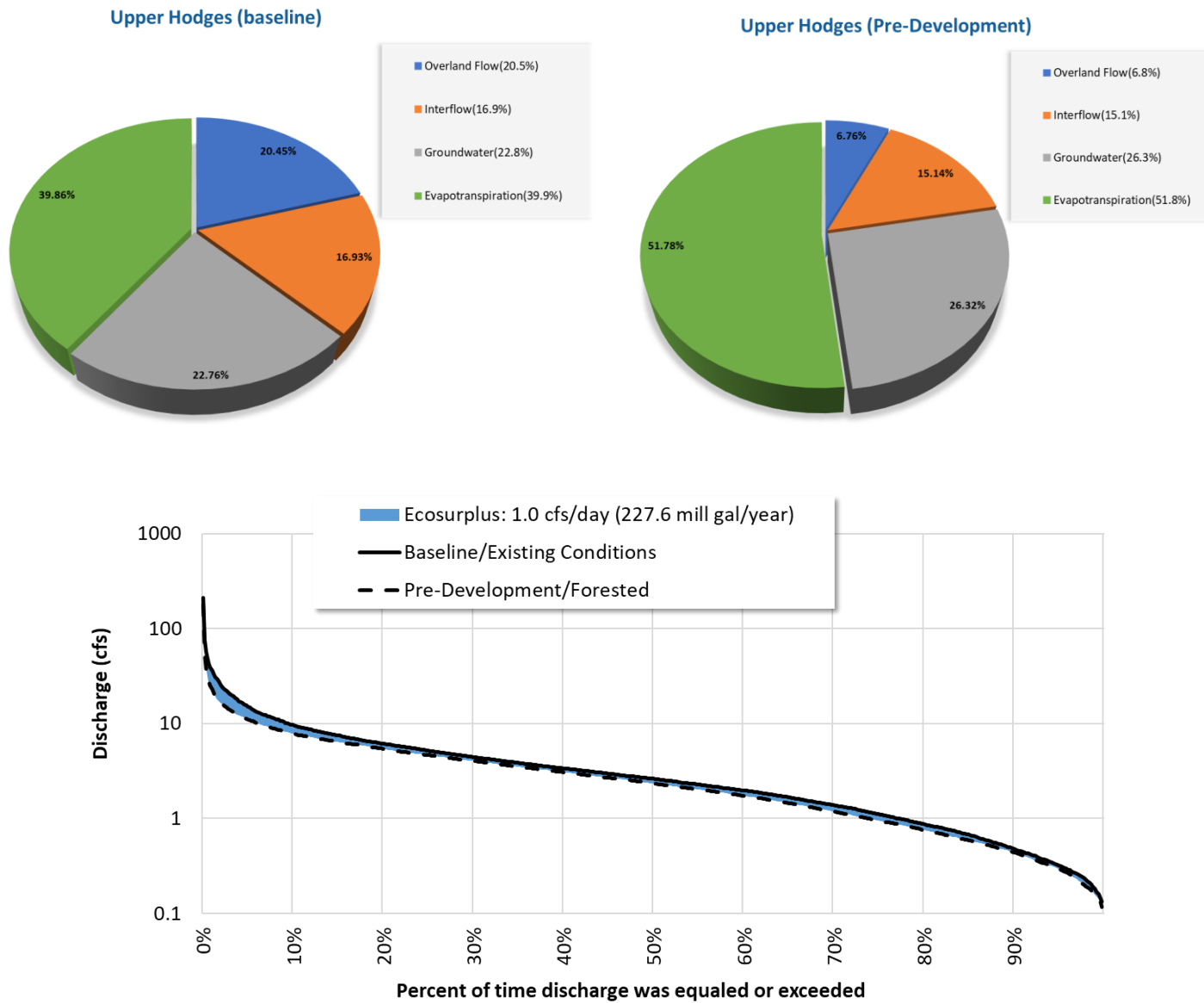


Figure 4-10. Water balances and Ecosurplus for Upper Hodges Brook watershed for baseline and forested/pre-development conditions. Ecosurplus calculated relative to forested/pre-development conditions.

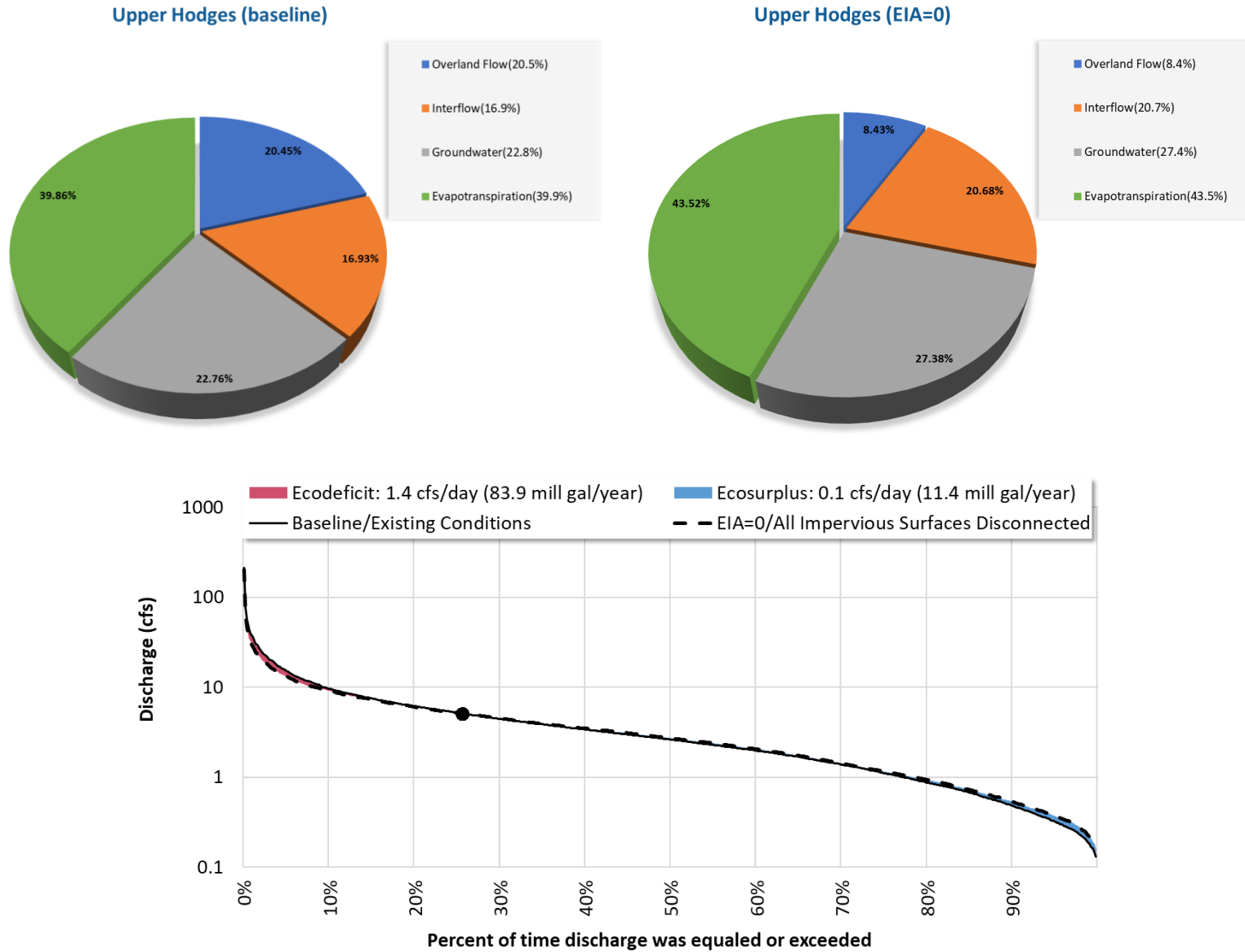


Figure 4-11. Water balances and Ecosurplus/Ecodeficit for Upper Hodges Brook watershed for baseline and EIA = 0 (all existing impervious surfaces disconnected). Ecosurplus/Ecodeficit calculated relative to baseline/existing condition. Black dots indicate places where FDCs cross each other.

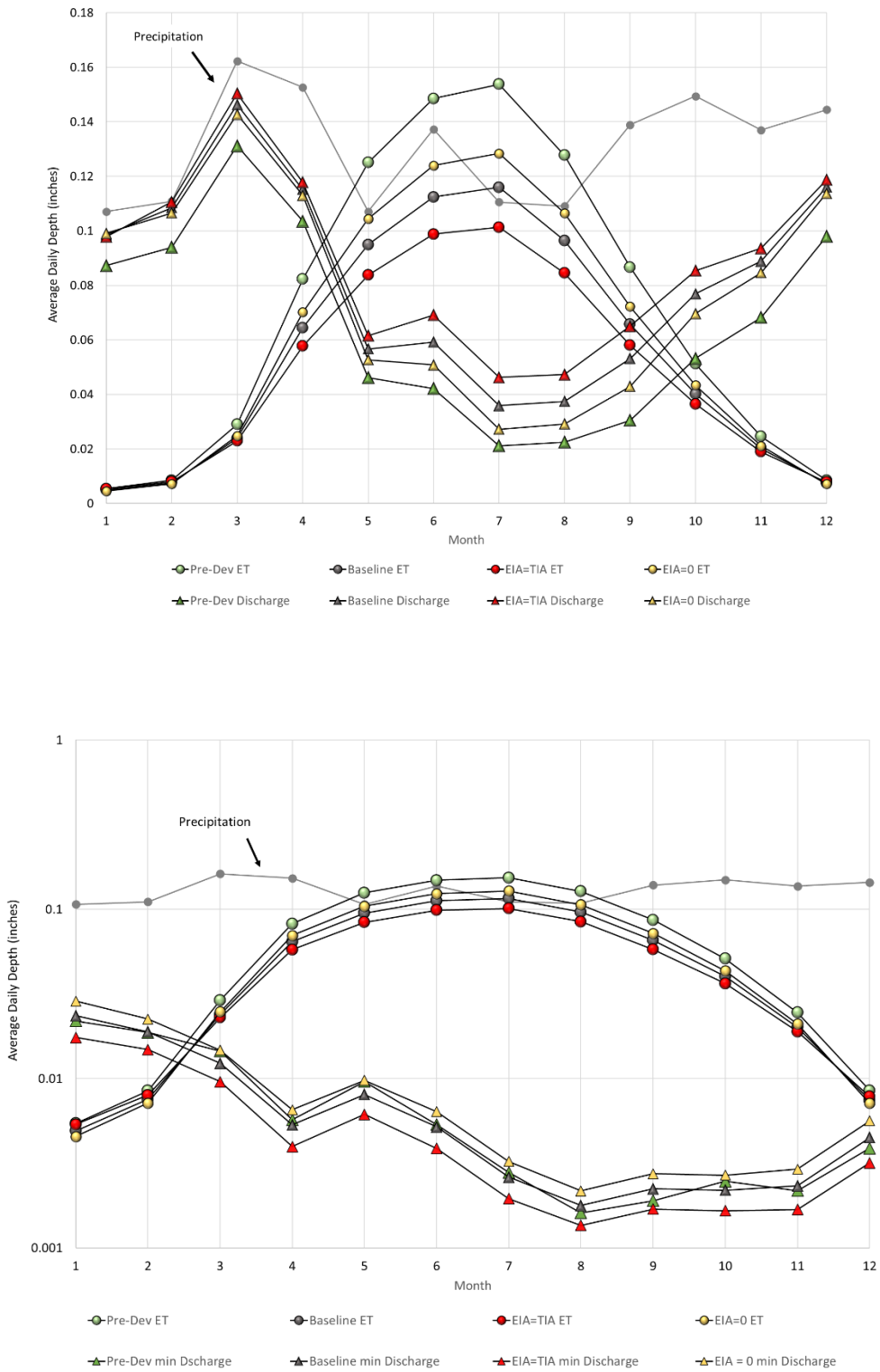


Figure 4-12. Average (top) and minimum (bottom) monthly flows for land use scenarios. Minimum flows are presented on a logarithmic scale.

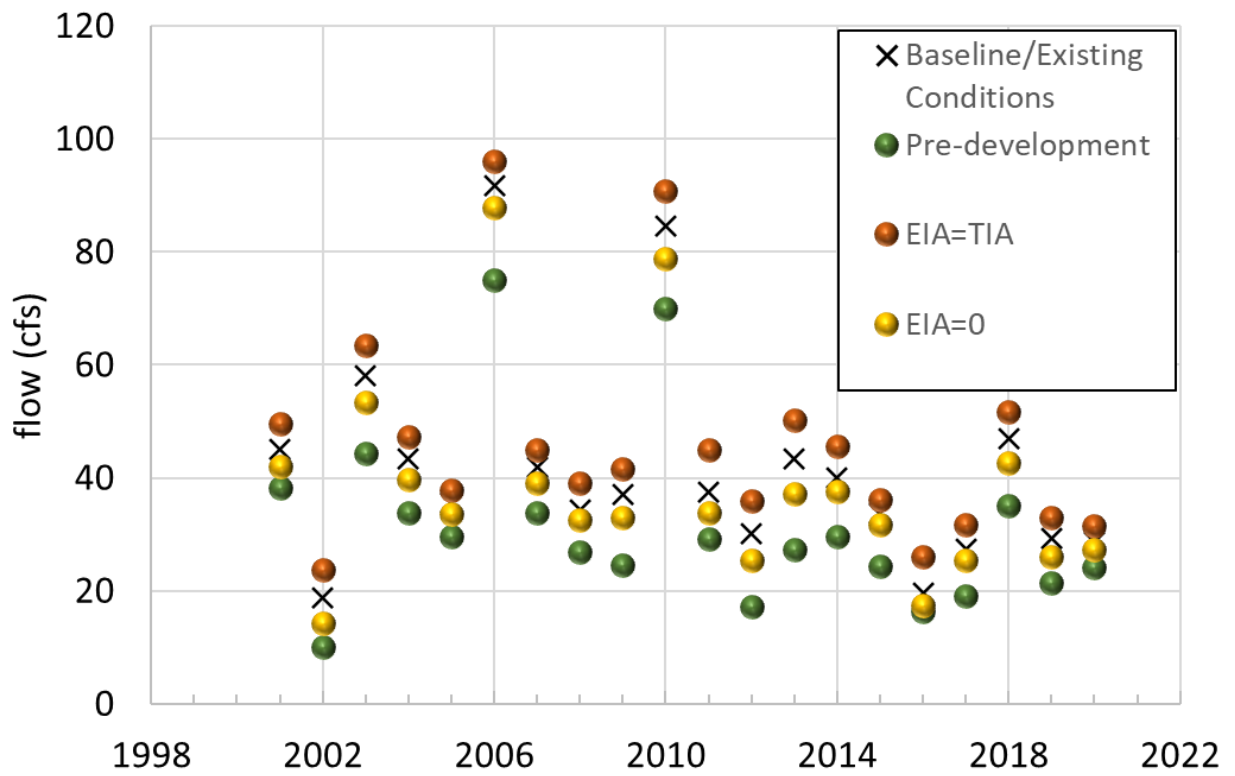
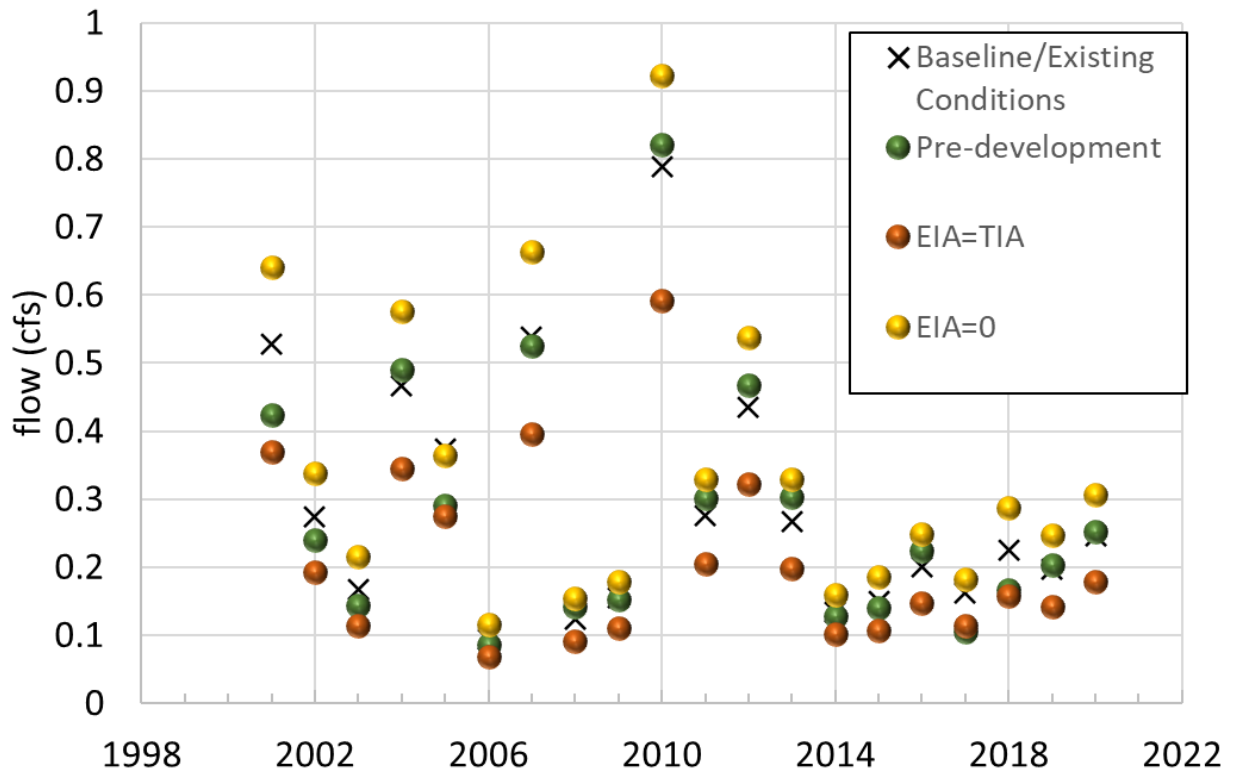


Figure 4-13. Three-day minimum (top) and maximum (bottom) flow for land use scenarios.

Table 4-2. Comparison of average 3-day minimum and maximum flows for baseline and land use scenarios

Average annual flows	Baseline	Pre-development/ Forested		EIA=TIA		EIA = 0	
	cfs	cfs	% diff from baseline	cfs	% diff from baseline	cfs	% diff from baseline
3-day minimum	0.29	0.28	-3.4%	0.21	-27.6%	0.35	20.7%
3-day maximum	41.38	31.51	-23.9%	46.05	11.3%	37.94	-8.3%

Table 4-3. Summary of average monthly flows and percent differences for land use scenarios

Month	Baseline	Pre-development /Forested		All existing impervious directly connected		All existing impervious disconnected	
	Average cfs	Average cfs	% Difference from baseline	Average cfs	% Difference from baseline	Average cfs	% Difference from baseline
January	5.56	4.91	-11.60%	5.52	-0.72%	5.58	0.42%
February	6.11	5.28	-13.50%	6.23	1.93%	5.99	-1.90%
March	8.25	7.39	-10.42%	8.47	2.67%	8.04	-2.52%
April	6.50	5.83	-10.30%	6.65	2.28%	6.36	-2.12%
May	3.20	2.60	-18.79%	3.47	8.56%	2.96	-7.24%
June	3.34	2.37	-29.02%	3.89	16.74%	2.86	-14.36%
July	2.02	1.18	-41.43%	2.60	28.73%	1.52	-24.51%
August	2.11	1.26	-40.29%	2.66	26.30%	1.63	-22.47%
September	2.99	1.71	-42.85%	3.67	22.47%	2.41	-19.38%
October	4.34	3.00	-30.95%	4.82	10.97%	3.92	-9.66%
November	5.01	3.84	-23.34%	5.28	5.35%	4.77	-4.87%
December	6.55	5.52	-15.72%	6.69	2.23%	6.40	-2.17%

4.1.3 Pollutant Export

The impact of land use scenarios on water quality was assessed by quantifying the average annual export of sediment, total phosphorus, total nitrogen, and zinc (Figure 4-14). Results are relatively straightforward, whereby a scenario of 32% completely connected impervious surfaces results in the highest loadings. Forested conditions and the scenario where all impervious surfaces are managed through disconnection have lower pollutant export rates.

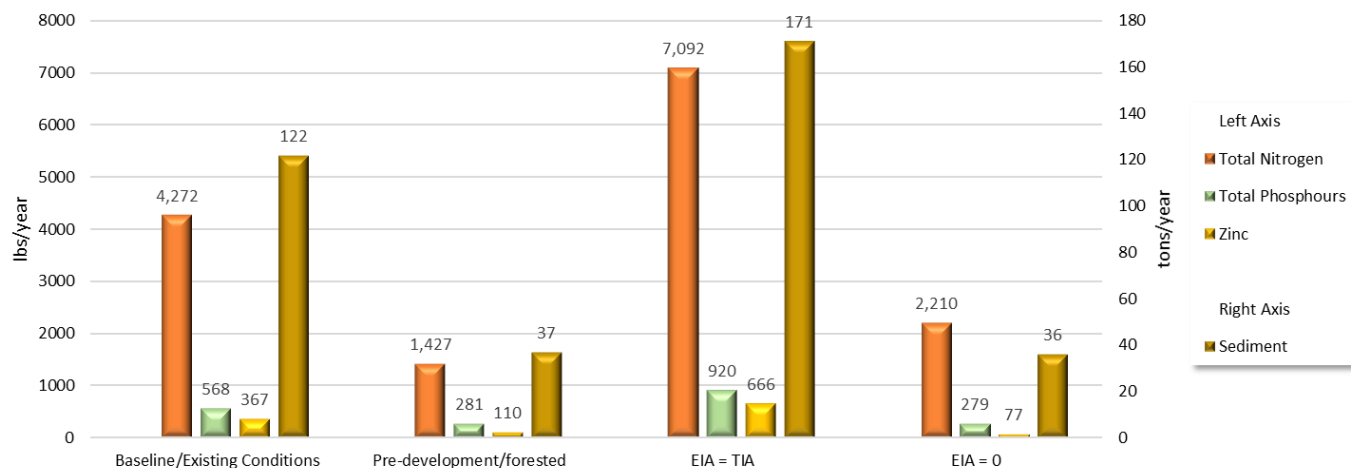


Figure 4-14. Pollutant export comparisons across land use scenarios.

4.1.4 Latent Heat and Carbon Sequestration

The effects of land use on heat exchange and carbon sequestration were investigated. Heat exchange was assessed for its impact on evaporative cooling. The impact that solar radiation has on a watershed depends on the land cover and the availability of water. When solar energy hits dry, non-vegetated surfaces, such as pavement or asphalt, that energy is converted to sensible heat, which warms up the ground and the air above it. However, vegetated surfaces use solar energy during evapotranspiration, in which water is taken up by roots, transferred via plant transport tissue to leaves where it then evaporates through the stomata. During evaporation, a phase change occurs where the liquid water in the plant is released as water vapor to the surrounding air. The energy that would have otherwise been sensible heat, warming the ground and air, is converted to latent heat. This results in a cooling effect due to energy (heat) being absorbed by water vapor as it changes from liquid to gas; humans beings take advantage of this same process by sweating to lower their body temperature. The cooling impact of land cover can therefore be quantified by the latent heat flux. Average annual HRU-level evapotranspiration rates (mm year^{-1}) were converted to latent heat flux ($\text{MJ m}^{-2} \text{year}^{-1}$) using a conversion factor of 2.45 and an assumed temperature of 20°C . Figure 4-15 presents maps showing the average annual latent heat flux across the three study sub-watersheds and the Wading River watershed. Upper Hodges had the lowest amount of latent heat flux, with an average of $1,244 \text{ MJ m}^{-2} \text{year}^{-1}$, while Pilot Tributary had the most ($1,617 \text{ MJ m}^{-2} \text{year}^{-1}$), Lower Hodges was between the two with $1,379 \text{ MJ m}^{-2} \text{year}^{-1}$. The cooling impact of forests on the air can be substantial. For example, a simulation of deforestation in northern Pennsylvania and southern New York showed decreased latent heat flux and an increase in summer air temperatures of at least 1.5°C (Klingaman et al., 2008). Similarly, modeling of land cover change in New Jersey indicates that compared to agricultural land cover, maximum daily temperatures are at least 1°C warmer in highly urban locations, but $0.3\text{-}0.6^{\circ}\text{C}$ cooler in reforested areas (Wichansky et al., 2008) The difference in latent heat flux between the Pilot Tributary and Upper Hodges in this research suggests that the difference in vegetative cover would also result in a difference in sensible heat, with the more urbanized Upper Hodges having higher temperatures.

Carbon sequestration is the process of capturing and storing atmospheric carbon dioxide (CO₂) which is the most produced greenhouse gas. Carbon is sequestered in vegetation such as grasslands or forests, as well as in soils as organic carbon. Activities that involve land conservation or restoration and some agricultural Nature-Based Solutions (NBS) and green infrastructure BMPs can sequester carbon. Forests, grasslands, peat swamps, and other terrestrial ecosystems collectively store much more carbon than does the atmosphere (Lal 2004). By storing this carbon in wood, other biomass, and soil, ecosystems keep CO₂ out of the atmosphere, where it would contribute to climate change. Beyond just storing carbon, many systems also continue to accumulate it in plants and soil over time, thereby “sequestering” additional carbon each year.

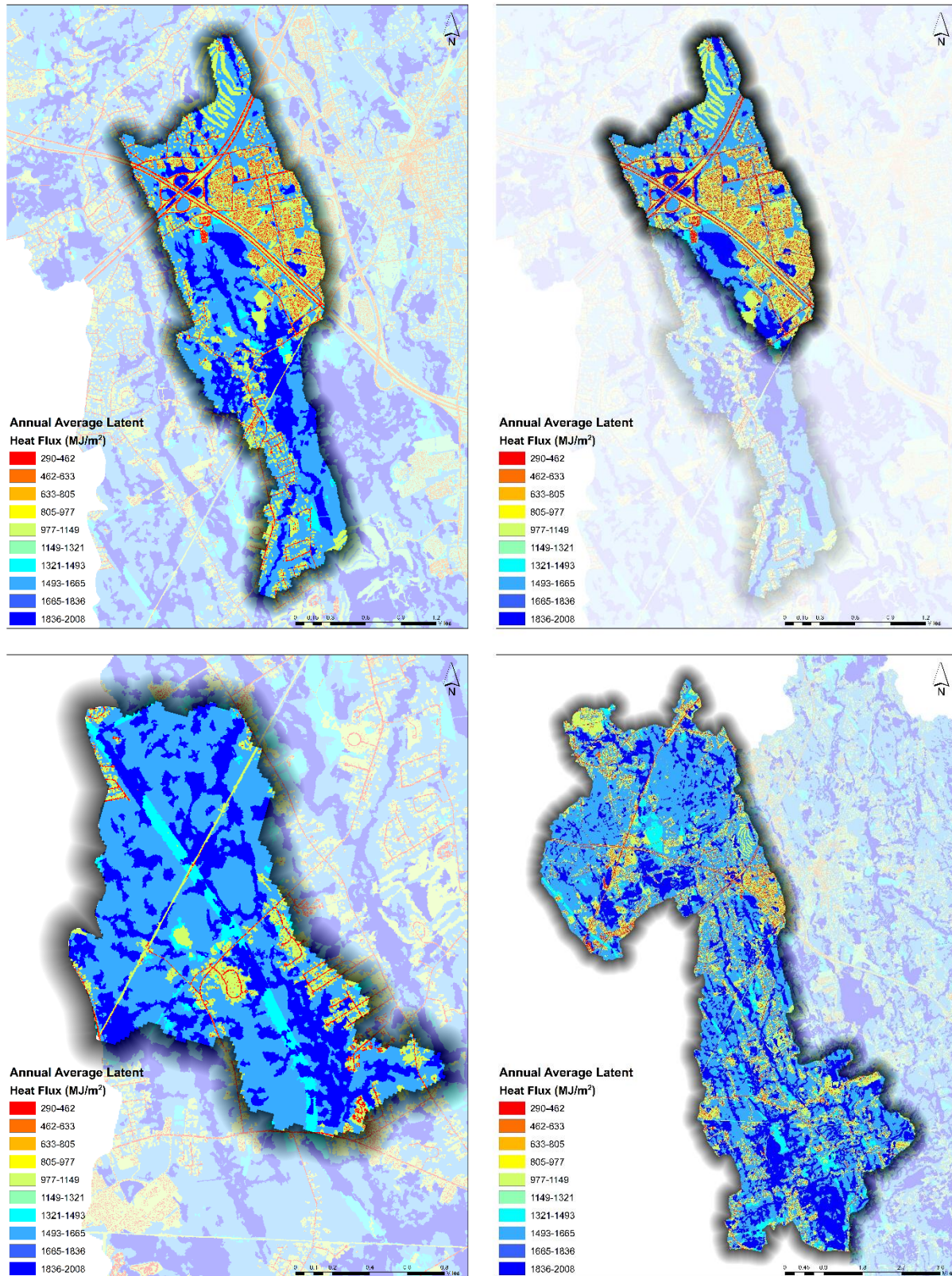


Figure 4-15. Average Annual Latent Heat Flux for Hodges Brook (top left), Upper Hodges Brook (top right), Pilot Tributary (bottom left), and Wading River (bottom right).

Disturbing these systems with fire, disease, or vegetation conversion (e.g., land use/land cover (LULC) conversion) can release large amounts of CO₂. Other management changes, like forest restoration or alternative agricultural practices, can lead to the storage of large amounts of CO₂. Therefore, managing terrestrial ecosystems is critical to regulating our climate (Brill et al., 2021). The Natural Capital Project's InVEST (Integrated Valuation of Ecosystem Services and Tradeoffs) open-source software uses a relatively simple terrestrial ecosystem biomass and soil carbon model to calculate net annual carbon balance (positive or negative) following a change from one land use/land cover (LULC) type to another and based on global datasets of LULC, soil carbon, and other parameters. Stock-change or gain-loss methods to estimate avoided CO₂ emissions or CO₂ removals (Table 4-4) are typically based on information regarding activity data (i.e., hectares of protected area) and emission factors (i.e., tons of avoided CO₂).

Given a range of data, carbon storage data should be set equal to the average carbon storage values for each LULC class. The ideal data source for all carbon stocks is a set of local field estimates, where carbon storage for all relevant stocks has been directly measured. These can be summarized to the LULC map, including any stratification by age or other variables. For this analysis, the default sample dataset from InVEST carbon model was used and a crosswalk table was developed for mapping the LULC classification of the carbon pool dataset with the HRU classification of the Wading River model ([Task 6 Memo](#)). The results from the InVEST Carbon model are presented in Table 4-5. The results show that the existing land use/land cover condition has reduced 58%, 27%, and 20% of the Carbon pool compared to the predevelopment/forested condition for Upper Hodges Brook, Lower Hodges Brook, and Pilot Tributary sub-watersheds, respectively.

The model limitations include; (1) the land use/land cover types are not gaining or losing carbon over time whereas in reality with age the same LULC could be accumulating more carbon, (2) carbon storage is fixed for a given LULC type and does not account for the age, so the storage varies only across the LULC types, (3) the model does not capture the movement of carbon from above-ground biomass to other dead organic material, (4) the carbon sequestration is assumed to be linear change over the time while most sequestration follows a non-linear path such that carbon is sequestered at a higher rate in the first few years and a lower rate in subsequent years.

Table 4-4. Carbon benefits and associated activities, indicators, and calculation methods (Brill et al., 2021)

Benefit	Habitat Intervention	Activity	Indicator	Calculation Method
Improved carbon sequestration	Land restoration, wetland, and mangrove restoration	Plant/restore native vegetation, introduce grazing management systems	CO ₂ removals by above and below-ground biomass and soil	Stock-change or gain-loss methods
	Agricultural management	Agricultural NBS (introduce grazing management systems, plant vegetation buffers)	CO ₂ removals by above and below-ground biomass and soil	Stock-change or gain-loss methods
Reduced/avoided carbon emissions	Land (forest, grassland) protection	Avoided habitat conversion (forest, grassland)	Avoided CO ₂ emissions from above- and belowground biomass and soil	Stock-change or gain-loss methods
	Agricultural management	Agricultural NBS (activities relating to rice management like restoring/improving soil health)	Avoided CH ₄ emissions from soil (rice fields)	Stock-change or gain-loss methods

Benefit	Habitat Intervention	Activity	Indicator	Calculation Method
	Wetland protection	Avoided habitat conversion	Avoided CH ₄ emissions from the soil at wetlands	Stock-change or gain-loss methods

Table 4-5. InVEST carbon model results for three pilot sub-watersheds

Total Carbon (megagrams)	Upper Hodge Brook	Lower Hodge Brook	Pilot Tributary
Predevelopment/Forested Condition	109,290	82,405	99,350
Existing Land Use/Land Cover Condition	45,628	60,065	79,233
Change in Carbon for Existing Condition	-63,662	-22,340	-20,117
Percent Change in Carbon for Existing Condition	-58%	-27%	-20%

Note: 1 megagram = 1.102 US ton

4.1.5 Climate Change Scenarios

Climate change scenario outputs are typically highly complex and can vary in many ways. For example, a time series could vary over time, with higher flows later in the century, and different GCM/RCP scenarios could have different characteristics, such as shorter, more intense storms in one GCM compared to another. Often, the size of downscaled GCM datasets can be overwhelming when analyzing hydrologic impacts. This presented a challenge—the size and number of datasets required a screening and selection process to identify a manageable subset of scenarios, but the complexity and richness of the data made summarizing such a complex dataset inherently difficult. To resolve this challenge, the screening of future climate scenarios was based on the ecosurpluses and deficits that they produced. The approach identified which models produced the 20th, 50th and 80th percentile ecosurpluses and ecodeficits for RCP 4.5 and 8.5 scenarios. Therefore, a total of 12 potential models were selected for further analysis: three models for ecosurpluses at RCP 4.5, three models for ecodeficits at RCP 4.5, three models for ecosurpluses at RCP 8.5, and three models for ecodeficits at RCP 8.5. The period of 2079-2099 was selected as a future period to compare to the baseline scenario, which was the 20 years from Oct 2000 – Sep 2020. For both the baseline/existing conditions simulation from 2000-2020 and the future climate simulations from 2079-2099, the HRU distribution remained the same, representing the most recently available landcover data, discussed in Section 2 and the [Task 5 Memo](#). Therefore, any changes to the flow regime may be attributable to changes in the meteorological conditions simulated. Figure 4-16 presents the ensemble model results for ecodeficits and surpluses. The results suggest that overall, the magnitude of change between deficits and surpluses is similar. The RCP 8.5 scenario produces larger ecodeficits than the RCP 4.5 scenario while RCP 4.5 and 8.5 have appeared to be relatively similar in terms of ecosurpluses.

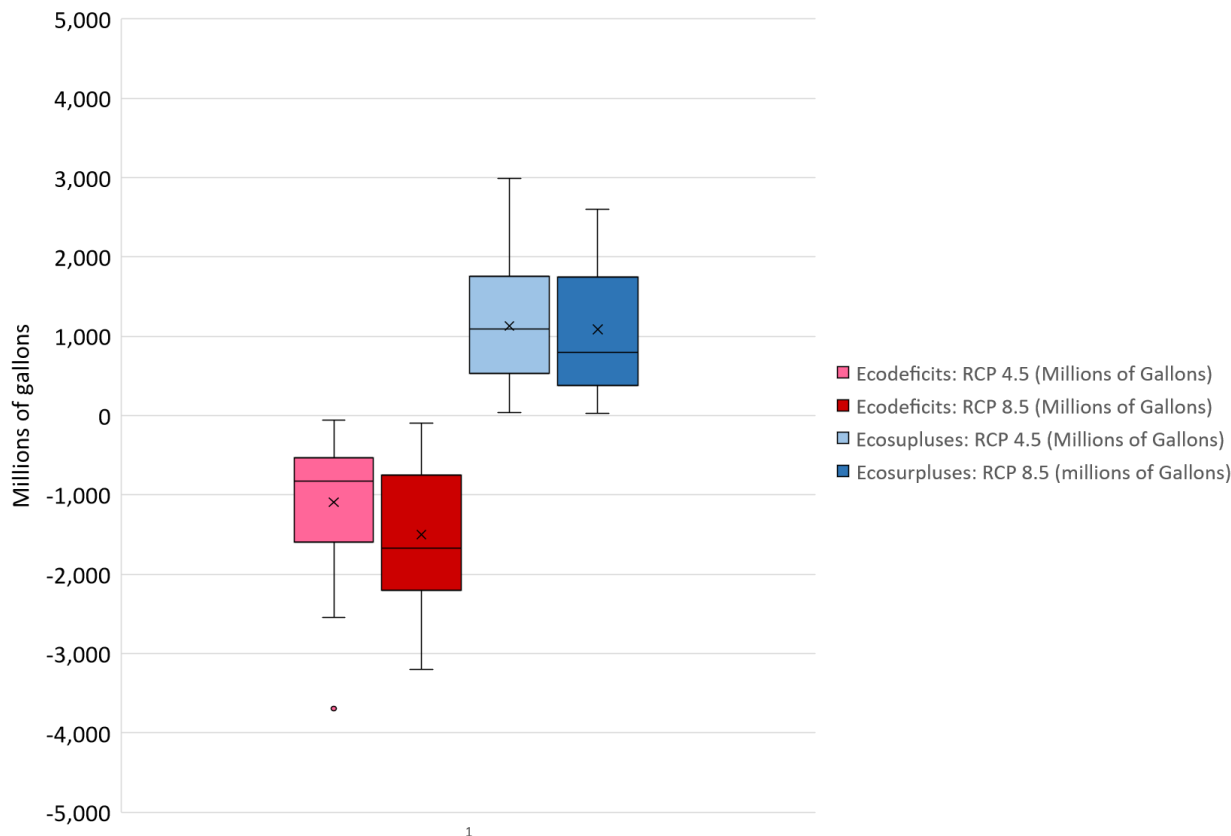


Figure 4-16. Ensemble results for ecosurplus and ecodeficits.

From the ensemble results, 12 models (Table 4-6) were selected to represent the range of potential scenarios producing ecodeficits and ecosurpluses. The selected models represent the 20th, median, and 80th percentile results. For example, for the ecodeficit models for RCP 4.5 miroc-esm-chem-1 was the 20th percentile model, producing relatively little ecodeficits, termed the ‘wet’ model, bcc-csm-1-m-1 produced the median, or 50th percentile result and was termed the ‘median’ model, and mpi-esm-mr-1 was the 80th percentile model producing a relatively high ecodeficit and was termed the ‘dry’ model. Figure 4-17 and Figure 4-18 present the FDCs from the models that produced the 20th, median, and 80th percentile ecodeficits and ecosurpluses, respectively, for the two RCPs. The FDCs are further compared to the baseline model results in Figure 4-19, Figure 4-20, Figure 4-21, and Figure 4-22. Ecosurplus and ecodeficits are presented in both cfs/day and millions of gallons per year (mgy). Table 4-7 presents a summary of ecosurpluses and ecodeficits for the two emission scenarios. For the ecodeficit models, ecodeficits ranged from a low 20th percentile (wet) of 470.5 mgy to an 80th percentile (dry) 1,829.1 mgy for an RCP 4.5 scenario. For RCP 8.5, the 20th percentile ecodeficit increased to 703.2 mgy and the 80th percentile ecodeficit increased to 2,281.8 mgy.

Table 4-6. Selected models from ensemble results for future climate projections (2079-2099)

RCP	Scenario ¹	Ecosuplus Model	Ecodeficit Model
RCP 4.5	Dry	hadgem2-cc-1	mpi-esm-mr-1
	Median	bcc-csm1-1-m-1	bcc-csm1-1-m-1
	Wet	bcc-csm1-1-1	miroc-esm-chem-1
RCP 8.5	Dry	inmcm4-1	miroc-esm-1
	Median	cesm1-cam5-1	cesm1-cam5-1
	Wet	cesm1-bgc-1	mri-cgcm3-1

1: Dry, Median, and Wet correspond to the 20th, 50th, and 80th percentile hydrological responses

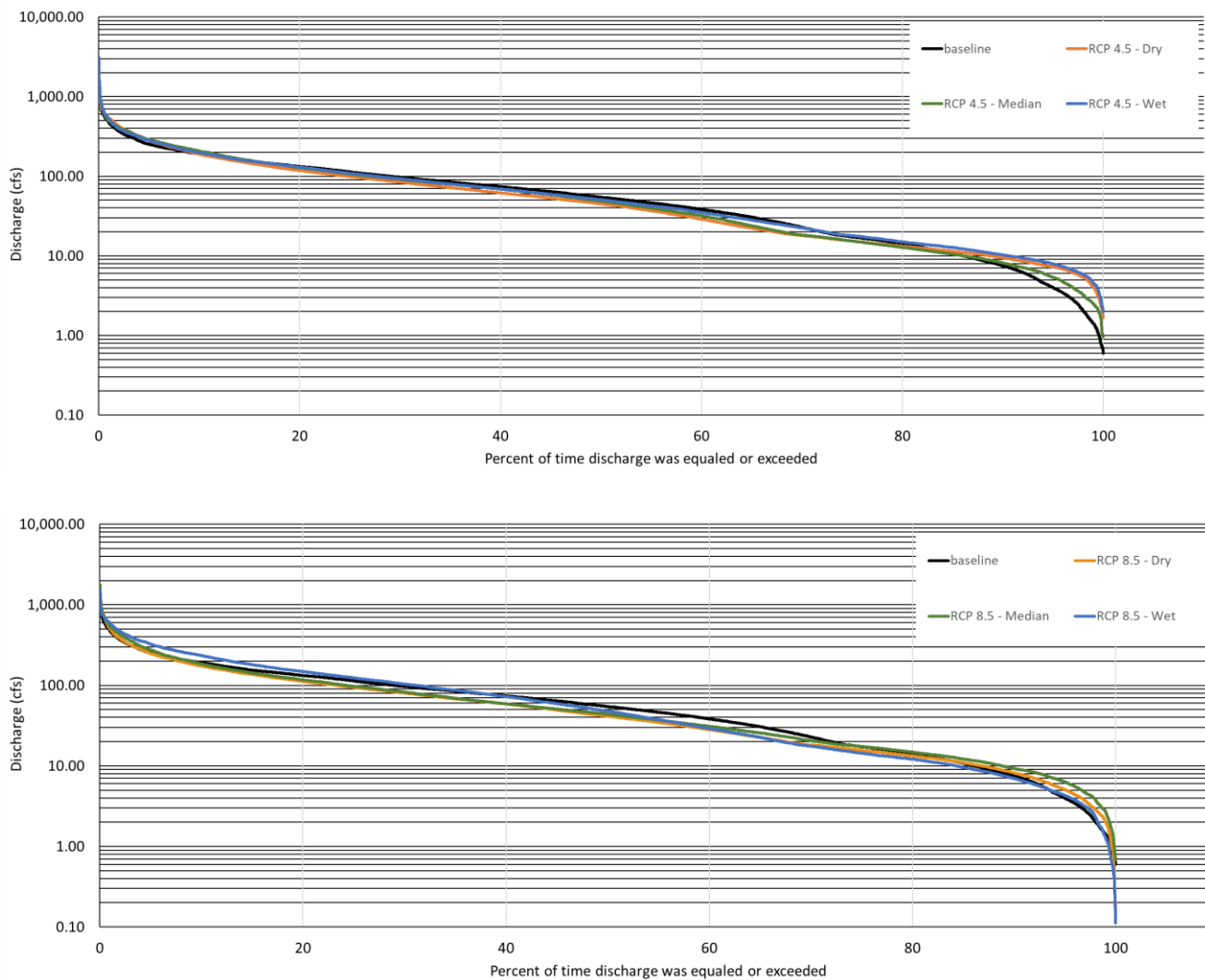


Figure 4-17. Ecodeficit FDCs at the Wading River USGS Gage (01109000) under baseline and climate change scenarios for RCP 8.5 (top) and RCP 4.5 (bottom).

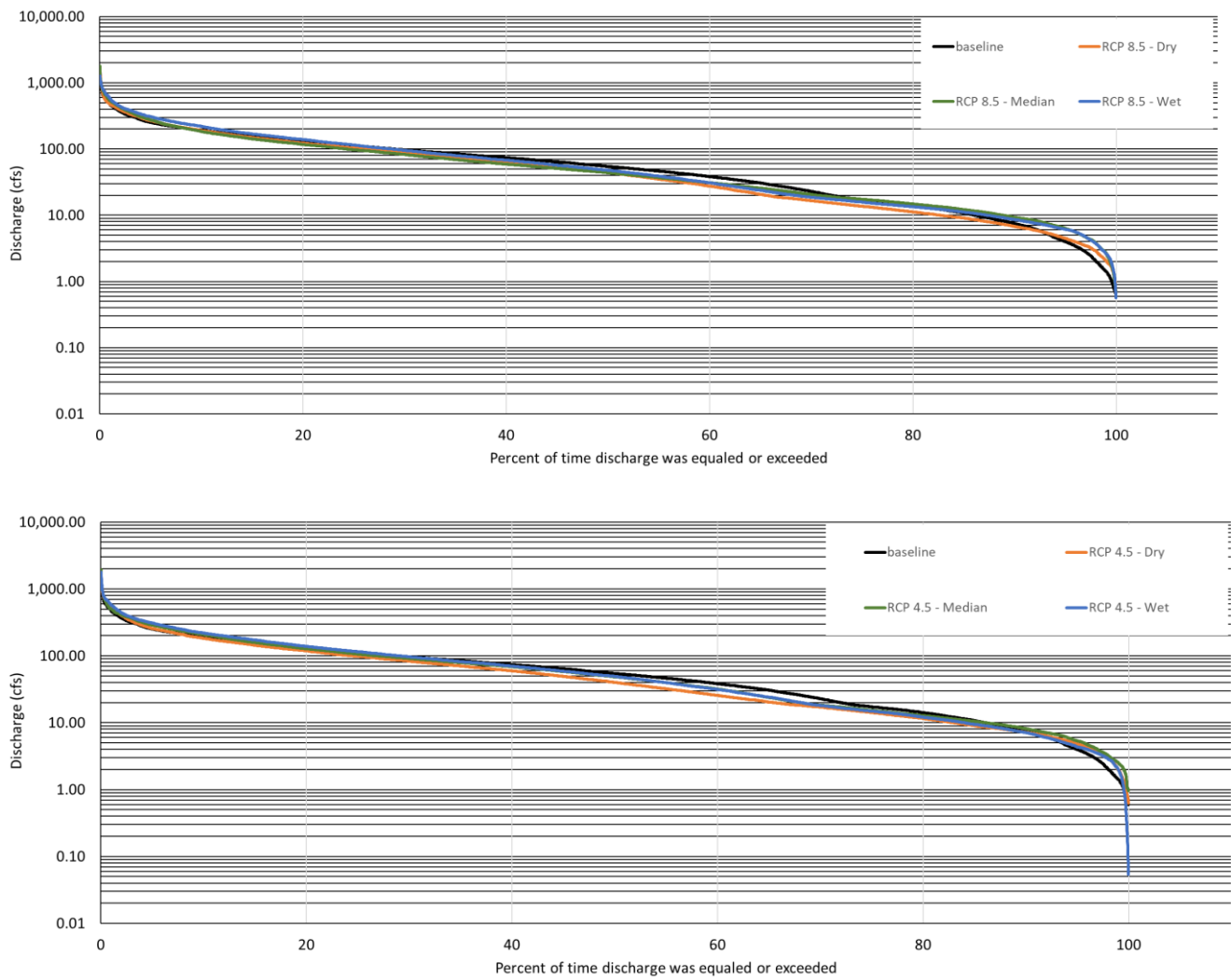


Figure 4-18. Ecosuplus FDCs at the Wading River USGS Gage (01109000) under baseline and climate change scenarios for RCP 8.5 (top) and RCP 4.5 (bottom).

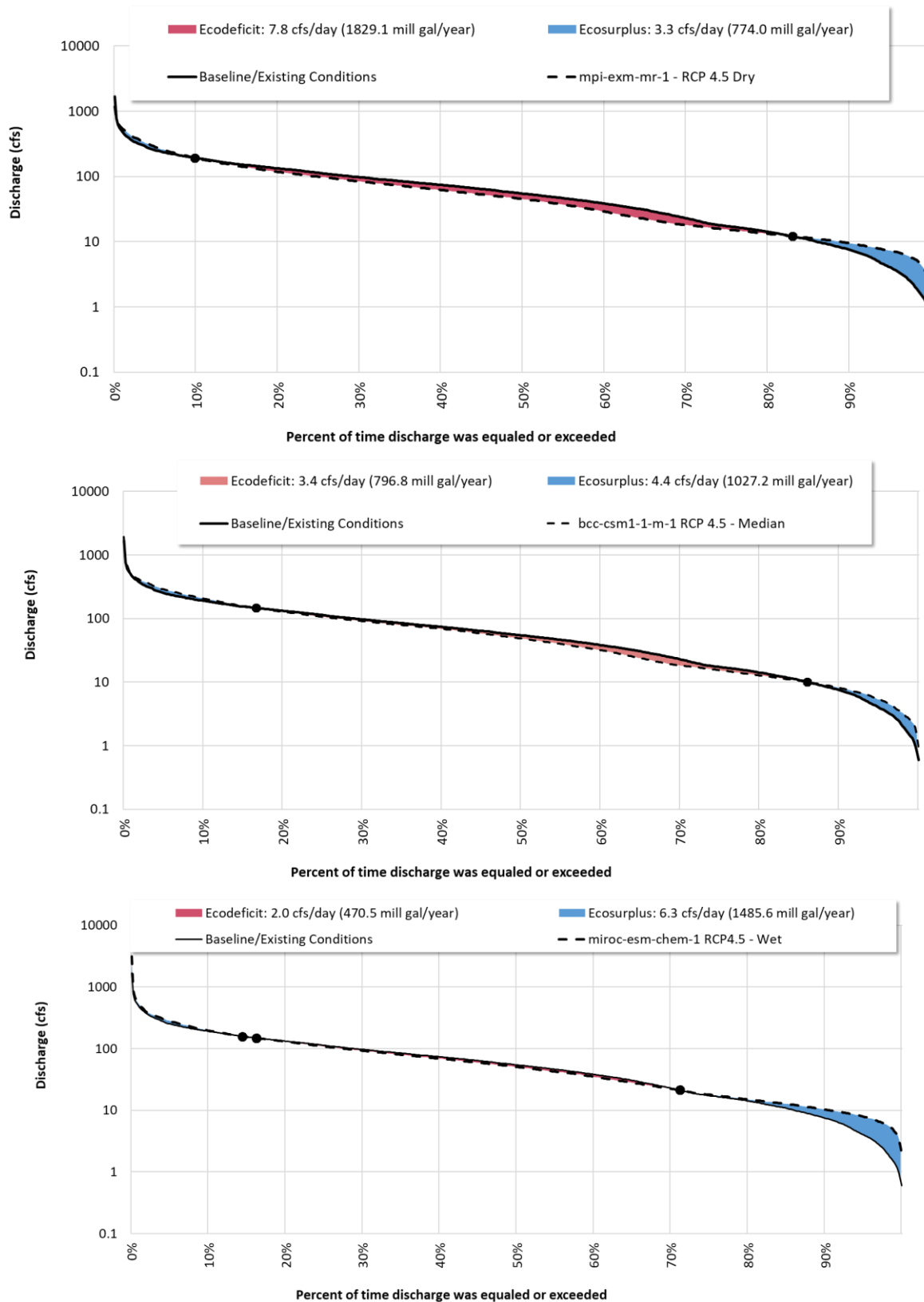


Figure 4-19. Results for the wet, median, and dry models for ecodeficits based on an RCP 4.5 scenario. Results are for the Wading River USGS Gage (01109000) under comparing baseline (2000-2020) to future climate scenarios (2079-2099).

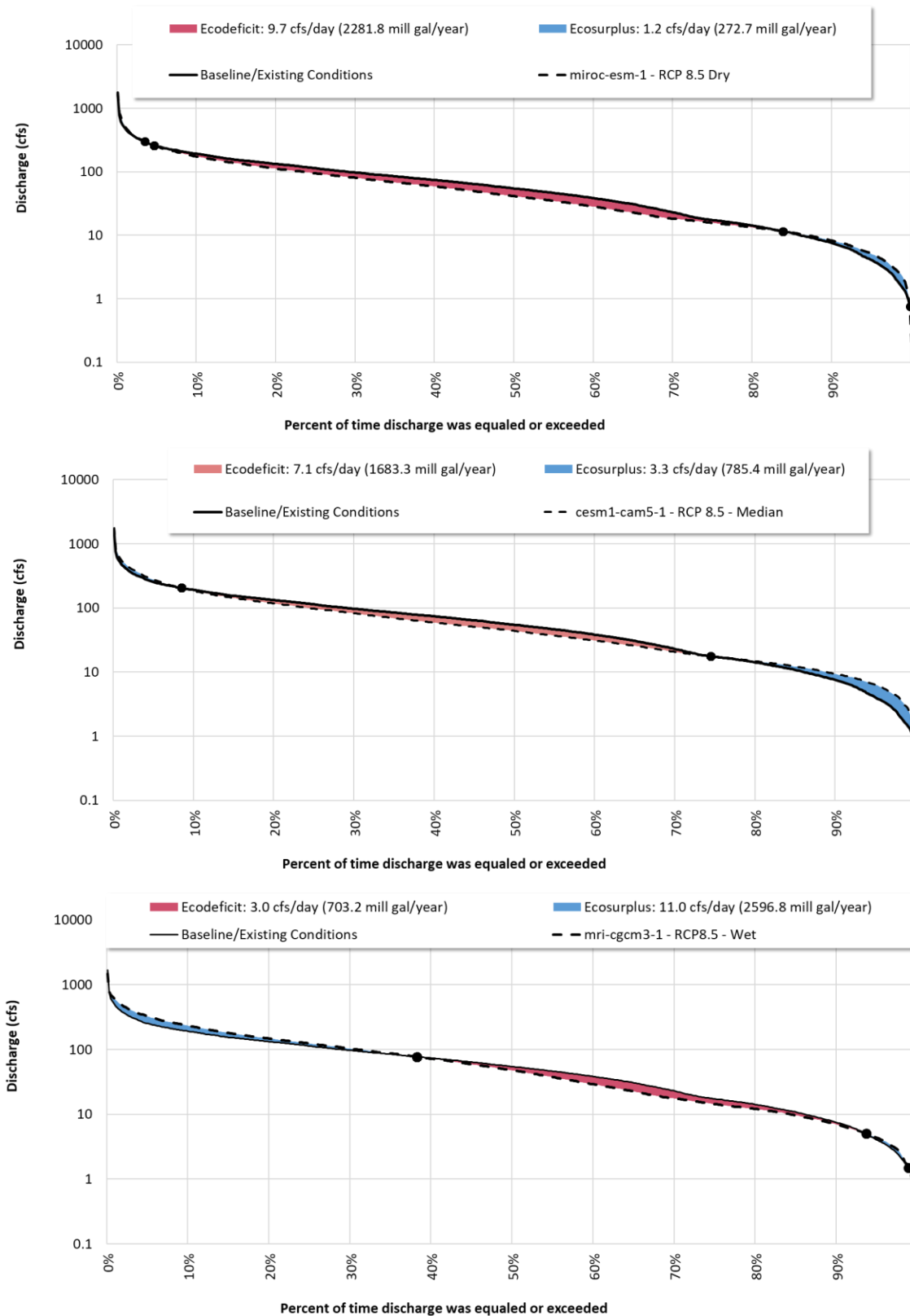


Figure 4-20. Results for the wet, median, and dry models for ecodficits based on an RCP 8.5 scenario. Results are for Wading River USGS Gage (01109000) comparing baseline (2000-2020) to future climate scenarios (2079-2099).

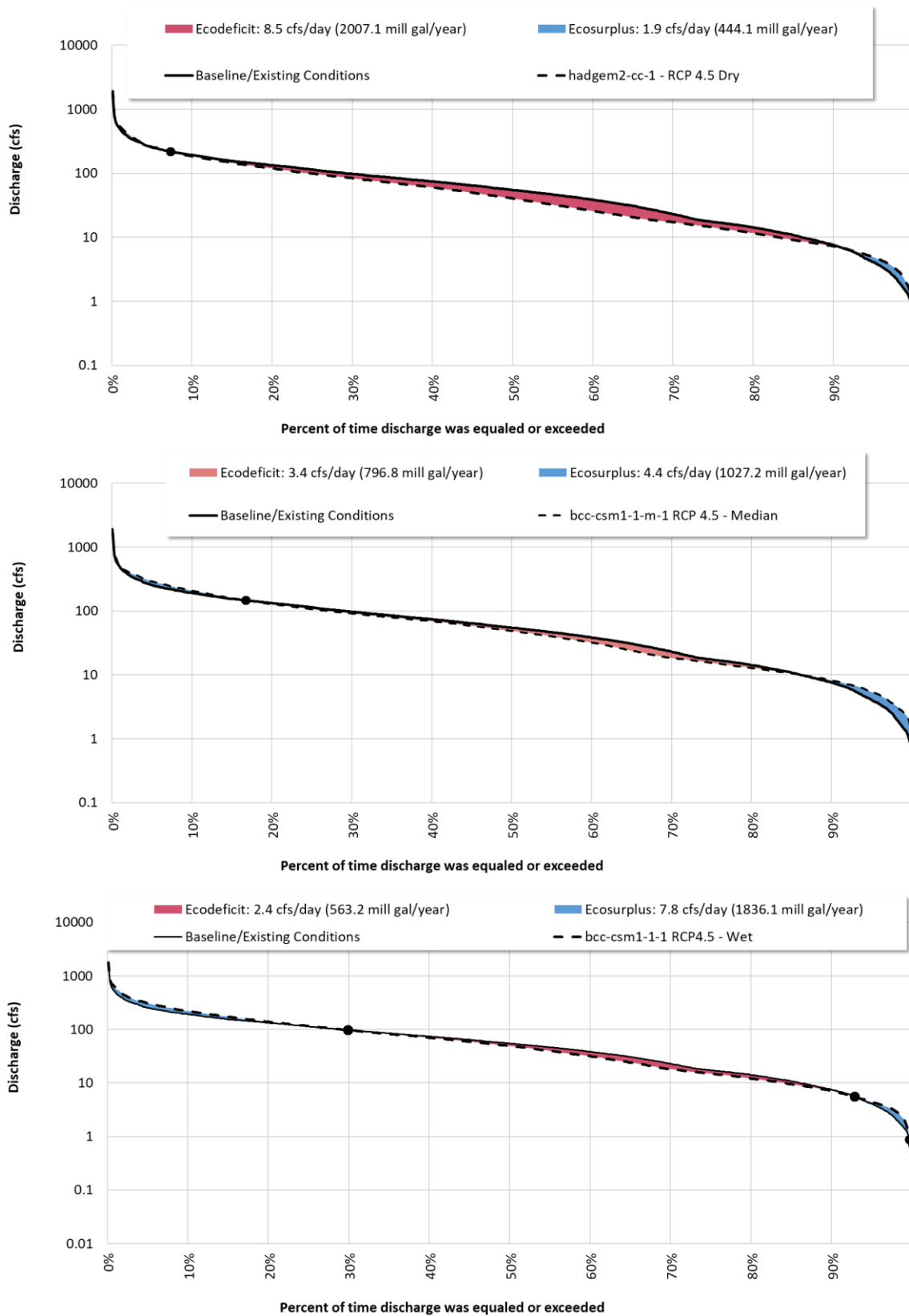


Figure 4-21. Results for the wet, median, and dry models for ecosurpluses based on an RCP 4.5 scenario. Results are for Wading River USGS Gage (01109000) comparing baseline (2000-2020) to future climate scenarios (2079-2099).

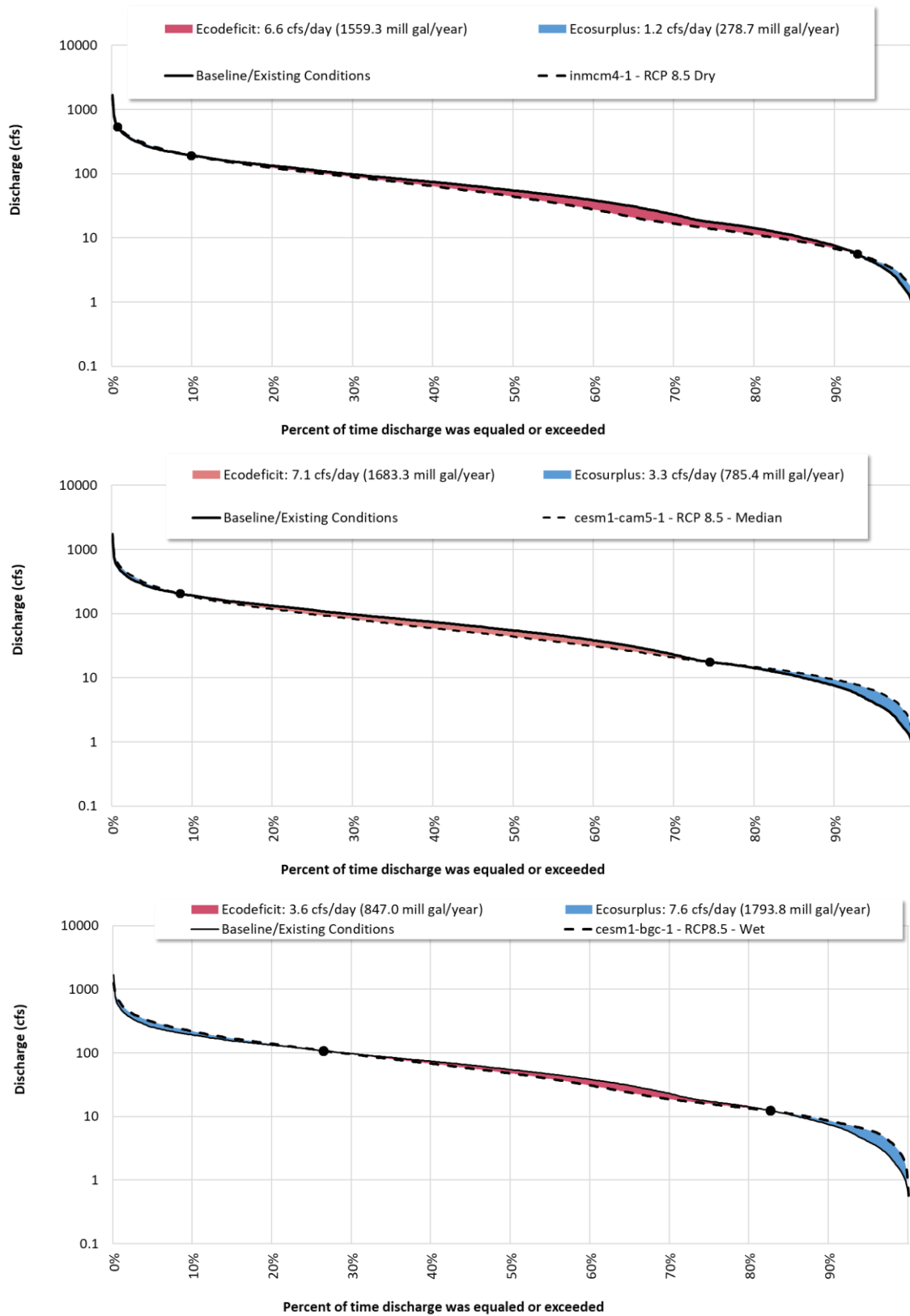


Figure 4-22. Results for the wet, median, and dry models for ecosurpluses based on an RCP 8.5 scenario. Results are for the Wading River USGS Gage (01109000) comparing baseline (2000-2020) to future climate scenarios (2079-2099).

Table 4-7. Summary of ecosurpluses and ecodeficits (millions of gallons per year) for RCP 4.5 and 8.5 scenarios

Scenario	Ecodeficit models					
	Ecodeficits			Ecosurplus		
	Dry	Median	Wet	Dry	Median	Wet
RCP 4.5	1,829.1	796.8	470.5	774.0	1,027.2	1,485.6
RCP 8.5	2,281.8	1,683.3	703.2	272.7	785.4	2,596.8
Scenario	Ecosurplus models					
	Ecodeficits			Ecosurplus		
	Dry	Median	Wet	Dry	Median	Wet
RCP 4.5	2,007.1	796.8	563.2	444.1	1,027.2	1,836.1
RCP 8.5	1,559.3	1,683.3	847.0	278.7	785.4	1,793.8

For the ecosurplus models, the result ranges from a 20th percentile ecosurplus of 441.1 mgly to an 80th percentile 1,836.1 mgly for the RCP 4.5 scenario. For the RCP 8.5 scenario, ecosurpluses for the 20th and 80th percentiles are almost lower to 278.2 and 1,793.8 mgly, respectively. Overall, these results support the conclusions of Demaria et al (2016a) who found that future climate scenarios may result in a decrease in the magnitude of low flow conditions in the northeast. Table 4-8 presents the analysis of average 3-day low flows and high flows for the RCP 4.5 and 8.5 model simulations compared against the baseline simulation. While FDC analysis helps to understand the overall trends, analysis of 3-day low and high flows provides greater information on extreme (drought vs flood) conditions. General trends in the data show the lowest flows (average 3-day minimum flow) became higher, which is expected given the prevalence of ecosurpluses at low flows on the climate change FDCs. Additionally, the high flows also became higher. The analysis removed two years from the observed annual 3-day maximum flow dataset. These were high flows resulting from tropical storm Tammy in October of 2005 and a nor'easter in March of 2010. The high flows from these two storms resulted in 2005 and 2010 having annual maximum high flows almost 3 times higher than the average from high flows across the other years (2000-2020). The two years were therefore removed to provide a better comparison of historical and future high flows that were not impacted by rare, extreme, historical events. Uncertainty surrounding future climate predictions is well documented and a field of active research. The results suggest that assuming no change to land use, future climate conditions will result in both low and high flows increasing in the Wading River. Figure 4-23 presents an analysis of how the selected models differ for changes in annual average precipitation and temperature. The graph also shows the median values for RCP 4.5 and 8.5. Compared to baseline conditions, the models varied for whether there was a net increase or decrease in precipitation, however, all models had an increase in average annual temperature. Unsurprisingly, the models that were identified as 'wet' based on their ecosurpluses also had the largest increases in precipitation. The causes of the ecodeficits produced by the 'dry' models appear to be more complex. As an example, the 'dry' RCP 8.5 ecodeficit model had an increase in average temperatures and a 5% increase in precipitation compared to baseline conditions while the 'dry' RCP 4.5 ecodeficit model had a 6% increase in average temperatures but a decrease (-2%) in precipitation. Table 4-9 shows that generally, the selected climate models have more days with a relatively high precipitation amount (≥ 0.5 in) compared to the baseline.

Table 4-10 shows how seasonal rainfall trends change. More precipitation generally occurs in the winter months. Interestingly, most models also have additional rain in August, which is typically the period for the lowest flows in the watershed. Table 4-11 provides information on possible future drought conditions by quantifying changes in the maximum amount of consecutive dry days that occur. Late spring and early summer appear to become drier while winter becomes wetter. Table 4-12, Table 4-13, and Table 4-14 present an analysis of future temperatures. Overall, the maximum, minimum, and average temperatures are expected to increase throughout the year. While the percent change to maximum temperatures does not appear to have a strong seasonal influence, the winter is expected to see large increases in minimum and average temperatures.

Table 4-8. Percent change in 3-day minimum and maximum flows for RCP 4.5 and 8.5 scenarios compared to baseline simulation

Model	RCP	Scenario	Average annual 3-day minimum (cfs)	Average annual 3-day maximum (cfs)
Baseline	NA	Historical	3.75	500.44
Ecodeficit Model	RCP45	Dry	38.53%	-12.37%
Ecodeficit Model	RCP45	Median	18.16%	-10.44%
Ecodeficit Model	RCP45	Wet	70.85%	6.64%
Ecodeficit Model	RCP85	Dry	38.10%	18.15%
Ecodeficit Model	RCP85	Median	51.23%	26.23%
Ecodeficit Model	RCP85	Wet	15.88%	13.29%
Ecosurplus Model	RCP45	Dry	-2.50%	27.88%
Ecosurplus Model	RCP45	Median	18.16%	15.40%
Ecosurplus Model	RCP45	Wet	8.02%	20.76%
Ecosurplus Model	RCP85	Dry	0.25%	24.95%
Ecosurplus Model	RCP85	Median	51.23%	26.23%
Ecosurplus Model	RCP85	Wet	19.08%	20.34%

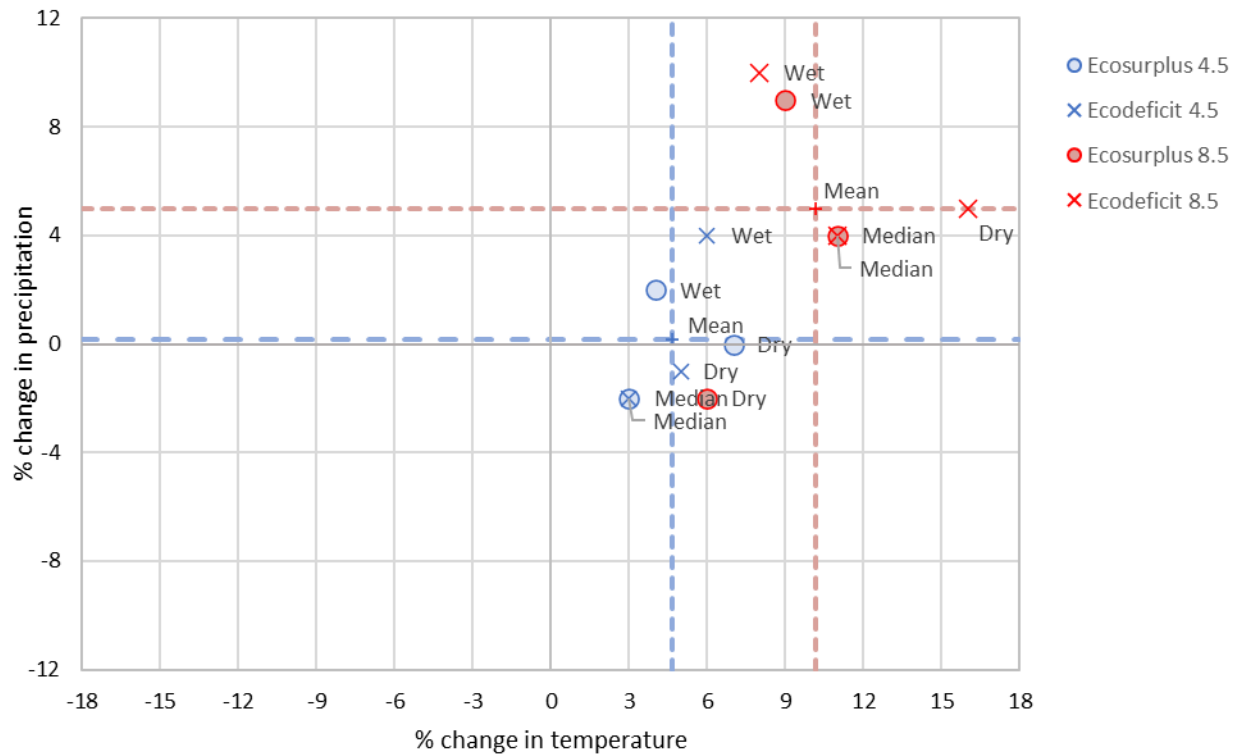


Figure 4-23. Percent change in annual average precipitation and temperature from baseline conditions for the selected models presented in Table 4-6.

Table 4-9. Dry days and days with precipitation for the selected future climate scenarios compared to the historical, observed conditions.

Model	RCP	Scenario	Maximum Consecutive Dry Days	Average No. Rain Days				
				≥0.01 in	≥0.10 in	≥0.50 in	≥1.00 in	≥2.00 in
Baseline	NA	Historical	8.4	128.0	78.2	29.9	12.6	2.4
Ecodeficit Model	RCP45	Dry	9.3	126.1	78.3	29.3	12.9	2.3
Ecodeficit Model	RCP45	Median	9.2	125.5	77.6	29.1	12.5	2.3
Ecodeficit Model	RCP45	Wet	8.7	126.8	77.0	31.2	13.9	3.4
Ecodeficit Model	RCP85	Dry	9.6	122.0	76.2	31.6	14.0	3.0
Ecodeficit Model	RCP85	Median	9.3	128.6	78.2	32.1	13.8	2.7
Ecodeficit Model	RCP85	Wet	8.5	126.0	79.3	34.6	15.3	3.4
Ecosurplus Model	RCP45	Dry	9.1	126.1	76.1	31.2	13.0	2.4
Ecosurplus Model	RCP45	Median	9.2	125.5	77.6	29.1	12.5	2.3
Ecosurplus Model	RCP45	Wet	9.5	130.2	77.0	31.1	13.9	2.4
Ecosurplus Model	RCP85	Dry	8.7	125.6	75.8	29.2	12.5	2.5
Ecosurplus Model	RCP85	Median	9.3	128.6	78.2	32.1	13.8	2.7
Ecosurplus Model	RCP85	Wet	8.8	132.8	82.2	33.2	15.1	2.7

Note: For maximum consecutive dry days, red shading indicates an increase in dry days. For rain days, red shading indicates a decrease in days greater than or equal to the associated depth, blue shading indicates an increase in days with precipitation greater than or equal to the associated depth.

Table 4-10. Percent change for average annual and monthly precipitation for future climate scenarios compared to the historical, observed conditions.

Model	RCP	Scenario	Percent Change of Average Monthly Precipitation (inches) by Scenario												
			Annual	Jan	Feb	Mar	Apr	May	Jun	Jul	Aug	Sep	Oct	Nov	Dec
NA	NA	Historical	46.9	3.3	3.2	4.9	4.6	3.5	4.1	3.5	3.1	4.1	4.4	3.9	4.2
Ecodeficit Model	RCP45	Dry	-1%	44%	16%	-8%	9%	-1%	-26%	-29%	36%	-14%	-7%	3%	-15%
Ecodeficit Model	RCP45	Median	-2%	36%	37%	-18%	-29%	-25%	-17%	1%	0%	-6%	-2%	1%	18%
Ecodeficit Model	RCP45	Wet	4%	17%	18%	-11%	-34%	-9%	14%	4%	33%	15%	-1%	12%	12%
Ecodeficit Model	RCP85	Dry	5%	20%	14%	-4%	-23%	2%	-2%	38%	-12%	-1%	-15%	51%	3%
Ecodeficit Model	RCP85	Median	4%	34%	7%	-8%	-15%	-13%	-43%	10%	72%	23%	6%	-13%	16%
Ecodeficit Model	RCP85	Wet	10%	47%	81%	33%	-33%	-3%	-30%	-14%	-3%	9%	-3%	35%	21%
Ecosurplus Model	RCP45	Dry	0%	19%	32%	-2%	-19%	7%	-20%	-2%	-2%	-4%	-39%	-9%	49%
Ecosurplus Model	RCP45	Median	-2%	36%	37%	-18%	-29%	-25%	-17%	1%	0%	-6%	-2%	1%	18%
Ecosurplus Model	RCP45	Wet	2%	28%	38%	-5%	3%	-17%	-34%	-18%	31%	-18%	5%	7%	20%
Ecosurplus Model	RCP85	Dry	-2%	30%	9%	-15%	5%	-4%	-31%	-14%	39%	-10%	-22%	16%	-1%
Ecosurplus Model	RCP85	Median	4%	34%	7%	-8%	-15%	-13%	-43%	10%	72%	23%	6%	-13%	16%
Ecosurplus Model	RCP85	Wet	9%	66%	54%	14%	-14%	-16%	-37%	39%	5%	18%	-29%	21%	8%

Note: Red shading indicates a decrease in precipitation, blue shading indicates an increase in precipitation

Table 4-11. Percent change for average maximum consecutive dry days for the future climate scenarios compared to the historical, observed conditions.

Model	RCP	Scenario	Percent Change for Average No. Maximum Consecutive Dry Days by Scenario												
			Annual	Jan	Feb	Mar	Apr	May	Jun	Jul	Aug	Sep	Oct	Nov	Dec
Baseline	NA	Historical	8	11	10	9	8	7	7	8	9	9	7	9	8
Ecodeficit Model	RCP45	Dry	11%	-33%	-16%	6%	6%	11%	31%	27%	6%	11%	73%	21%	21%
Ecodeficit Model	RCP45	Median	9%	-21%	-14%	-8%	5%	42%	38%	23%	25%	16%	36%	1%	-2%
Ecodeficit Model	RCP45	Wet	4%	-9%	-12%	-12%	2%	45%	30%	18%	-19%	-13%	36%	12%	2%
Ecodeficit Model	RCP85	Dry	15%	-27%	-15%	-17%	17%	82%	36%	40%	57%	18%	30%	4%	-9%
Ecodeficit Model	RCP85	Median	11%	-13%	5%	12%	-1%	26%	61%	29%	-24%	-19%	37%	38%	10%
Ecodeficit Model	RCP85	Wet	1%	-17%	-33%	-22%	11%	19%	41%	22%	5%	14%	33%	-19%	-9%
Ecosurplus Model	RCP45	Dry	8%	-34%	-29%	-8%	28%	28%	40%	33%	15%	14%	75%	-6%	-10%
Ecosurplus Model	RCP45	Median	9%	-21%	-14%	-8%	5%	42%	38%	23%	25%	16%	36%	1%	-2%
Ecosurplus Model	RCP45	Wet	13%	-28%	-17%	-21%	-11%	38%	5%	60%	2%	50%	83%	36%	-3%
Ecosurplus Model	RCP85	Dry	4%	-21%	-23%	-29%	-6%	20%	47%	36%	-6%	1%	66%	11%	-5%
Ecosurplus Model	RCP85	Median	11%	-13%	5%	12%	-1%	26%	61%	29%	-24%	-19%	37%	38%	10%
Ecosurplus Model	RCP85	Wet	4%	-21%	-26%	-12%	-8%	18%	47%	21%	1%	-10%	52%	10%	16%

Note: Red shading indicates an increase in dry days, blue shading indicates a decrease in dry days

Table 4-12. Percent change in average maximum daily temperature for the selected future climate scenarios compared to the historical, observed conditions

Model	RCP	Scenario	Average Maximum Daily Temperature (F) / Percent Change by Scenario												
			Annual	Jan	Feb	Mar	Apr	May	Jun	Jul	Aug	Sep	Oct	Nov	Dec
Baseline	NA	Historical	65	48	46	53	63	72	78	81	79	75	67	60	54
Ecodeficit Model	RCP45	Dry	3%	-1%	-2%	5%	3%	3%	4%	2%	3%	5%	3%	3%	5%
Ecodeficit Model	RCP45	Median	1%	-4%	0%	2%	0%	3%	2%	3%	3%	3%	-2%	-2%	-2%
Ecodeficit Model	RCP45	Wet	2%	-5%	4%	7%	3%	4%	3%	3%	5%	4%	0%	1%	-4%
Ecodeficit Model	RCP85	Dry	10%	9%	18%	14%	11%	10%	9%	8%	9%	9%	8%	9%	3%
Ecodeficit Model	RCP85	Median	7%	3%	8%	3%	6%	8%	7%	6%	9%	8%	5%	7%	8%
Ecodeficit Model	RCP85	Wet	5%	7%	11%	4%	9%	3%	5%	4%	4%	6%	2%	3%	2%
Ecosurplus Model	RCP45	Dry	5%	-2%	5%	5%	8%	2%	3%	4%	7%	4%	6%	9%	5%
Ecosurplus Model	RCP45	Median	1%	-4%	0%	2%	0%	3%	2%	3%	3%	3%	-2%	-2%	-2%
Ecosurplus Model	RCP45	Wet	1%	-5%	6%	4%	2%	-1%	2%	2%	3%	3%	-1%	-2%	-5%
Ecosurplus Model	RCP85	Dry	4%	4%	11%	8%	7%	4%	3%	2%	3%	6%	2%	6%	0%
Ecosurplus Model	RCP85	Median	7%	3%	8%	3%	6%	8%	7%	6%	9%	8%	5%	7%	8%
Ecosurplus Model	RCP85	Wet	5%	7%	8%	4%	7%	6%	6%	5%	7%	7%	4%	-2%	3%

Note: Red shading indicates an increase in temperature, blue shading indicates a decrease in temperature.

Table 4-13. Percent change in average minimum daily temperature for the selected future climate scenarios compared to the historical, observed conditions

Model	RCP	Scenario	Average Minimum Daily Temperature (F) / Percent Change by Scenario												
			Annual	Jan	Feb	Mar	Apr	May	Jun	Jul	Aug	Sep	Oct	Nov	Dec
Baseline	NA	Historical	38	12	18	24	37	47	55	64	62	52	40	29	21
Ecodeficit Model	RCP45	Dry	6%	67%	-1%	11%	7%	2%	3%	1%	5%	5%	4%	15%	-3%
Ecodeficit Model	RCP45	Median	5%	36%	8%	14%	1%	-1%	3%	2%	4%	2%	4%	12%	3%
Ecodeficit Model	RCP45	Wet	9%	46%	27%	28%	11%	0%	6%	6%	7%	3%	7%	12%	2%
Ecodeficit Model	RCP85	Dry	24%	110%	46%	51%	26%	13%	20%	14%	17%	16%	15%	32%	27%
Ecodeficit Model	RCP85	Median	14%	87%	46%	25%	1%	1%	5%	8%	11%	7%	13%	33%	34%
Ecodeficit Model	RCP85	Wet	14%	70%	34%	27%	9%	6%	8%	7%	8%	6%	12%	28%	33%
Ecosurplus Model	RCP45	Dry	10%	70%	10%	16%	5%	4%	7%	4%	7%	-1%	10%	21%	30%
Ecosurplus Model	RCP45	Median	5%	36%	8%	14%	1%	-1%	3%	2%	4%	2%	4%	12%	3%
Ecosurplus Model	RCP45	Wet	7%	48%	0%	24%	6%	5%	5%	4%	6%	7%	7%	10%	1%
Ecosurplus Model	RCP85	Dry	5%	66%	22%	27%	5%	-4%	3%	-2%	1%	-1%	1%	16%	2%
Ecosurplus Model	RCP85	Median	14%	87%	46%	25%	1%	1%	5%	8%	11%	7%	13%	33%	34%
Ecosurplus Model	RCP85	Wet	13%	85%	40%	24%	6%	3%	9%	6%	8%	6%	8%	25%	29%

Note: Red shading indicates an increase in temperature, blue shading indicates a decrease in temperature.

Table 4-14. Percent change in average daily temperature for the selected future climate scenarios compared to the historical, observed conditions

Model	RCP	Scenario	Average Daily Temperature (F) / Percent Change by Scenario												
			Annual	Jan	Feb	Mar	Apr	May	Jun	Jul	Aug	Sep	Oct	Nov	Dec
Baseline	NA	Historical	51.1	29.6	31.7	38.1	48.1	58.1	66.5	72.7	71.0	63.7	53.5	43.7	35.1
Ecodeficit Model	RCP45	Dry	5%	11%	3%	8%	5%	4%	4%	2%	3%	5%	2%	6%	6%
Ecodeficit Model	RCP45	Median	3%	6%	1%	6%	3%	2%	3%	3%	3%	2%	1%	4%	
Ecodeficit Model	RCP45	Wet	6%	10%	10%	15%	9%	5%	6%	4%	6%	4%	5%	2%	
Ecodeficit Model	RCP85	Dry	16%	27%	27%	27%	20%	14%	13%	11%	13%	13%	17%	15%	
Ecodeficit Model	RCP85	Median	11%	18%	18%	12%	7%	8%	7%	7%	10%	10%	13%	19%	
Ecodeficit Model	RCP85	Wet	9%	17%	18%	11%	11%	6%	8%	5%	6%	7%	10%	14%	
Ecosurplus Model	RCP45	Dry	7%	11%	4%	7%	9%	5%	6%	5%	8%	6%	8%	13%	
Ecosurplus Model	RCP45	Median	3%	6%	1%	6%	3%	2%	3%	3%	3%	2%	1%	4%	
Ecosurplus Model	RCP45	Wet	4%	3%	4%	10%	6%	2%	4%	4%	4%	6%	2%	0%	
Ecosurplus Model	RCP85	Dry	6%	14%	12%	14%	10%	5%	5%	2%	4%	4%	5%	3%	
Ecosurplus Model	RCP85	Median	11%	18%	18%	12%	7%	8%	7%	7%	10%	10%	13%	19%	
Ecosurplus Model	RCP85	Wet	9%	20%	17%	9%	10%	8%	7%	6%	8%	8%	8%	14%	

Note: Red shading indicates an increase in temperature.

4.2 Opti-Tool Optimization of SCMs to Achieve Flow Duration Curve Objectives.

4.2.1 GIS Screening to Identify SCM Opportunities

The approach to identifying the SCM opportunities were based on the approach used in [EPA Region 1's Tisbury, MA Impervious Cover Disconnection Project](#). A GIS spatial data analysis was performed for the Taunton River basin to identify potential stormwater control technologies that would be technically feasible based on the available GIS data. Table 4-15 presents the matrix of suitability criteria and management categories used for this study. Figure 4-24 presents the locations of SCM opportunities identified in the Lower Hodges, Upper Hodges, and Pilot Tributary sub-watersheds as well as the larger Wading River watershed. The treated impervious areas by land use group were split into two categories: roofs and other impervious surfaces. For this pilot study, it was assumed that rooftops could be disconnected by redirecting their runoff to infiltrations trenches, while all other types of impervious areas, such as roads and driveways, could be disconnected by diverting their runoff to infiltration basins. When poorly drained soils (HSG = D) were present, a biofiltration device was used. Both public and private property were assumed to be available for GIS SCM implementation. Seven practices from a range of potential stormwater management methods were evaluated. The seven practices were two infiltration techniques, basins and trenches, on soil groups A, B, and C, and a biofiltration device on soil group D. Infiltration trenches were used to treat roof runoff while infiltration basins were used to treat runoff from all other impervious surfaces. The design specifications are presented in Table 4-16.

4.2.2 Estimating SCM Footprints and Drainage Treatment Areas

The distribution of the SCM opportunity areas (i.e., SCM footprints) was estimated by land use category group. This distribution represents the maximum available SCM footprint in the pilot watersheds, based on GIS spatial data analysis, and does not necessarily represent the feasibility of such opportunity areas. Table 4-18 presents the total amount of impervious area that was able to be treated during optimization. While all impervious surfaces were routed to an SCM, treatment was contingent on the SCM size. For this project, the maximum SCM footprints that could be considered during optimization were limited to capture up to 2 inches of runoff from the impervious drainage areas by land use group (Table 4-19).

Table 4-15. Site suitability criteria for stormwater management categories

Land Use	Within 200 feet of impervious surface	Landscape Slope (%)	Within FEMA Hazard Areas	Within Surface Water Protection Zone	Within 100 feet of Stream/Coastline	Within Wetland	Within 25 feet of Structure?	Hydrologic Soil Group	Management Category	SCM Type(s) in Opti-Tool
Pervious Area	Yes	<= 15	Yes	Yes	Yes	Yes	Yes	All	SCM with complicating characteristics	--
			No	No	No	No	No	A/B/C	Surface Infiltration	Surface Infiltration Basin (e.g., Rain Garden)
		D	Biofiltration	Biofiltration with underdrain option						
	> 15	--	--	--	--	--	--	SCM with complicating characteristics	--	
	No	--	--	--	--	--	--	--	No SCM opportunity	--
Impervious Area	<= 5	<= 5	Yes	Yes	Yes	Yes	Yes	All	SCM with complicating characteristics	--
			No	No	No	No	No	A/B/C	Subsurface Infiltration	Infiltration Trench
		D	Shallow filtration	Porous Pavement						
	> 5	--	--	--	--	--	--	SCM with complicating characteristics	--	

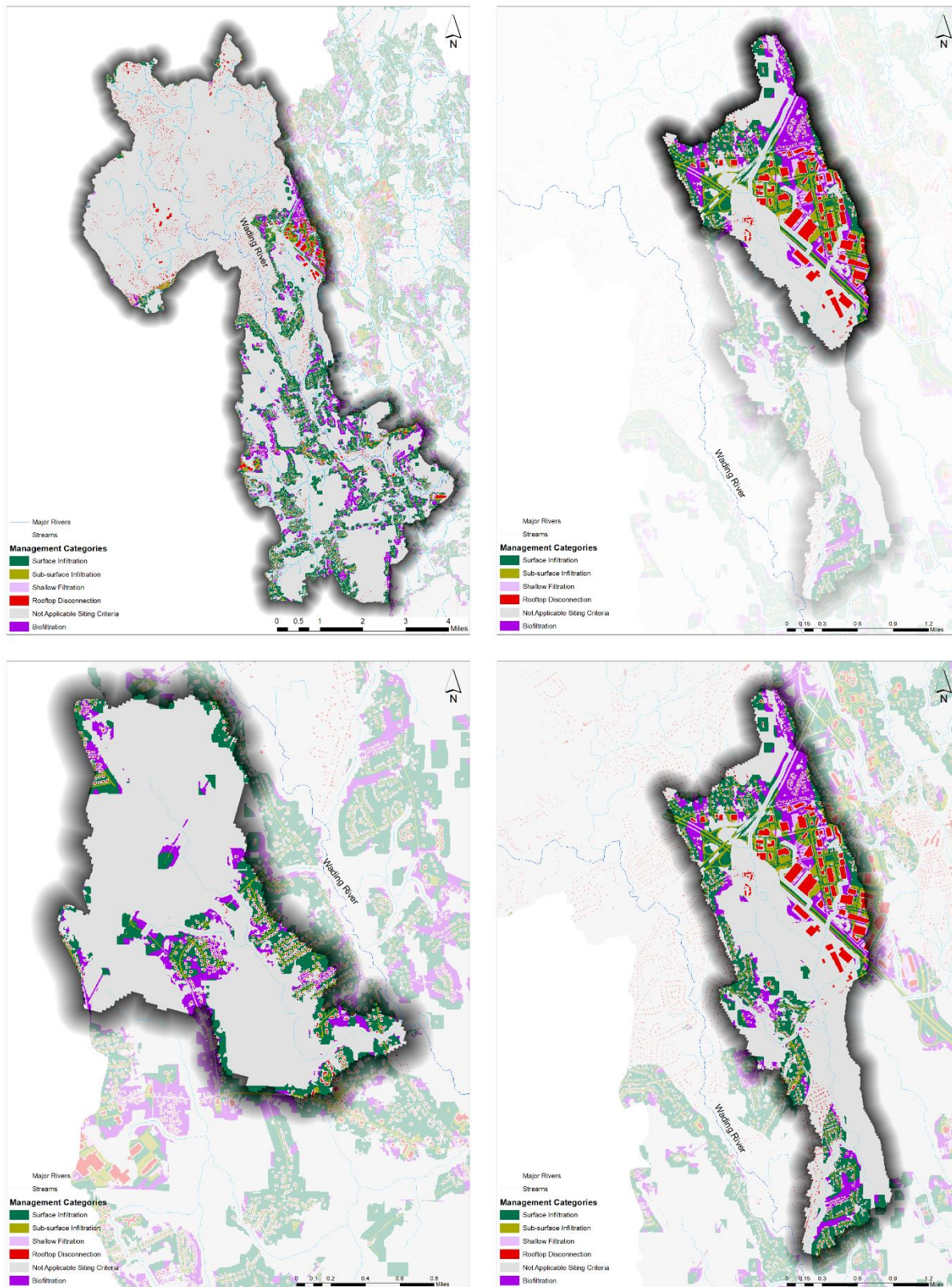


Figure 4-24. SCM opportunities for Wading River (top left), Upper Hodges Brook (top right), Pilot Tributary (bottom left), and Lower Hodges Brook (bottom right).

Table 4-16. SCM Design Specifications

General Information	SCM Parameters	Infiltration Trench HSG – A, B, C	Infiltration Basin HSG – A, B, C	Biofiltration HSG – D
SCM Dimensions	Surface Area (ac)	Table 4-19	Table 4-19	Table 4-19
Surface Storage Configuration	Orifice Height (ft)	0	0	0
	Orifice Diameter (in.)	0	0	0
	Rectangular or Triangular Weir	Rectangular	Rectangular	Rectangular
	Weir Height (ft)/Ponding Depth (ft)	0.5	2	0.5
	Crest Width (ft)	30	30	30
Soil Properties	Depth of Soil (ft)	6	0	2.5
	Soil Porosity (0-1)	0.4	0.4	0.2
	Vegetative Parameter A	0.9	0.9	0.9
	Soil Infiltration (in/hr)	8.27, 2.41, 1.02	8.27, 2.41, 1.02	2.5
Underdrain Properties	Consider Underdrain Structure?	No	No	Yes
	Storage Depth (ft)	0	0	1
	Media Void Fraction (0-1)	0	0	0.4
	Background Infiltration (in/hr)	N/A	N/A	0.1
Cost Parameters	Storage Volume Cost (\$/ft ³)	\$25.64	\$12.82	\$31.74
Cost Function Adjustment	SCM Development Type	New SCM in Developed Area	New SCM in Developed Area	New SCM in Developed Area
	Cost Adjustment Factor	2	2	2
Decay Rates	TSS (1/hr)	0.74	0.74	0.79
	TN (1/hr)	0.42	0.42	0.03
	TP (1/hr)	0.27	0.27	0.13
	ZN (1/hr)	0.45	0.45	0.49
Underdrain Removal Rates	TSS (% 0-1)	N/A	N/A	0.89
	TN (% 0-1)	N/A	N/A	0.41
	TP (% 0-1)	N/A	N/A	0.43
	ZN (% 0-1)	N/A	N/A	0.84

4.2.3 *Opti-Tool Setup*

The following steps were performed to set up and run the Opti-Tool for the optimization analysis.

- Identify representative climate boundary condition: An average water year of precipitation in the recent historical period (1999 – 2020) as climate boundary condition was selected for running thousands of GI SCM simulation iterations to develop the cost-effectiveness curves (CE-Curves). The analysis identified 2012 as an average water year (Table 4-17). By using a single water year instead of a full 20-year period to develop the CE-Curve, simulation time was reduced from ~72 hours to ~4 hours for running 10,000 model iterations.
- Establish baseline condition: Unit-area HRU time series for the period of interest (October 2000 – September 2020) were used as the boundary condition to the SCM simulation model. These time series were generated from the calibrated LSPC model and represent the hourly flow and pollutant loadings from the surface runoff. The interflow and groundwater outflow to the streams were also output as hourly time series from the calibrated LSPC model. An Opti-Tool baseline model was set up for each selected sub-watershed with HRU-based runoff time series and baseflow time series were routed to the stream segment configured in the Opti-Tool. The flow routing in the stream was modeled using the F-table representation from the calibrated LSPC model to be consistent with the watershed model. The Opti-Tool was run for 20 years without any GI SCM configured in the model to establish the baseline. The Opti-Tool daily outflow time series at the sub-watershed outlet were compared against the calibrated LSPC baseline daily outflow time series. The comparison shows a satisfactory representation of the baseline in the Opti-Tool (Figure 4-25) that was used as an existing condition for simulating the GI SCM controls for the FDC optimization objective.
- Set target condition: An hourly outflow time series for the pre-development/forested condition was created for each study sub-watershed in the LSPC model. Those time series were used to generate the pre-development target FDC for SCM optimization in the Opti-Tool.
- Set management objective: The management objective was to identify the mixture of the most cost-effective stormwater controls (types and sizes) for minimizing the difference between the pre-development and existing conditions FDC for each of the three study sub-watersheds.
- Set optimization target: Cost-effectiveness curves showing a wide range of best solutions for reducing the area between the FDC curves were developed.
- Incorporate land use information: The area distribution for the major land use groups within the study watersheds was estimated. Each land use group in the model was assigned the corresponding unit-area HRU time series. The impervious areas were routed to the SCM type by land use group and HSG soil group (Table 4-18). The untreated pervious areas were routed directly to the downstream channel.
- Incorporate SCM information: Three SCM types, infiltration trench, infiltration basin, and biofiltration were selected by major land use group and HSG soil group based on the GIS screening of Management Category analysis. SCM design specifications were set using the default parameters and SCM cost function available in the Opti-Tool (Table 4-16). The maximum footprint opportunity used in the optimization decision matrix for each SCM type was limited to capture up to 2-inch runoff from the treated impervious cover (Table 4-19).
- Run optimization scenario: The simulation period (water year 2012), the stormwater evaluation factor (FDC), the objective function (minimize cost) were defined, and input files were created for the optimization runs. The optimization was performed using the continuous hourly simulation SCM model to reflect precipitation conditions for an average water year that included a wide range of actual storm sizes to find the optimal SCM storage capacities that provided the most cost-effective




solution at the watershed scale. Twenty thousand iterations were performed for each optimization scenario for the study sub-watersheds that generated a CE-Curve showing a wide range of optimal solutions frontier that minimize the area between FDCs for existing conditions and the pre-development/forested condition (Figure 4-26).

- Identify the best solution: The CE-Curve presents solutions from all 20,000 iterations made during the optimization run. The gray dots are the inferior solutions because they cost more as compared to the best solution on the frontier of the curve for the same optimization target reduction. Even though the frontier of the curve represents the best solution for the specific optimization reduction target, the best solution at the knee of the curve represents the most cost-effective solution that provides the maximum benefits at the minimum cost (Figure 4-27).
- Evaluate the selected best solution: The optimization runs were made for an average water year to save the model run time in identifying the mixture of the most cost-effective SCM types and sizes. The selected best solution for the optimized SCM storage capacities was simulated for 20 years (2000-2020) to stress test for a wide range of weather conditions including dry and wet climate years and a wide range of storm sizes span over the long-term period. The FDCs for the selected best solution were compared against the existing baseline condition and pre-development/forested condition for the study sub-watersheds (Figure 4-28).
- Test resiliency to climate change: The selected best solution for the Upper Hodges sub-watershed was further evaluated against the predicted future climate conditions by using the 12 selected climate change models in Section 4.1.5 (Table 4-6). The FDCs for the selected best solution using the future climate conditions (2079-2099) were compared against the historical climate condition (2000-2020).

Table 4-17. Precipitation analysis for the baseline model period

Taunton Airport							
Water Year (Oct-Sept)	Rainfall (in)	Percentile	Difference (inches)	Number of Rain Days per Year:			
			All Years	≥ 0.1in	≥ 0.5in	≥ 1.0in	≥1.5in
1999	39.02	22%	-7.04	60	23	14	4
2000	47.84	57%	1.78	83	34	12	4
2001	44.24	39%	-1.82	73	33	10	7
2002	33.55	4%	-12.51	61	21	7	5
2003	59.46	96%	13.40	99	36	21	9
2004	35.02	9%	-11.04	58	23	10	5
2005	37.77	17%	-8.29	60	26	10	4
2006	57.38	91%	11.32	81	34	14	8
2007	45.91	43%	-0.15	74	25	16	8
2008	49.08	65%	3.02	85	25	12	6
2009	50.57	70%	4.51	96	37	9	6
2010	55.82	87%	9.76	81	37	18	8
2011	51.17	74%	5.11	84	34	16	5
2012	46.18	48%	0.12	72	32	13	5
2013	46.23	52%	0.17	86	33	13	1
2014	40.03	26%	-6.03	78	24	7	5
2015	48.67	61%	2.61	81	34	13	6
2016	35.5	13%	-10.56	81	24	5	1
2017	41.89	29%	-4.17	76	24	12	5
2018	52.56	79%	6.50	82	32	18	8
2019	53.27	83%	7.21	94	37	15	3
2020	42.23	33%	-3.83	86	27	10	3
Average (1999-2020)	46.06	--	--	79	30	13	5

Legend

-  10th %-tile Year
-  Average Year
-  90th %-tile Year

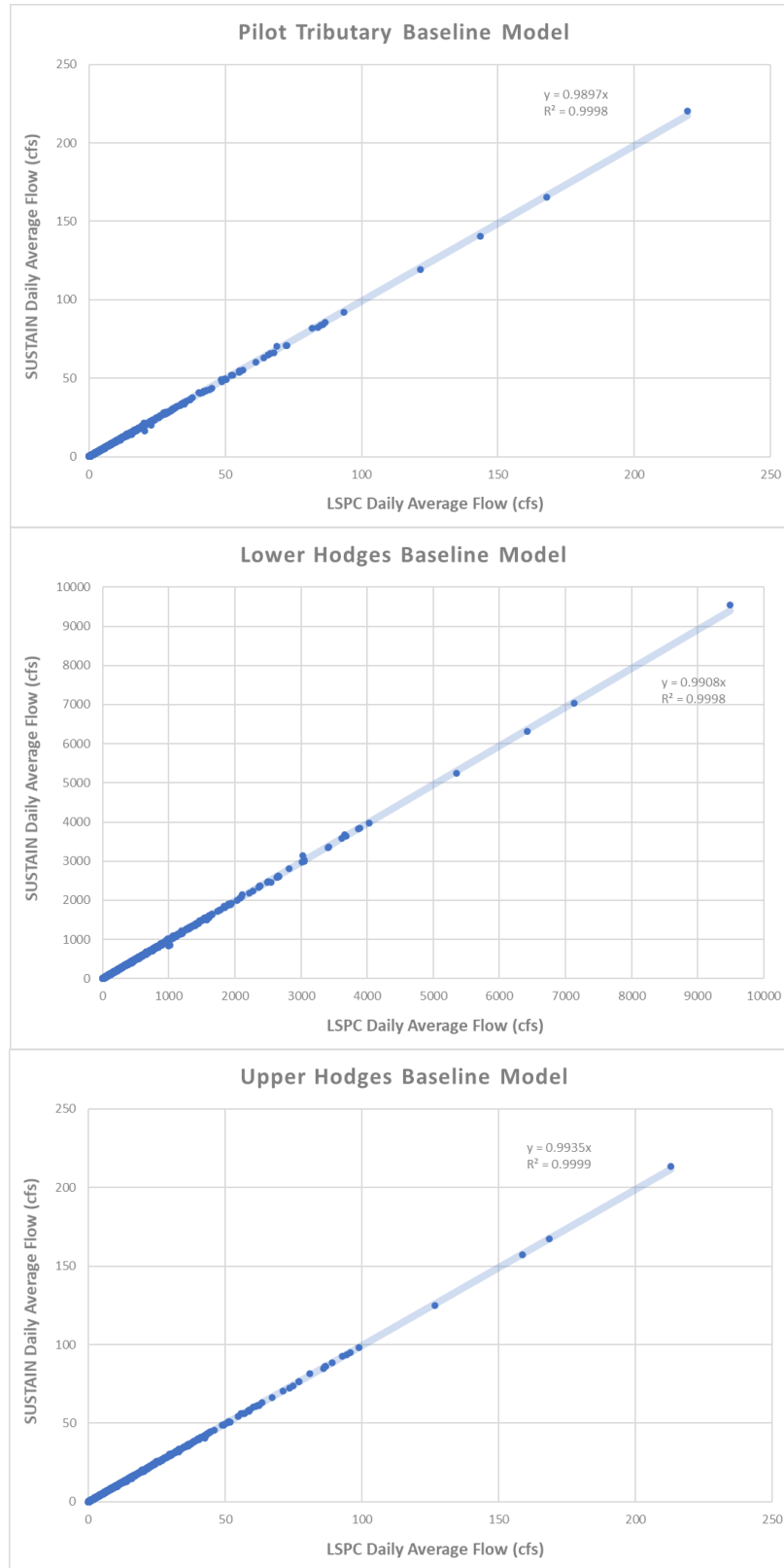


Figure 4-25. Opti-Tool baseline verification for Pilot Tributary (top), Lower Hodges (middle), and Upper Hodges (bottom) sub-watersheds. Sub-watersheds ordered from top to bottom as least developed (Pilot Tributary) to most Developed (Upper Hodges).

Table 4-18. Impervious area treated by SCMs (impervious cover disconnection) in the three study sub-watersheds.

Land Use Group	Disconnection Type	SCM Type	HSG	Treated Impervious Area (acres)		
				Pilot Tributary	Upper Hodges	Lower Hodges
Forest	Rooftop	Infiltration Trench	A	--	--	--
			B	--	--	--
			C	--	--	--
	Other IC	Infiltration basin	A	--	--	--
			B	--	--	--
		Biofiltration	C	--	--	--
Agriculture	Rooftop	Infiltration Trench	D	--	--	--
			A	--	--	--
			B	--	--	--
	Other IC	Infiltration basin	C	--	--	--
			A	--	--	--
		Biofiltration	B	--	--	--
Commercial	Rooftop	Infiltration Trench	C	--	--	--
			A	0.05	2.69	0.11
			B	--	0.03	--
	Other IC	Infiltration basin	A	0.09	4.00	--
			B	--	0.15	--
		Biofiltration	C	--	2.57	--
Industrial	Rooftop	Infiltration Trench	D	0.07	3.09	--
			A	--	1.82	--
			B	--	0.20	--
	Other IC	Infiltration basin	C	--	30.61	--
			A	0.01	1.33	--
		Biofiltration	B	0.01	0.47	--
Low Density Residential	Rooftop	Infiltration Trench	C	0.03	17.16	--
			D	0.03	18.72	--
			A	1.66	0.73	1.77
	Other IC	Infiltration basin	B	0.03	0.24	0.58
			A	1.29	0.41	2.07
		Biofiltration	C	0.50	0.35	0.77
Medium Density Residential	Rooftop	Infiltration Trench	D	1.08	0.87	1.06
			A	0.02	--	--
			B	--	0.08	0.03
	Other IC	Infiltration basin	C	--	0.05	0.02
			A	0.10	--	0.24

Land Use Group	Disconnection Type	SCM Type	HSG	Treated Impervious Area (acres)		
				Pilot Tributary	Upper Hodges	Lower Hodges
		Biofiltration	B	--	0.11	0.01
			C	--	0.11	--
			D	0.03	0.24	--
High Density Residential	Rooftop	Infiltration Trench	A	1.36	--	--
			B	0.15	2.00	0.50
			C	0.02	0.37	0.09
	Other IC	Infiltration basin	A	1.32	0.01	0.07
			B	0.14	1.57	0.01
			C	0.34	0.47	0.26
		Biofiltration	D	0.66	2.39	0.21
Highway	Rooftop	Infiltration Trench	A	--	--	--
			B	--	--	--
			C	--	--	0.01
	Other IC	Infiltration basin	A	6.52	23.43	15.95
			B	0.98	7.99	5.77
			C	6.29	36.92	4.65
		Biofiltration	D	5.48	28.01	3.22
Open Land	Rooftop	Infiltration Trench	A	0.01	0.09	0.02
			B	--	0.03	0.01
			C	--	0.26	0.05
	Other IC	Infiltration basin	A	0.09	0.37	0.05
			B	0.02	0.20	0.03
			C	0.14	0.93	0.06
		Biofiltration	D	0.09	1.26	0.06

Table 4-19. Potential SCM opportunity areas (maximum modeled footprints) in the three study sub-watersheds.

Land Use Group	Disconnection Type	SCM Type	HSG	Maximum Modeled Footprint* (acres)		
				Pilot Tributary	Upper Hodges	Lower Hodges
Forest	Rooftop	Infiltration Trench	A	--	--	--
			B	--	--	--
			C	--	--	--
	Other IC	Infiltration basin	A	--	--	--
			B	--	--	--
		Biofiltration	D	--	--	--
Agriculture	Rooftop	Infiltration Trench	A	--	--	--
			B	--	--	--
			C	--	--	--
	Other IC	Infiltration basin	A	--	--	--
			B	--	--	--
		Biofiltration	D	--	--	--
Commercial	Rooftop	Infiltration Trench	A	--	0.15	0.01
			B	--	--	--
			C	--	0.10	--
	Other IC	Infiltration basin	A	0.01	0.33	--
			B	--	0.01	--
		Biofiltration	C	--	0.21	--
Industrial	Rooftop	Infiltration Trench	D	0.01	0.37	--
			A	--	0.10	--
			B	--	0.01	--
	Other IC	Infiltration basin	C	--	1.76	--
			A	--	0.11	--
		Biofiltration	B	--	0.04	--
Low Density Residential	Rooftop	Infiltration Trench	C	--	1.43	--
			D	--	2.23	--
			A	0.10	0.04	0.10
	Other IC	Infiltration basin	B	--	0.01	0.03
			C	0.02	0.04	0.09
		Biofiltration	A	0.11	0.03	0.17
Medium Density Residential	Rooftop	Infiltration Trench	B	0.01	0.01	0.05
			C	0.04	0.03	0.06
	Other IC	Infiltration basin	D	0.13	0.10	0.13
Medium Density Residential	Rooftop	Infiltration Trench	A	--	--	--
			B	--	--	--
			C	--	--	--
	Other IC	Infiltration basin	A	0.01	--	0.02

Land Use Group	Disconnection Type	SCM Type	HSG	Maximum Modeled Footprint* (acres)		
				Pilot Tributary	Upper Hodges	Lower Hodges
		Biofiltration	B	--	0.01	--
			C	--	0.01	--
			D	--	0.03	--
High Density Residential	Rooftop	Infiltration Trench	A	0.08	--	--
			B	0.01	0.11	0.03
			C	--	0.02	0.01
	Other IC	Infiltration basin	A	0.11	--	0.01
			B	0.01	0.13	--
			C	0.03	0.04	0.02
		Biofiltration	D	0.08	0.28	0.02
Highway	Rooftop	Infiltration Trench	A	--	--	--
			B	--	--	--
			C	--	--	--
	Other IC	Infiltration basin	A	0.54	1.95	1.33
			B	0.08	0.67	0.48
			C	0.52	3.08	0.39
		Biofiltration	D	0.65	3.33	0.38
Open Land	Rooftop	Infiltration Trench	A	--	0.01	--
			B	--	--	--
			C	--	0.02	--
	Other IC	Infiltration basin	A	0.01	0.03	--
			B	--	0.02	--
			C	0.01	0.08	0.01
		Biofiltration	D	0.01	0.15	0.01

* The maximum modeled footprint represents the maximum opportunity used in the optimization decision matrix to capture up to 2 inches of runoff from the treated impervious cover. The actual available footprint on the ground could be higher to allow larger design storage volume to capture larger storms for flood control management objective.

4.3 Optimization Results

The optimal mix of GI SCM types and sizes was assessed for the management objective of reducing the difference between the baseline and pre-development/forested FDCs for the three study sub-watersheds. Figure 4-26 presents the cost-effectiveness curve (CE-Curve) for the FDC objective for Pilot Tributary, Lower Hodges, and Upper Hodges. The blue diamonds form the most cost-effective combination of GI SCM configurations for FDC differences. The grey dots on the curve are inferior solutions; compared to these solutions, cheaper alternatives exist that would achieve the same optimization target reduction. The red triangle presents a theoretical target solution. Figure 4-26 highlights the maximum simulated reductions in each sub-watershed. As outlined in Section 4.2.3, the CE-Curves were developed using the 2012 water year. The cost estimates are based on regional unit cost information for the control types, a 35% add-on for engineering and contingencies and a site factor multiplier to account for anticipated difficulties associated with installations. For this analysis, a multiplier of 2X was assumed for all controls. Perhaps unsurprisingly, Figure 4-26 suggests that implementing SCMs in a less developed watershed has a relatively smaller impact on the FDC than SCMs implemented in a more developed watershed. SCM implementation in the relatively undeveloped Pilot Tributary can only achieve a 7% reduction between the baseline and pre-development FDCs while SCM implementation in Upper Hodges, which was the most developed sub-watershed, can achieve a 16% reduction. This result is likely due to increased development resulting in additional divergence from the pre-development condition. Therefore, when SCMs are implemented in such watersheds, the impact is more readily observed compared to less developed watersheds whose hydrological functions are relatively un-impaired. While the highlighted reductions are the maximum modeled, they are also some of the least cost-effective. The CE-Curves, which have a reduction on the x-axis and cost on the y-axis, become steeper from left to right. Therefore, the further right on the curve, the more expensive any additional reduction becomes.

Figure 4-29 presents a generalized, annotated FDC that assigns five conditions, ranging from low flows to high flows, across the curve. These flow regimes were used to compare model results for the Pilot Tributary sub-watershed (Table 4-20), Lower Hodges sub-watershed (Table 4-21), and Upper Hodges sub-watershed (Table 4-22). The results support the LSPC-based land use scenario findings discussed in Section 4.1.2. The pre-development conditions had the lowest flows across the FDC, which can be attributed to the ability of forests to store and attenuate water, as well as high ET rates during the summer. The SCM implementation results support the results from the disconnected (EIA = 0) land use scenario. At the high flows, SCMs result in lower flows compared to existing conditions; however, other flow regimes experience an increase in streamflow. The stormwater runoff that SCMs infiltrate is routed to the Opti-Tool aquifer and allowed to become return flows to the stream. These return flows are likely the cause of the increased flows in other flow regimes. The pollutant load reductions (TSS, TN, TP, and Zn) for the same selected solutions were also estimated for the study sub-watersheds (Table 4-23). Table 4-24 and Table 4-25 show the BMP selection details for the maximum and best solutions for the Upper Hodges sub-watershed.

Figure 4-30 through Figure 4-34 present the results of the climate change analysis. The resilience of the implementation solution for Upper Hodges, highlighted in Figure 4-27 was assessed by running the 12 climate change models identified in Table 4-6. The climate change runs were made for 20 years (2079-2099) consistent with the 20-year baseline period (2000-2020). The results suggest that overall, climate change is expected to produce lower low flows and higher high flows in the Upper Hodges, which was the most developed watershed. These results differ from those presented in Figure 4-19 through Figure 4-23, however, those results were assessed at the mouth of the Wading River as compared to the outlet of Upper Hodges. Climate change models produced ecosurpluses at the lowest flows in the Wading River but ecodeficits for low flows in Upper Hodges. The results are likely due to differences in watershed characteristics, including size, land cover, and the presence of wetlands and small dams. Overall, the results support the findings of Demaria et al (Demaria et al., 2016b) who found that low flows and base flows are expected to decrease due to climate change. The implementation of SCMs may help to mitigate some of these losses in baseflows by encouraging infiltration and groundwater recharge.

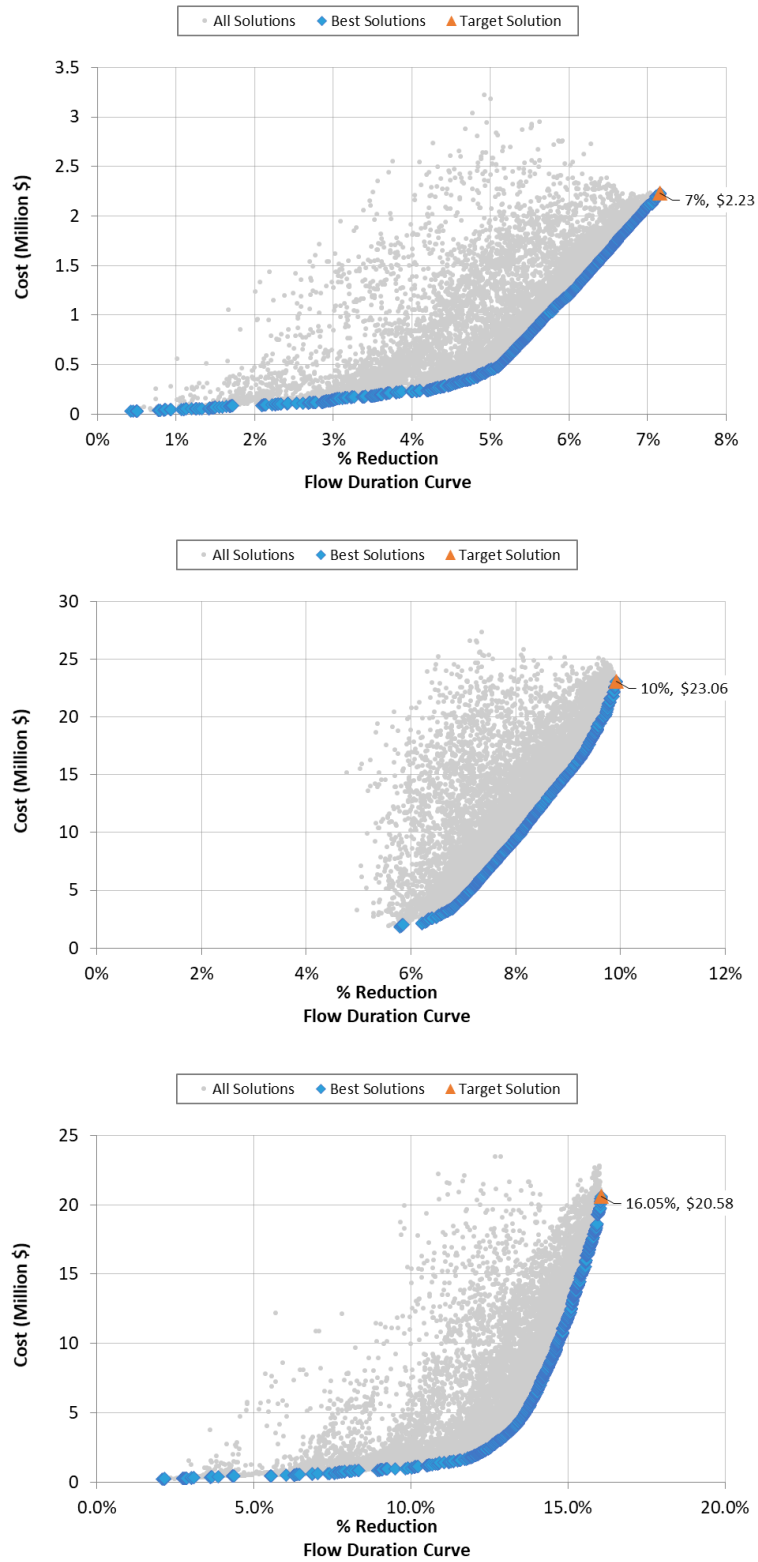


Figure 4-26. Opti-Tool FDC cost-effectiveness curves for Pilot Tributary (top), Lower Hodges (middle), and Upper Hodges (bottom) sub-watersheds. The maximum solutions are highlighted. Sub-watersheds ordered from top to bottom as least developed (Pilot Tributary) to most Developed (Upper Hodges).

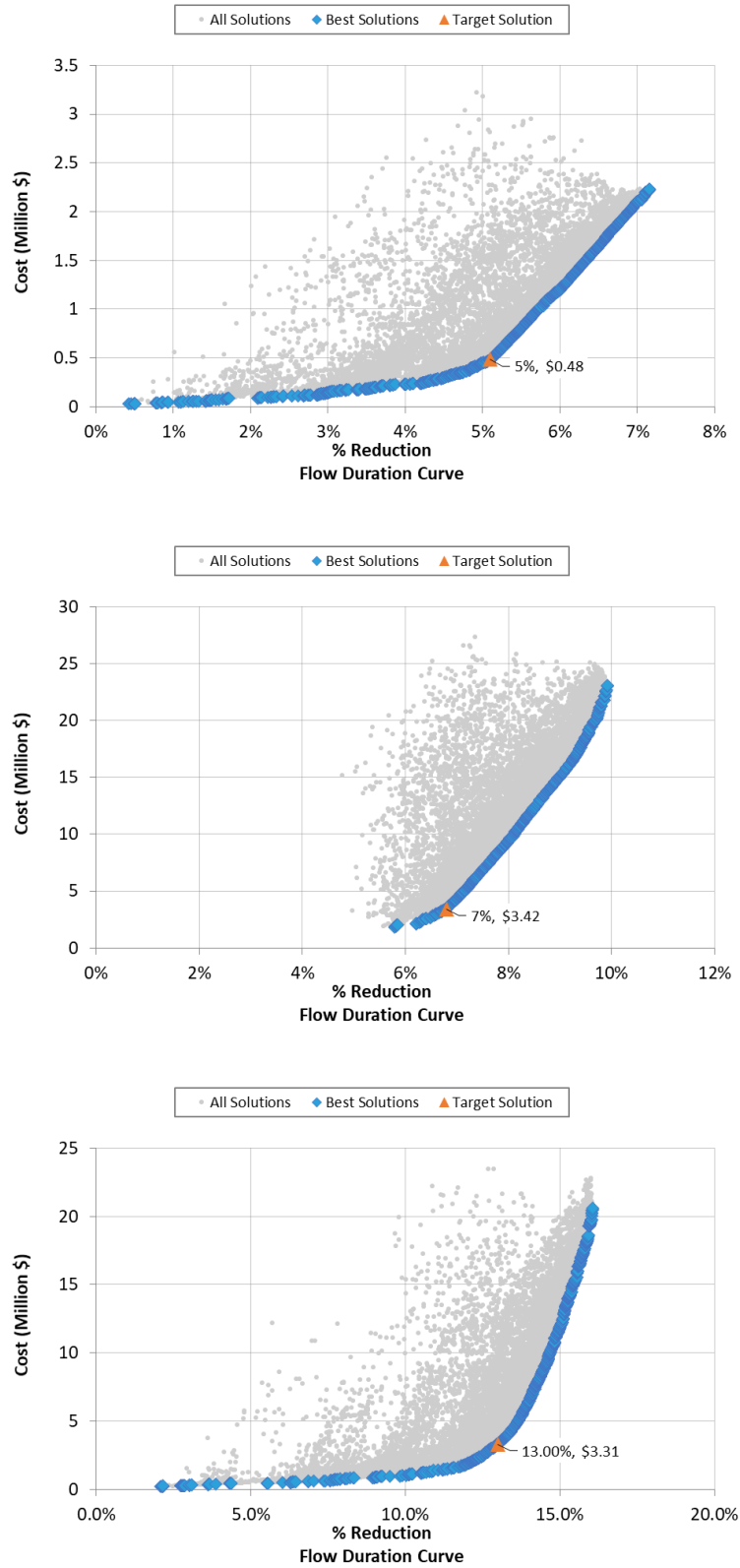


Figure 4-27. Opti-Tool FDC cost-effectiveness curves for Pilot Tributary (top), Lower Hodges (middle), and Upper Hodges (bottom) sub-watersheds. Highly cost-effective solutions, located around the knee of the curves, are highlighted. Sub-watersheds ordered from top to bottom as least developed (Pilot Tributary) to most Developed (Upper Hodges).

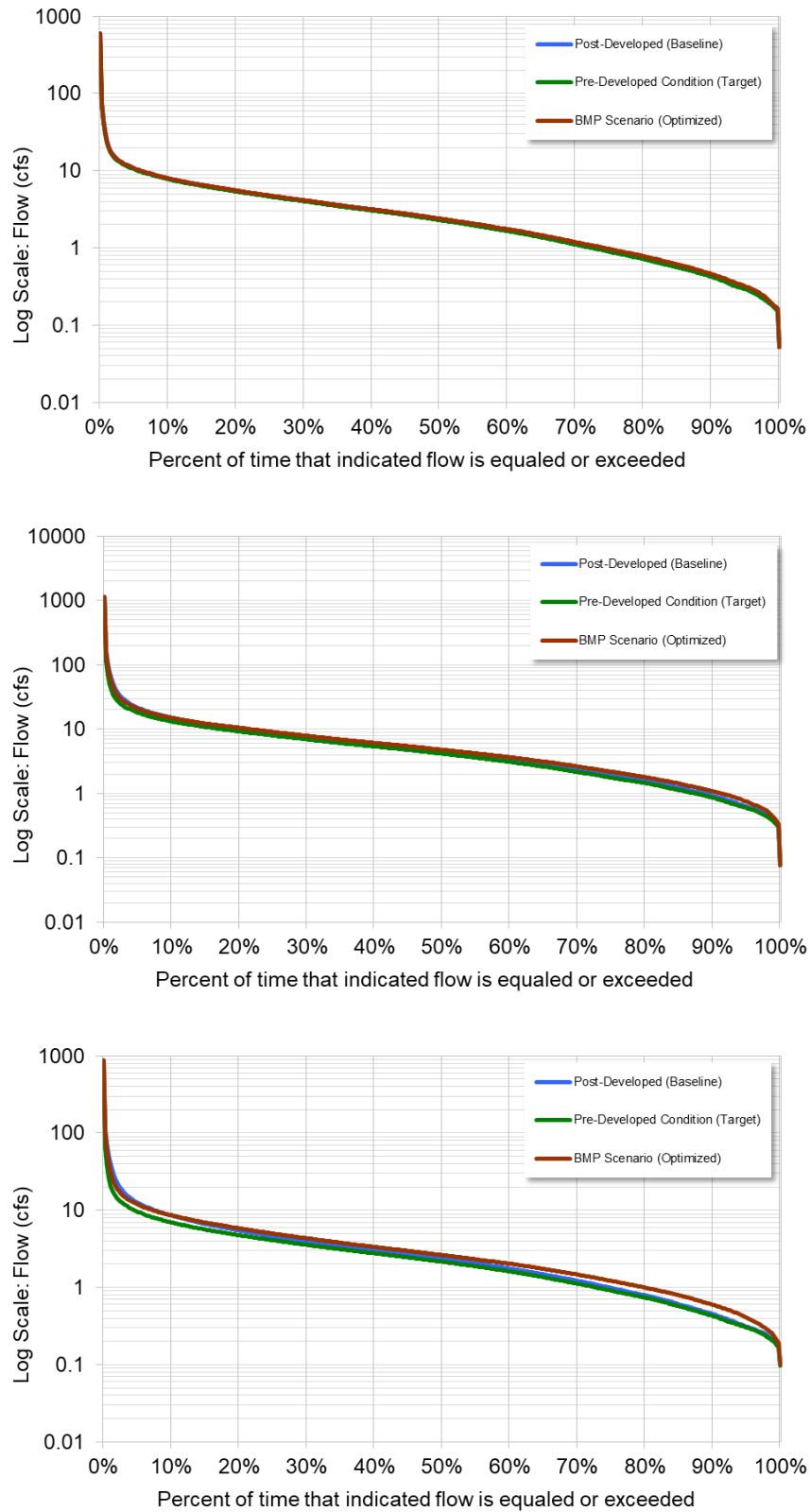


Figure 4-28. Opti-Tool FDCs for Pilot Tributary (top), Lower Hodges (middle), and Upper Hodges (bottom) sub-watersheds. Results are based on the solutions highlighted in Figure 4-27. Sub-watersheds ordered from top to bottom as least developed (Pilot Tributary) to most Developed (Upper Hodges).

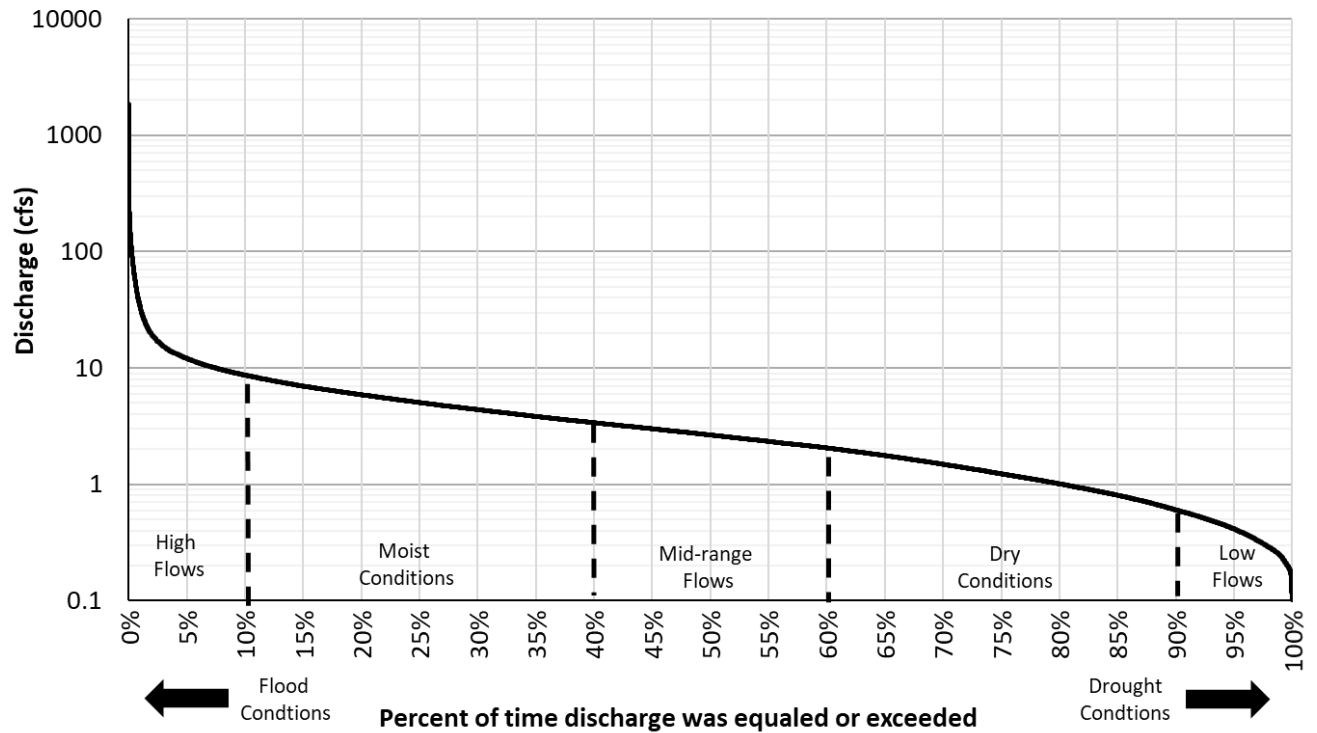


Figure 4-29. Annotated flow duration curve. Adapted from U.S. EPA, 2007.

Table 4-20. Average daily flow by flow regime (gallons per day) for Pilot Tributary sub-watershed. Results are based on the FDCs shown in Figure 4-28.

FDC Flow Regime	Pre-development	Existing Conditions	SCM Implementation	Difference between Existing Conditions and SCM Implementation
High Flows (<10%)	11,012,039	11,530,783	11,424,319	-106,465
Moist Conditions (10% - 40%)	3,179,165	3,262,186	3,278,555	16,369
Mid-range Flows (40% - 60%)	1,522,348	1,580,935	1,588,452	7,516
Dry Conditions (60% - 90%)	621,713	658,184	668,450	10,267
Low Flows (>90%)	187,063	196,962	204,940	7,978

Table 4-21. Average daily flow by flow regime (gallons per day) for Lower Hodges sub-watershed. Results are based on the FDCs shown in Figure 4-28.

FDC Flow Regime	Pre-development	Existing Conditions	SCM Implementation	Difference between Existing Conditions and SCM Implementation
High Flows (<10%)	18,479,200	24,094,669	22,906,197	-1,188,473
Moist Conditions (10% - 40%)	5,440,956	6,048,528	6,172,442	123,914
Mid-range Flows (40% - 60%)	2,736,726	3,000,845	3,145,674	144,830
Dry Conditions (60% - 90%)	1,210,179	1,331,404	1,474,435	143,031
Low Flows (>90%)	383,402	408,548	480,178	71,630

Table 4-22. Average daily flow by flow regime (gallons per day) for Upper Hodges sub-watershed. Results are based on the FDCs shown in Figure 4-28.

FDC Flow Regime	Pre-development	Existing Conditions	SCM Implementation	Difference between Existing Conditions and SCM Implementation
High Flows (<10%)	10,328,678	15,542,489	14,047,584	-1,494,905
Moist Conditions (10% - 40%)	2,821,690	3,249,150	3,452,334	203,184
Mid-range Flows (40% - 60%)	1,418,780	1,545,519	1,730,688	185,169
Dry Conditions (60% - 90%)	625,365	676,662	821,837	145,174
Low Flows (>90%)	195,743	204,887	263,553	58,666

Table 4-23. Pollutant load reductions (%) from the surface runoff for the best solutions (highlighted in Figure 4-27) for the study sub-watersheds.

Parameter	Pilot Tributary	Lower Hodges	Upper Hodges
TSS Load	23.3%	49.8%	51.2%
TN Load	11.7%	32.2%	36.0%
TP Load	9.8%	31.5%	36.7%
Zn Load	21.5%	49.5%	52.8%

Table 4-24. Optimized SCM opportunities for the maximum solution (highlighted in Figure 4-26) for the Upper Hodges sub-watershed.

SCM ID	SCM Type	Land Use-HSG	Treated Impervious Area (acres)	Runoff Depth (in.)	SCM Storage Capacity (gallon)	SCM Cost (\$)
SCM1	INFILTRATIONBASIN	Commercial-A	4.00	0.2	21,708	\$37,202
SCM2	INFILTRATIONBASIN	Commercial-B	0.15	0.2	833	\$1,428
SCM3	INFILTRATIONBASIN	Commercial-C	2.57	0.6	41,899	\$71,805
SCM4	BIORETENTION	Commercial-D	3.09	2.0	167,929	\$712,527
SCM5	INFILTRATIONBASIN	Industrial-A	1.33	0.2	7,217	\$12,369
SCM6	INFILTRATIONBASIN	Industrial-B	0.47	0.2	2,559	\$4,386
SCM7	INFILTRATIONBASIN	Industrial-C	17.15	0.6	279,557	\$478,669
SCM8	BIORETENTION	Industrial-D	18.72	2.0	1,016,860	\$4,314,560
SCM9	INFILTRATIONBASIN	Low Density Residential-A	0.41	0.4	4,416	\$7,568
SCM10	INFILTRATIONBASIN	Low Density Residential-B	0.15	0.8	3,262	\$5,591
SCM11	INFILTRATIONBASIN	Low Density Residential-C	0.35	0.8	7,680	\$13,162
SCM12	BIORETENTION	Low Density Residential-D	0.87	1.4	32,922	\$139,690
SCM13	INFILTRATIONBASIN	Medium Density Residential-B	0.11	0.4	1,219	\$2,090
SCM14	INFILTRATIONBASIN	Medium Density Residential-C	0.11	0.4	1,183	\$2,028
SCM15	BIORETENTION	Medium Density Residential-D	0.24	1.6	10,340	\$43,871
SCM16	INFILTRATIONBASIN	High Density Residential-A	0.01	1.0	351	\$601
SCM17	INFILTRATIONBASIN	High Density Residential-B	1.57	0.4	17,095	\$29,298
SCM18	INFILTRATIONBASIN	High Density Residential-C	0.47	0.6	7,659	\$13,127
SCM19	BIORETENTION	High Density Residential-D	2.39	2.0	129,549	\$549,681
SCM20	INFILTRATIONBASIN	Highway-A	23.43	0.2	127,296	\$218,158
SCM21	INFILTRATIONBASIN	Highway-B	7.99	0.4	86,836	\$148,819
SCM22	INFILTRATIONBASIN	Highway-C	36.92	0.6	601,580	\$1,030,979
SCM23	BIORETENTION	Highway-D	28.01	2.0	1,521,124	\$6,454,160
SCM24	INFILTRATIONBASIN	Open Land-A	0.37	0.2	2,034	\$3,485
SCM25	INFILTRATIONBASIN	Open Land-B	0.20	0.6	3,201	\$5,486
SCM26	INFILTRATIONBASIN	Open Land-C	0.93	0.6	15,198	\$26,046
SCM27	BIORETENTION	Open Land-D	1.26	1.6	54,687	\$232,038
SCM28	INFILTRATIONTRENCH	Commercial-A	2.69	0.4	29,195	\$123,876
SCM29	INFILTRATIONTRENCH	Commercial-B	0.03	0.2	171	\$727
SCM30	INFILTRATIONTRENCH	Commercial-C	1.80	1.4	68,489	\$290,602

SCM ID	SCM Type	Land Use-HSG	Treated Impervious Area (acres)	Runoff Depth (in.)	SCM Storage Capacity (gallon)	SCM Cost (\$)
SCM31	INFILTRATIONTRENCH	Industrial-A	1.82	0.4	19,786	\$83,953
SCM32	INFILTRATIONTRENCH	Industrial-B	0.20	1.0	5,381	\$22,832
SCM33	INFILTRATIONTRENCH	Industrial-C	30.61	1.4	1,163,549	\$4,936,963
SCM34	INFILTRATIONTRENCH	Low Density Residential-A	0.74	0.4	7,983	\$33,871
SCM35	INFILTRATIONTRENCH	Low Density Residential-B	0.24	0.6	3,963	\$16,814
SCM36	INFILTRATIONTRENCH	Low Density Residential-C	0.63	1.4	24,054	\$102,061
SCM37	INFILTRATIONTRENCH	Medium Density Residential-B	0.08	1.4	3,124	\$13,254
SCM38	INFILTRATIONTRENCH	Medium Density Residential-C	0.05	1.0	1,405	\$5,960
SCM39	INFILTRATIONTRENCH	High Density Residential-B	2.00	1.4	75,891	\$322,006
SCM40	INFILTRATIONTRENCH	High Density Residential-C	0.37	1.0	10,042	\$42,608
SCM41	INFILTRATIONTRENCH	Highway-A	0.00	0.0	0	\$0
SCM42	INFILTRATIONTRENCH	Highway-B	0.00	0.0	0	\$0
SCM43	INFILTRATIONTRENCH	Highway-C	0.00	0.0	0	\$0
SCM44	INFILTRATIONTRENCH	Open Land-A	0.00	0.0	0	\$0
SCM45	INFILTRATIONTRENCH	Open Land-B	0.03	0.6	499	\$2,115
SCM46	INFILTRATIONTRENCH	Open Land-C	0.26	0.8	5,704	\$24,201
Total			194.84	1.1	5,585,431	\$20,580,666

Table 4-25. Optimized SCM opportunities for the best solutions (highlighted in Figure 4-27) for the Upper Hodges sub-watershed.

SCM ID	SCM Type	Land Use-HSG	Treated Impervious Area (acres)	Runoff Depth (in.)	SCM Storage Capacity (gallon)	SCM Cost (\$)
SCM1	INFILTRATIONBASIN	Commercial-A	4.00	0.2	21,708	\$37,202
SCM2	INFILTRATIONBASIN	Commercial-B	0.15	0.8	3,334	\$5,714
SCM3	INFILTRATIONBASIN	Commercial-C	2.57	0.6	41,899	\$71,805
SCM4	BIORETENTION	Commercial-D	0.00	0.0	0	\$0
SCM5	INFILTRATIONBASIN	Industrial-A	1.33	0.2	7,217	\$12,369
SCM6	INFILTRATIONBASIN	Industrial-B	0.47	0.2	2,559	\$4,386
SCM7	INFILTRATIONBASIN	Industrial-C	17.15	0.6	279,557	\$478,669
SCM8	BIORETENTION	Industrial-D	0.00	0.0	0	\$0
SCM9	INFILTRATIONBASIN	Low Density Residential-A	0.41	0.2	2,208	\$3,784
SCM10	INFILTRATIONBASIN	Low Density Residential-B	0.15	0.4	1,631	\$2,795

SCM ID	SCM Type	Land Use-HSG	Treated Impervious Area (acres)	Runoff Depth (in.)	SCM Storage Capacity (gallon)	SCM Cost (\$)
SCM11	INFILTRATIONBASIN	Low Density Residential-C	0.35	0.8	7,680	\$13,162
SCM12	BIORETENTION	Low Density Residential-D	0.00	0.0	0	\$0
SCM13	INFILTRATIONBASIN	Medium Density Residential-B	0.11	1.0	3,048	\$5,224
SCM14	INFILTRATIONBASIN	Medium Density Residential-C	0.11	0.4	1,183	\$2,028
SCM15	BIORETENTION	Medium Density Residential-D	0.24	1.2	7,755	\$32,903
SCM16	INFILTRATIONBASIN	High Density Residential-A	0.00	0.0	0	\$0
SCM17	INFILTRATIONBASIN	High Density Residential-B	1.57	0.4	17,095	\$29,298
SCM18	INFILTRATIONBASIN	High Density Residential-C	0.47	0.6	7,659	\$13,127
SCM19	BIORETENTION	High Density Residential-D	0.00	0.0	0	\$0
SCM20	INFILTRATIONBASIN	Highway-A	23.43	0.2	127,296	\$218,158
SCM21	INFILTRATIONBASIN	Highway-B	7.99	0.6	130,254	\$223,228
SCM22	INFILTRATIONBASIN	Highway-C	36.92	0.6	601,580	\$1,030,979
SCM23	BIORETENTION	Highway-D	0.00	0.0	0	\$0
SCM24	INFILTRATIONBASIN	Open Land-A	0.37	0.6	6,101	\$10,456
SCM25	INFILTRATIONBASIN	Open Land-B	0.20	1.0	5,335	\$9,144
SCM26	INFILTRATIONBASIN	Open Land-C	0.93	0.2	5,066	\$8,682
SCM27	BIORETENTION	Open Land-D	0.00	0.0	0	\$0
SCM28	INFILTRATIONTRENCH	Commercial-A	2.69	0.4	29,195	\$123,876
SCM29	INFILTRATIONTRENCH	Commercial-B	0.00	0.0	0	\$0
SCM30	INFILTRATIONTRENCH	Commercial-C	1.80	0.4	19,568	\$83,029
SCM31	INFILTRATIONTRENCH	Industrial-A	1.82	0.2	9,893	\$41,977
SCM32	INFILTRATIONTRENCH	Industrial-B	0.20	0.6	3,229	\$13,699
SCM33	INFILTRATIONTRENCH	Industrial-C	30.61	0.2	166,221	\$705,280
SCM34	INFILTRATIONTRENCH	Low Density Residential-A	0.74	0.2	3,991	\$16,936
SCM35	INFILTRATIONTRENCH	Low Density Residential-B	0.24	0.6	3,963	\$16,814
SCM36	INFILTRATIONTRENCH	Low Density Residential-C	0.00	0.0	0	\$0
SCM37	INFILTRATIONTRENCH	Medium Density Residential-B	0.08	0.8	1,785	\$7,574
SCM38	INFILTRATIONTRENCH	Medium Density Residential-C	0.05	1.4	1,967	\$8,344
SCM39	INFILTRATIONTRENCH	High Density Residential-B	2.00	0.2	10,842	\$46,001

SCM ID	SCM Type	Land Use-HSG	Treated Impervious Area (acres)	Runoff Depth (in.)	SCM Storage Capacity (gallon)	SCM Cost (\$)
SCM40	INFILTRATIONTRENCH	High Density Residential-C	0.37	0.2	2,008	\$8,522
SCM41	INFILTRATIONTRENCH	Highway-A	0.00	0.0	0	\$0
SCM42	INFILTRATIONTRENCH	Highway-B	0.00	0.0	0	\$0
SCM43	INFILTRATIONTRENCH	Highway-C	0.00	0.0	0	\$0
SCM44	INFILTRATIONTRENCH	Open Land-A	0.09	0.6	1,526	\$6,475
SCM45	INFILTRATIONTRENCH	Open Land-B	0.03	0.6	499	\$2,115
SCM46	INFILTRATIONTRENCH	Open Land-C	0.26	0.6	4,278	\$18,151
Total			139.92	0.4	1,539,130	\$3,311,903

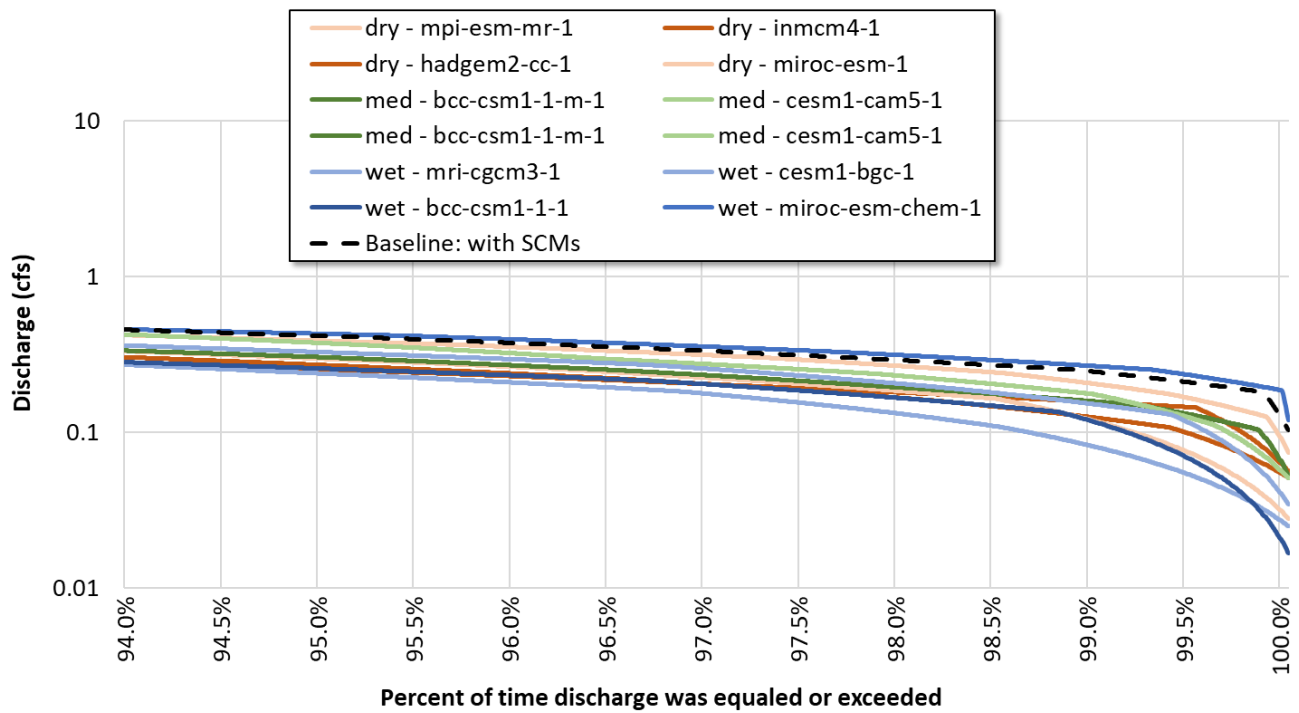
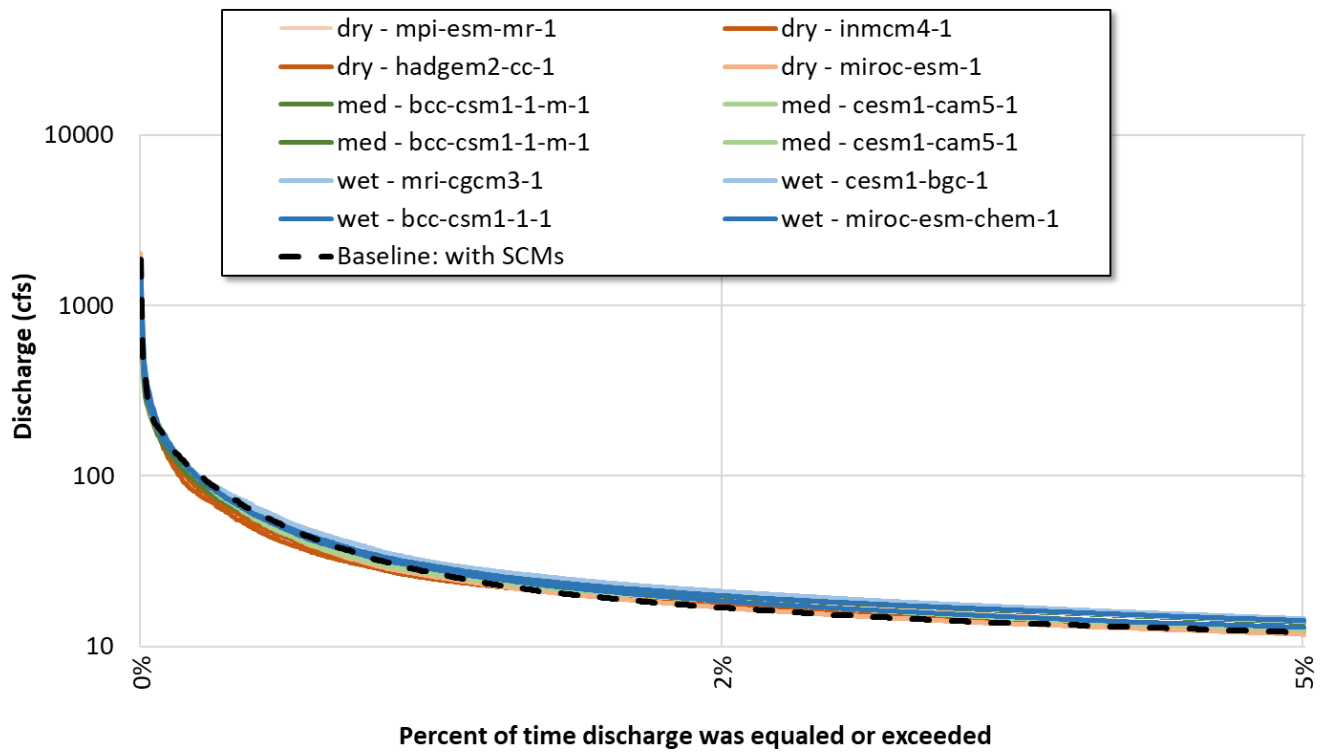


Figure 4-30. Comparison of FDCs resulting from optimized SCM implementation under baseline conditions and those same SCMs under climate change conditions for Upper Hodges sub-watershed. Graphs highlight separate sections of the same FDCs. The top graph shows the high flows and the bottom graph highlight the low flows.

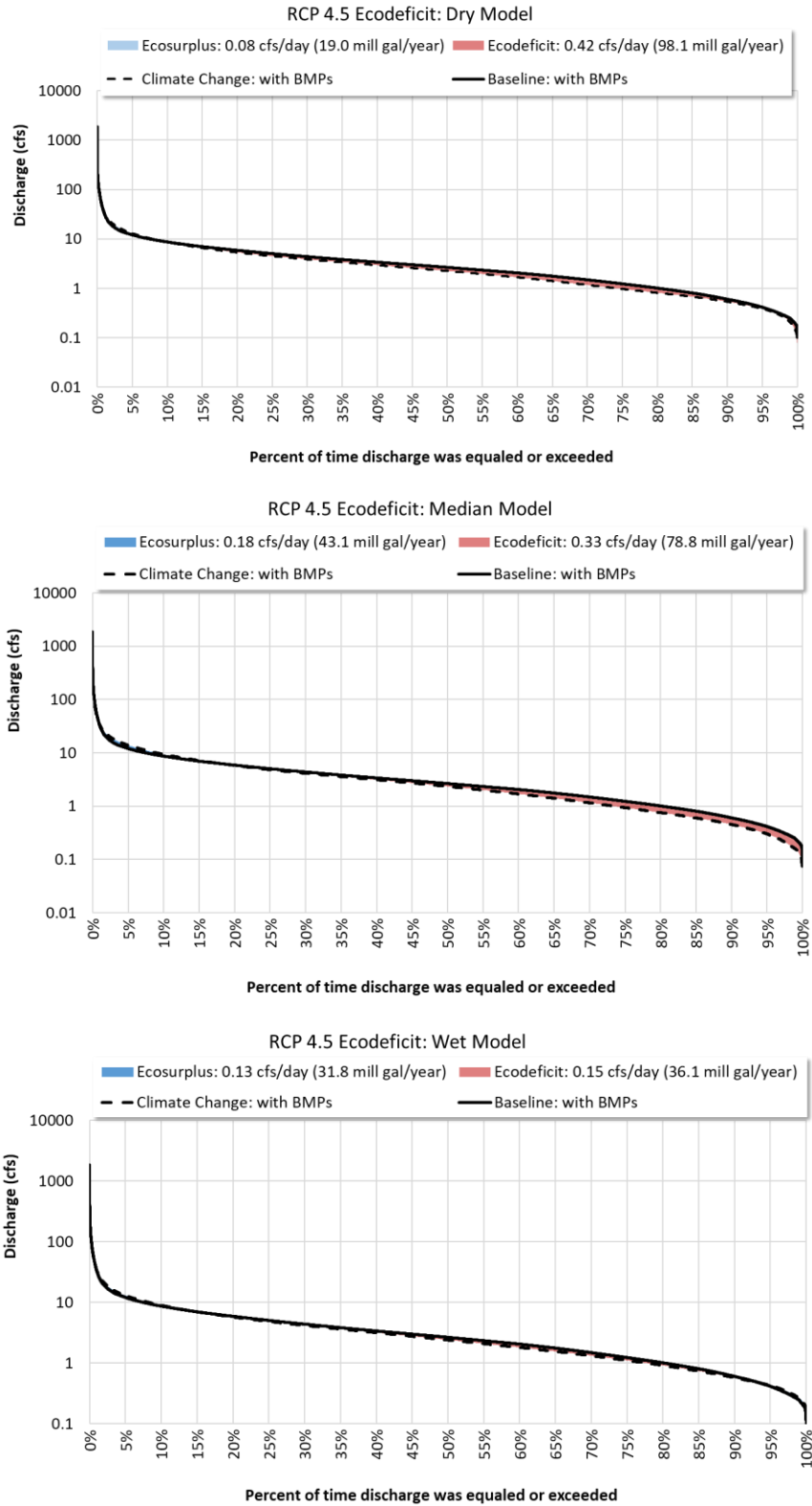


Figure 4-31. Evaluation of the response of optimized SCM implementation to climate change scenarios (RCP 4.5 Ecodeficit Models for Upper Hodges sub-watershed.

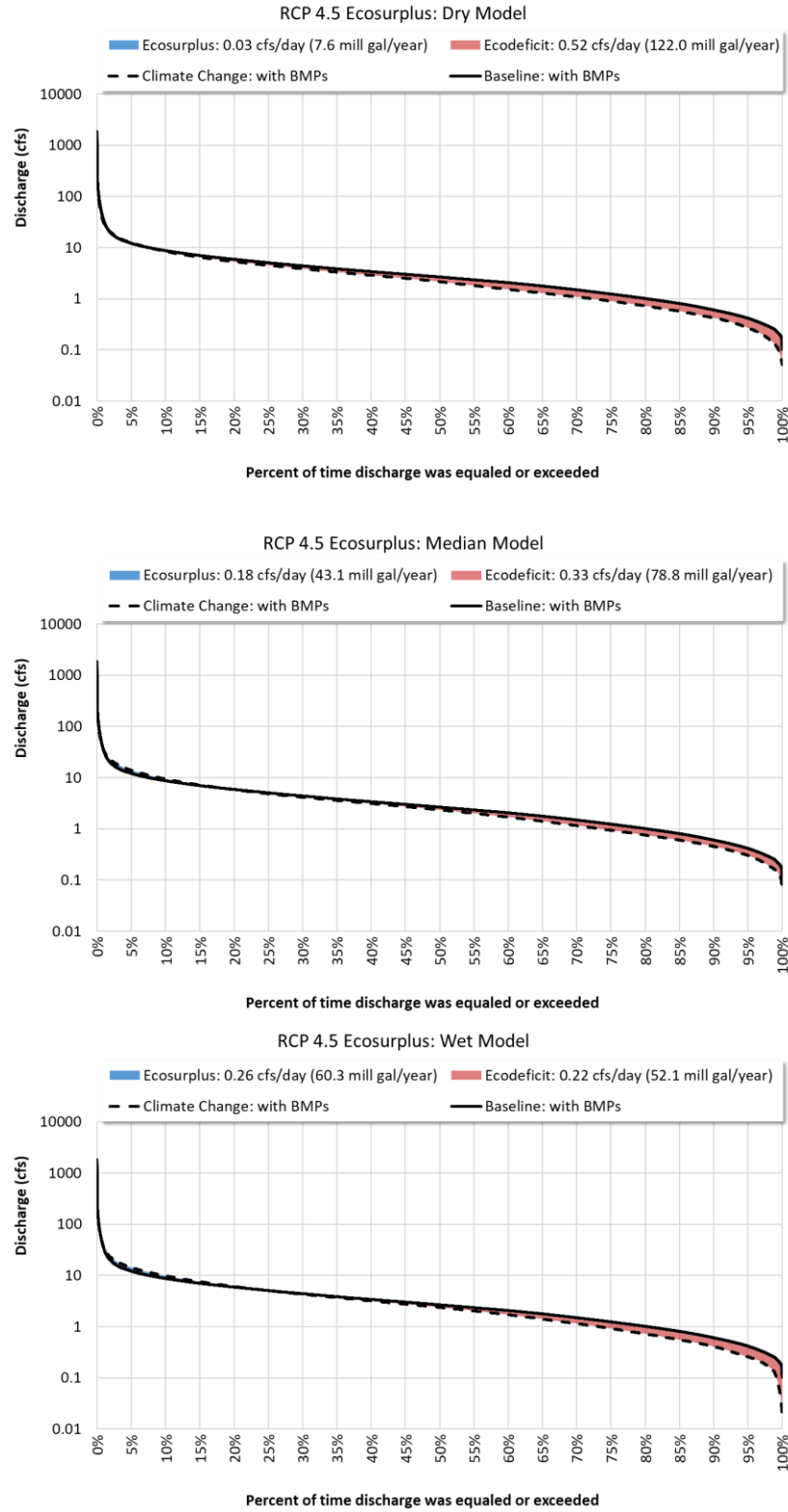


Figure 4-32. Evaluation of the response of optimized SCM implementation to climate change scenarios (RCP 4.5 Ecosurplus Models for Upper Hodges sub-watershed.

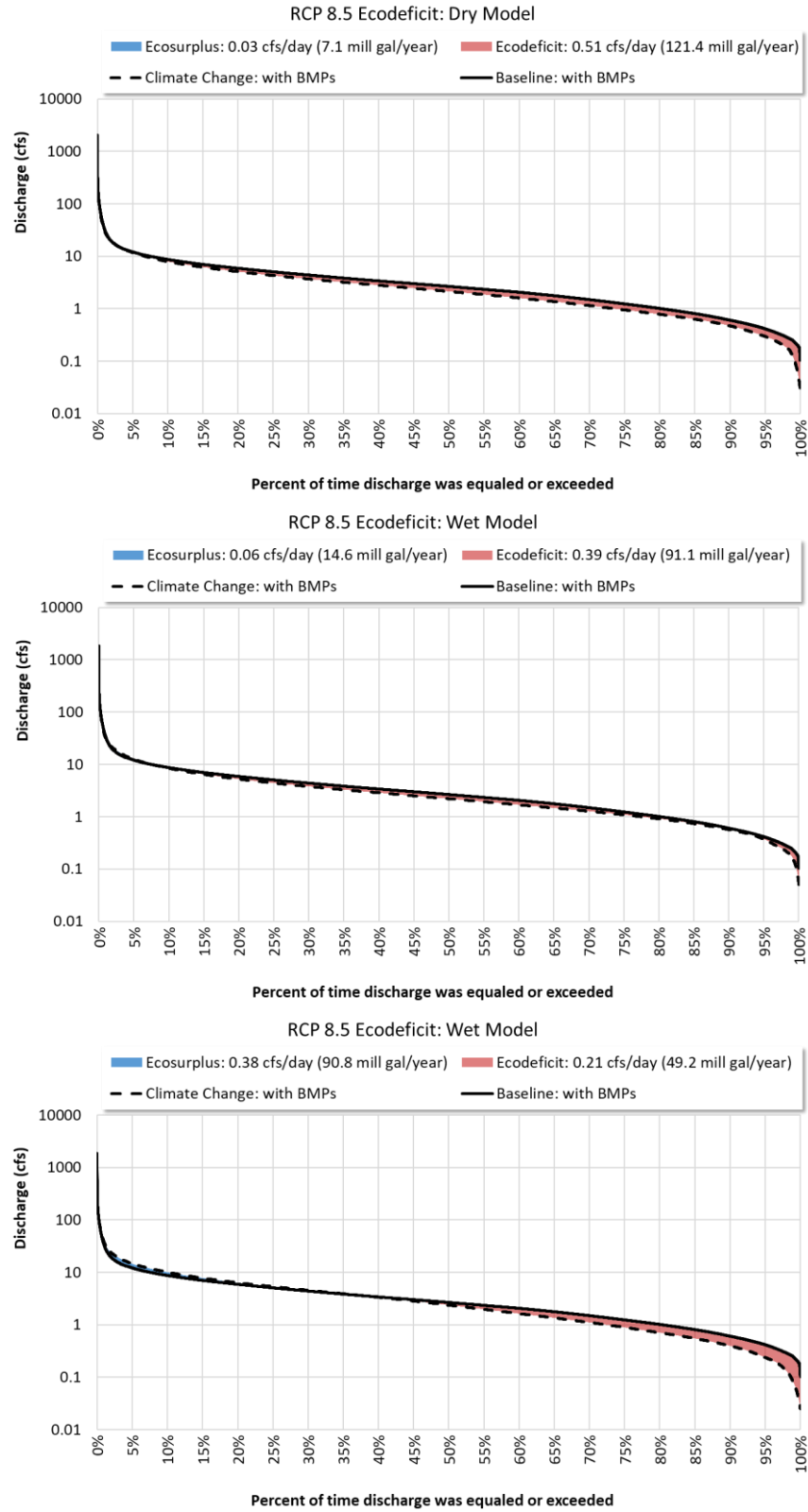


Figure 4-33. Evaluation of the response of optimized SCM implementation to climate change scenarios (RCP 8.5 Ecodeficit Models for Upper Hodges sub-watershed).

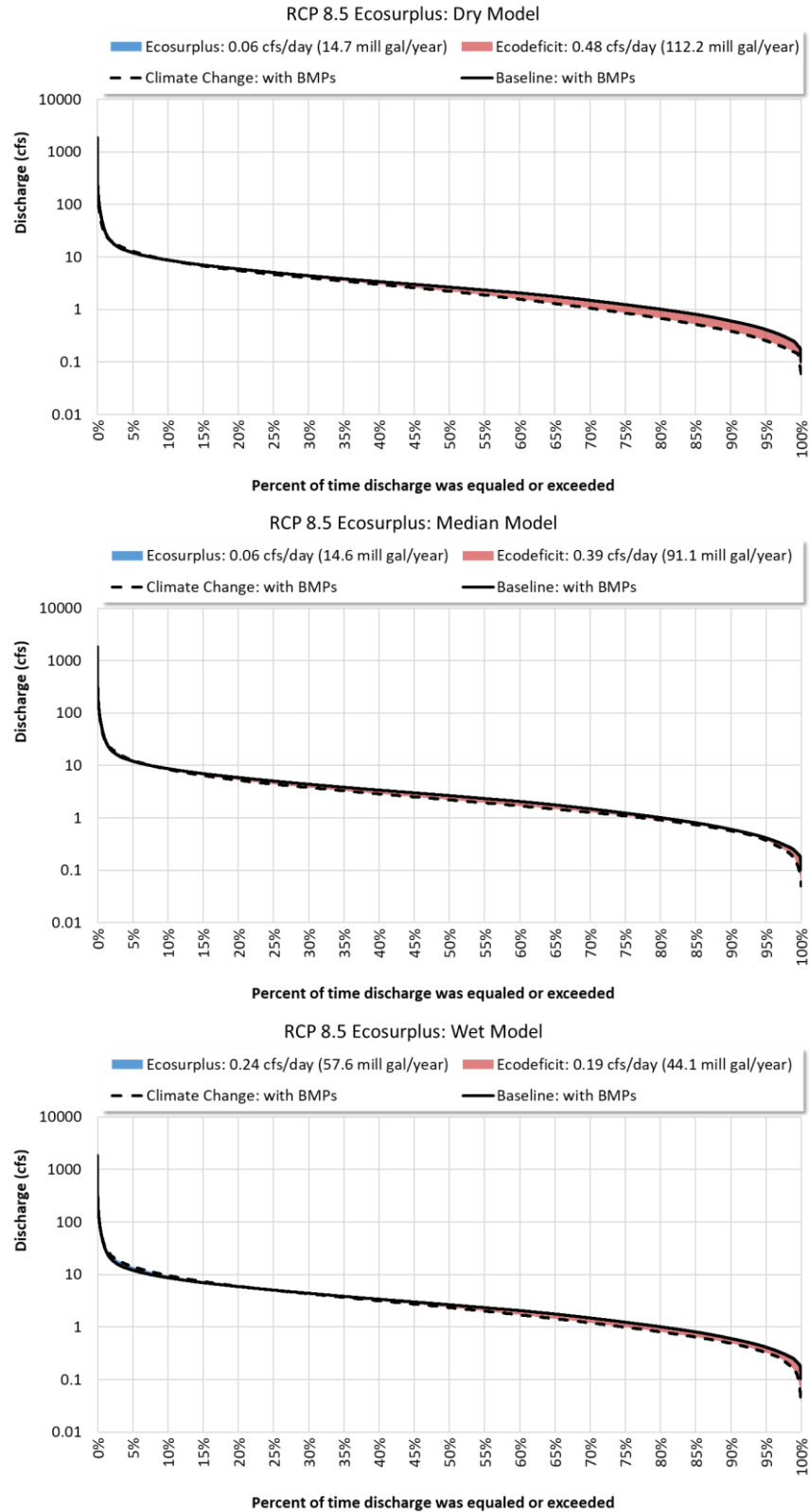


Figure 4-34. Evaluation of the response of optimized SCM implementation to climate change scenarios (RCP 8.5 Ecosurplus Models for Upper Hodges sub-watershed).

Figure 4-35 demonstrates that optimized SCM implementation had the effect of lowering the days in which bankfull discharges occurred in the Upper Hodges watershed. On an average annual basis, SCM implementation reduced bankfull discharges by 0.65 days. Bankfull discharge was assumed to be 30.4 cfs and was obtained by delineating the watershed and generating flow statistics using the [Streamstats](#) website. For the study area, the website uses the same local reference (Bent and Waite, 2013) used to configure channel geometry in the LSPC model (Section 3.3.1.5).

Figure 4-36 presents a conceptual model established by Hawley and Vietz (2016) that identifies broad ranges of flow thresholds and management targets for different sediment particle sizes. The authors suggest that an order-of-magnitude prediction for the critical discharge for bed particle entrainment can be predicted based solely on the material class (e.g., cobble vs sand) and the 2-year peak discharge of the stream under undeveloped conditions. If bed material information is available, future work can leverage the work of Hawley and Vietz (2016) as well as model simulations for undeveloped, forested conditions to better understand the impact of potential management scenarios on the mobilization of sediment.

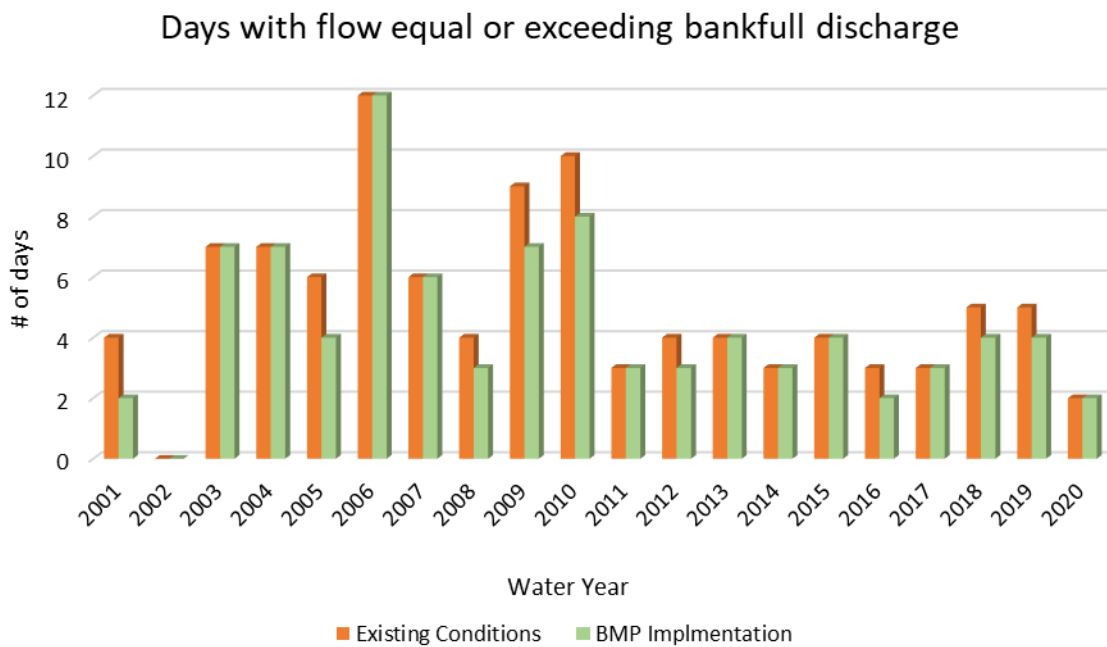


Figure 4-35. Evaluation of the impact of optimized BMP implementation to bankfull discharge for the Upper Hodges watershed.

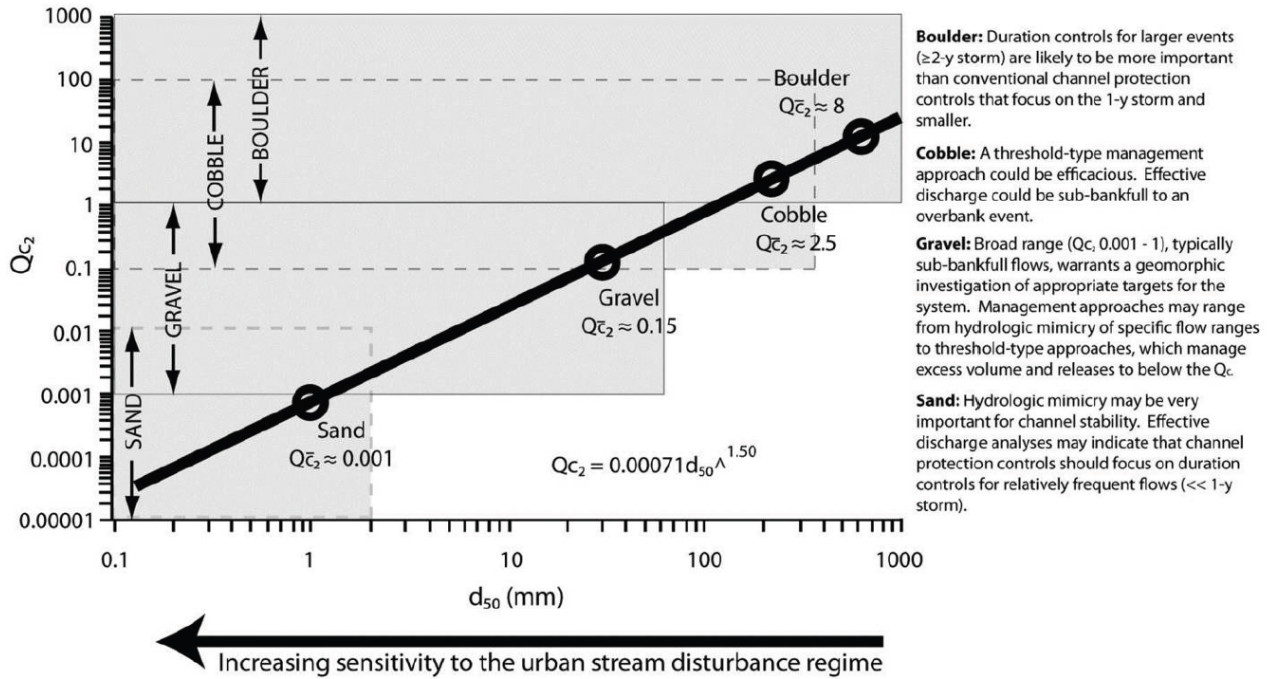


Figure 4-36. From (Hawley and Vietz, 2016). Bed-sediment mobilization along a sensitivity gradient. Q_c = critical discharge for incipient motion, Q_2 = 2-y peak discharge, $Q_c/2=Q_c$ standardized by Q_2 , $Q_c/2$ = mean threshold values for each particle size.

4.4 Conclusions

The results of this streamflow modeling analysis support many well-established concepts about how impervious surfaces influence streamflow, especially stormflows. Additionally, the results suggest that the impact development has on baseflows can vary depending on the intensity of development. Compared to pre-development/forested conditions, development, including development that includes disconnected impervious surfaces, increased baseflows. However, baseflows fell below pre-development conditions when the amount of connected impervious surfaces was substantially increased. There appears to be a threshold somewhere between the developed and forested watershed conditions where increasing infiltration in a developed watershed with less vegetation (and therefore, less ET) may increase baseflows above an equally sized forested watershed with more ET. The results improve our understanding of the extent to which SCMs restore predevelopment streamflows and improve watershed functions. While SCM implementation can mitigate some of the impacts of impervious surfaces, it may be difficult to attain pre-development watershed functions without landscape-level changes that promote additional evapotranspiration. Further investigation may be conducted in the future to test the sensitivity of the system between MIA and EIA and find the threshold where managing runoff meets or exceeds predeveloped conditions baseflow levels.

The optimization analysis provides these key findings:

- Cost-effective management strategies (e.g., the knee of the cost-effectiveness curve) were identified through optimization by searching through the screened SCM selection and placement opportunity in the example watersheds.
- Allowing the SCM sizing rules (in terms of BMP-to-drainage area ratio) to vary by watershed increases the cost-effectiveness of the optimized solutions. Using a standard design storm or sizing rule globally results in oversized SCMs in some places, which increases the overall management cost. For example, a maximum reduction solution for the Upper Hodges sub-watershed that captures on average 1.1-inches of runoff volume from the treated impervious cover (Table 4-24) would cost

\$20.58 Million as compared to a solution at the knee of the curve that captures on average 0.4-inches of runoff volume from the treated impervious cover (Table 4-25) would cost only \$3.31 Million with cost savings of \$17.27 Million (84%). The difference in FDC optimization target for those two solutions is only 3% as shown in Figure 4-26 and Figure 4-27.

- Although the recharge benefits in the FDC low-flow regime (lowest 10% of flows) are marginally different between a maximum solution (58,188 gallons per day) and the best solution (58,666 gallons per day), the associated cost at the knee of the CE-Curve suggests a large cost savings of \$17.27 Million for the Upper Hodges sub-watershed (84% of the maximum cost).
- On the other hand, the benefit of reduction in the highest 10% flows is reduced by about 20% going from the maximum solution to the best solution (1,874,124 vs. 1,494,905 gallons per day, respectively); however, the 20% reduction in performance for the best solution is associated with an 84% reduction in cost compared to the maximum solution.

The model results were also tested for climate resiliency using an ensemble of locally downscaled future climate projections. The ensemble approach tested climate futures from 32 GCMs and 2 RCP scenarios (4.5 and 8.5). Because each GCM/RCP scenario combination represents different projected emissions trajectories and global responses that vary over the century, representative models could not be selected in advance. Instead, the model was run using the full ensemble and summarized as ranges of low/median/high models (i.e., 20th, 50th, and 80th percentile hydrological responses, respectively) for ecosurplus/ecodeficit FDC conditions, and for RCP 4.5/RCP 8.5 scenarios, for the future projection of 2079-2099. This represented a subset of 12 representative GCM projections for evaluating climate resiliency in the watershed (3 ranges × 2 FDC conditions × 2 RCP scenarios).

5. FUTURE WORK – PHASE II

Phase II will evaluate a wide range of potential management measures including GI SCMs, removal of existing IC, and potential future CD practices that can be reasonably simulated in the hydrologic modeling. Future land use management strategies will be identified which protect water resources from future watershed development activities. These strategies will inform the development of next-generation municipal ordinances and bylaws that incorporate next-generation nD/rD practices, or “Conservation Development” (CD) practices, that include among other things, a de-emphasis on use and application of impervious cover (IC), an increasing role of landscape architecture to achieve enhanced ET and better geospatial distribution of nD/rD site runoff, preservation of naturally vegetated areas and incorporation of architecture for increased sustainability and resilience and which preserves the predevelopment hydrological condition.

Phase II of this project will also include the drafting of model bylaws intended to be disseminated to communities to guide development and protect water resources. Model ordinances and bylaws provide language for municipalities to incorporate and adapt to public regulatory laws. The Fact Sheets in Appendix F may be used in the drafting of companion outreach material associated with the model bylaws. Outreach material may be in the form of figures, schematics, and text that provide a plain-language explanation of the model bylaws to be used in outreach to town planning and select boards as well as the public.

Phase II may also include recommendations for successful dissemination and adoption of bylaws. Adoption of bylaws that impact development in a community can be encouraged through incentives. An example of such an incentive is that provided in the state of Vermont for River Corridor/Flood Hazard (RC/FH) protections. Municipalities that adopt approved bylaws that meet RC/FH protections are eligible to receive the maximum 17.5% Vermont Emergency Relief and Assistance Fund (ERAF) cost share of non-federal match requirements for FEMA Public Assistance Grants. To receive the maximum match, municipalities have two options; (1) Enroll in the National Flood Insurance Program Community Rating System and adopt a bylaw that prohibits new structures in the Flood Hazard Area, or (2) Adopt River Corridor protection standards that meet Agency of Natural Resources (ANR) criteria (State of Vermont, 2018).

Similar to model ordinances that guide floodplain development and can require hydraulic modeling to demonstrate compliance (Vermont Agency of Natural Resources, 2018), the Phase II model ordinances may use the metrics and models (Opti-Tool) presented in this final report to demonstrate that future development and redevelopment has no adverse impact to an FDC.

6. REFERENCES

- Barbaro, J.R., Sorenson, J.R., 2013a. Nutrient and sediment concentrations, yields, and loads in impaired streams and rivers in the Taunton River Basin, Massachusetts, 1997–2008: U.S. Geological Survey Scientific Investigations Report 2012–5277.
- Barbaro, J.R., Sorenson, J.R., 2013b. Nutrient and sediment concentrations, yields, and loads in impaired streams and rivers in the Taunton River Basin, Massachusetts, 1997–2008: U.S. Geological Survey Scientific Investigations Report 2012–5277.
- Bent, G.C., Waite, A.M., 2013. Equations for Estimating Bankfull Channel Geometry and Discharge for Streams in Massachusetts. USGS Scientific Investigations Report 2013–5155.
- Bhaskar, A.S., Hogan, D.M., Archfield, S.A., 2016. Urban base flow with low impact development. *Hydrol. Process.* 30, 3156–3171. <https://doi.org/10.1002/hyp.10808>
- Brill, G., Shiao, T., Kammeyer, C., Diringler, S., Vigerstol, K., Ofosu-Amaah, N., Matosich, M., Müller-Zantop, C., Larson, W., Dekker, T., 2021. Benefit Accounting of Nature-Based Solutions for Watersheds: Guide. Oakland, CA.
- Demaria, E.M.C., Palmer, R.N., Roundy, J.K., 2016a. Regional climate change projections of streamflow characteristics in the Northeast and Midwest U.S. *J. Hydrol. Reg. Stud.* 5, 309–323. <https://doi.org/https://doi.org/10.1016/j.ejrh.2015.11.007>
- Demaria, E.M.C., Palmer, R.N., Roundy, J.K., 2016b. Regional climate change projections of streamflow characteristics in the Northeast and Midwest U.S. *J. Hydrol. Reg. Stud.* 5, 309–323. <https://doi.org/https://doi.org/10.1016/j.ejrh.2015.11.007>
- EPA, 2020. Basins Framework and Features [WWW Document]. URL <https://www.epa.gov/ceam/basins-framework-and-features>
- EPA, 2016. What climate change means for Massachusetts. EPA 430-F-16-023.
- Fan, C., Li, J., 2004. A Modelling Analysis of Urban Stormwater Flow Regimes and their Implication for Stream Erosion. *Water Qual. Res. J.* 39, 356–361. <https://doi.org/10.2166/wqrj.2004.048>
- Friends of Lake Mirimichi, 2020. Historical information about our Lake [WWW Document]. URL <http://lakemirimichi.org/History.html>
- Hawley, R.J., Vietz, G.J., 2016. Addressing the urban stream disturbance regime. *Freshw. Sci.* 35, 278–292. <https://doi.org/10.1086/684647>
- Hayhoe, C.P., Wake, T.G., Huntington, L., Luo, M.D., Schrawtz, J., Sheffield, E., Wood, E., Anderson, B., Bradbury, A., Degaetano, T.J., Wolfe, D., 2006. Past and Future Changes in Climate and Hydrological Indicators in the U.S. Northeast. *Clim. Dyn.* 28, 381–707. <https://doi.org/10.1007>
- Hopkins, K.G., Morse, N.B., Bain, D.J., Bettez, N.D., Grimm, N.B., Morse, J.L., Palta, M.M., Shuster, W.D., Bratt, A.R., Suchy, A.K., 2015. Assessment of regional variation in streamflow responses to urbanization and the persistence of physiography. *Environ. Sci. Technol.* 49, 2724–2732. <https://doi.org/10.1021/es505389y>
- Huang, J., Zhan, J., Yan, H., Wu, F., Deng, X., 2013. Evaluation of the Impacts of Land Use on Water Quality. *Sci. World Journal*.
- Hwang, S., Graham, W.D., 2014. Assessment of Alternative Methods for Statistically Downscaling Daily GCM Precipitation Outputs to Simulate Regional Streamflow. *JAWRA J. Am. Water Resour. Assoc.* 50, 1010–1032. <https://doi.org/https://doi.org/10.1111/jawr.12154>
- International Institute for Applied Systems Analysis, 2009. Representative Concentration Pathways (RCP) Database, version 2.0 [WWW Document].
- Jewell, T.K., Nunno, T.J., Adrian, D.D., 1978. Methodology for Calibrating Stormwater Models. *J. Environ. Eng. Div.* 104, 485–501. <https://doi.org/10.1061/JEEGAV.0000772>
- Klingaman, N.P., Butke, J., Leathers, D.J., Brinson, K.R., Nickl, E., 2008. Mesoscale Simulations of the Land Surface Effects of Historical Logging in a Moist Continental Climate Regime. *J. Appl. Meteorol. Climatol.* 47, 2166–2182. <https://doi.org/10.1175/2008JAMC1765.1>
- Laroche, A.-M., Gallichand, J., Lagacé, R., Pesant, A., 1996. Simulating Atrazine Transport with HSPF in an Agricultural Watershed. *J. Environ. Eng.* 122, 622–630. [101](https://doi.org/10.1061/(ASCE)0733-</p></div><div data-bbox=)

9372(1996)122:7(622)

- Leopold, L.B., 1994. A view of the river. Harvard University Press, Cambridge, MA.
- Li, C., Fletcher, T.D., Duncan, H.P., Burns, M.J., 2017. Can stormwater control measures restore altered urban flow regimes at the catchment scale? *J. Hydrol.* 549, 631–653. <https://doi.org/10.1016/j.jhydrol.2017.03.037>
- MA EOOE, 2011. Climate Change Adaptation Report.
- Naito, K., Parker, G., 2019. Can Bankfull Discharge and Bankfull Channel Characteristics of an Alluvial Meandering River be Cospecified From a Flow Duration Curve? *J. Geophys. Res. Earth Surf.* 124, 2381–2401. <https://doi.org/10.1029/2018JF004971>
- Northeast Climate Adaptation Science Center, 2018a. Massachusetts Climate Change Projections - Statewide and for Major Drainage Basins Temperature, Precipitation, and Sea Level Rise Projections.
- Northeast Climate Adaptation Science Center, 2018b. Massachusetts Climate Change Projections - Statewide and for Major Drainage Basins Temperature, Precipitation, and Sea Level Rise Projections.
- Northwest Hydraulic Consultants, 2017. Little Bear Creek Basin Plan, A Final Watershed-Scale Stormwater Plan Prepared in Fulfillment of Special Condition S5.C.5.c.vi of the Phase I Municipal Stormwater Permit. Prepared for Snohomish County.
- Norton Conservation Commission, 2010. Norton's Lakes and Ponds. Norton, MA.
- Reichold, L., Zechman, E.M., Brill, E.D., Holmes, H., 2010. Simulation-Optimization Framework to Support Sustainable Watershed Development by Mimicking the Predevelopment Flow Regime. *J. Water Resour. Plan. Manag.* 136, 366–375. [https://doi.org/10.1061/\(asce\)wr.1943-5452.0000040](https://doi.org/10.1061/(asce)wr.1943-5452.0000040)
- Resilient Massachusetts Action Team, 2020. Climate Resilience Design Standards and Guidelines (DRAFT).
- Richter, B.D., Baumgartner, J. V, Powell, J., David, P., Richter, B.D., Baumgartner, J. V, Powell, J., Braunt, D.P., 1996. A Method for Assessing Hydrologic Alteration within Ecosystems Published by : Wiley for Society for Conservation Biology All use subject to <https://about.jstor.org/terms> A Method for Assessing Hydrologic Alteration within Ecosystems 10, 1163–1174.
- Richter, B.D., Baumgartner, J. V, Wigington, R., Braun, David, P., 1997. How much water does a river need. *Freshw. Biol.* 37.
- Said, A., 2014. Generalized Method for Estimating Variability in Directly Connected Impervious Areas. *Glob. J. Eng. Sci. Res. Manag.* 1.
- Searcy, J., 1959. Flow-Duration Curves. *Manual of Hydrology: Part 2. Low-Flow Techniques.* Washington, DC.
- State of Vermont, 2018. Emergency Relief & Assistance Fund Eligibility Criteria – 17.5% State Share.
- Sutherland, R., 2000. Methods for Estimating the Effective Impervious Area of Urban Watersheds. In: *The Practice of Watershed Protection. Technical Note 58.* Center for Watershed Protection, Ellicott City, MD.
- Swanson, S., 2002. Indicators of Hydrologic Alteration. *Resource Notes No 58.*
- Tong, S., Chen, W., 2002. Modeling the relationship between land use and surface water quality. *J. Environ. Manage.* 66, 377–393.
- Tunsaker, C., Levine, D., 1995. Hierarchical Approaches to the Study of Water Quality in Rivers. *Bioscience* 45, 193–203.
- U.S. EPA, 2007. An Approach for Using Load Duration Curves in the Development of TMDLs. EPA 841-B-07-006. Washington DC.
- USDA, 2019. SSURGO2 (Soil Survey Geographic Database).
- USDA, 2003. National Soil Survey Handbook.
- USGS, 2002. NED (National Elevation Dataset). [WWW Document]. URL <https://catalog.data.gov/dataset/usgs-national-elevation-dataset-ned>
- Vermont Agency of Natural Resources, 2018. Vermont Model Flood Hazard Bylaws. Montpelier, VT.
- Vogel, R.M., Sieber, J., Archfield, S.A., Smith, M.P., Apse, C.D., Huber-Lee, A., 2007. Relations among storage, yield, and instream flow. *Water Resour. Res.* 43, 1–12. <https://doi.org/10.1029/2006WR005226>
- Walsh, C.J., Roy, A.H., Feminella, J.W., Cottingham, P.D., Groffman, P.M., Ii, R.P.M., Ii, R.A.P.M.O., 2015. The urban stream syndrome : current knowledge and the search for a cure *The urban stream*

syndrome : current knowledge and 24, 706–723. <https://doi.org/10.1899/04-028.1>

Wichansky, P.S., Steyaert, L.T., Walko, R.L., Weaver, C.P., 2008. Evaluating the effects of historical land cover change on summertime weather and climate in New Jersey: Land cover and surface energy budget changes. *J. Geophys. Res. Atmos.* 113, 10107. <https://doi.org/10.1029/2007JD008514>

Wilson, C., 2015. Land use/land cover water quality nexus: quantifying anthropogenic influences on surface water quality. *Environ. Monit. Assess.* 187.